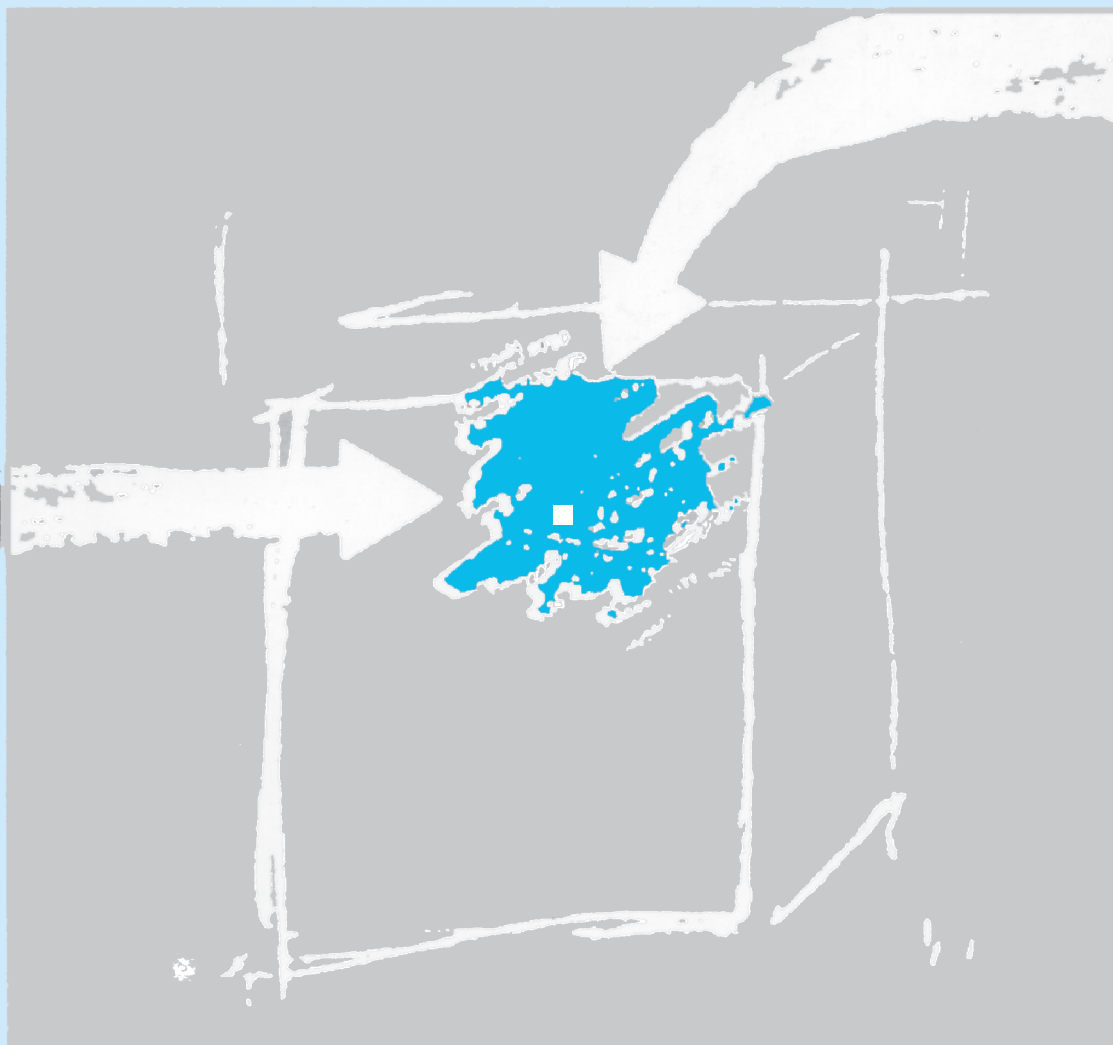


ANALYSIS AND MODELLING OF SORPTION PROCESSES IN COMPLEX MATERIALS



TIZIANA MISSANA
MIGUEL JULIÁN GARCÍA GUTIERREZ
URSULA BLANCA ALONSO DE LOS RÍOS



GOBIERNO
DE ESPAÑA

MINISTERIO
DE CIENCIA, INNOVACIÓN
Y UNIVERSIDADES

Ciemat

Centro de Investigaciones
Energéticas, Medioambientales
y Tecnológicas

Publication available in [General catalog of official publications](#)

© CIEMAT, 2019

Legal Deposit: M-34124-2019

ISBN: 978-84-7834-819-0

NIPO: 693-19-026-3

Edition and Publication:

Editorial CIEMAT

Avda. Complutense, 40 28040-MADRID

e-mail: editorial@ciemat.es

[Editorial news](#)

CIEMAT do not share necessarily the opinions expressed in this published work, whose responsibility corresponds to its author(s).

All rights reserved. No part of this published work may be reproduced, stored in a retrieval system, or transmitted in any form or by any existing or future means, electronic, mechanical, photocopying, recording, or otherwise, without written permission from the publisher.

ÍNDICE

1	INTRODUCTION.....	1
2	EXPERIMENTAL METHODS TO DETERMINE THE SOLID SORPTION CAPACITY.....	4
2.1	STATIC SORPTION TESTS (BATCH)	4
2.1.1	SORPTION EDGES.....	6
2.1.2	SORPTION ISOTHERMS	7
2.2	DYNAMIC SORPTION TESTS (COLUMN)	8
3	ANALYSIS OF SORPTION DATA: K_D AND SORPTION ISOTHERMS.....	14
3.1	LINEAR ISOTHERM MODEL AND DISTRIBUTION COEFFICIENT.....	14
3.2	FREUNDLICH ISOTHERM MODEL	16
3.3	LANGMUIR ISOTHERM MODEL.....	17
3.4	MODIFIED LANGMUIR ISOTHERM.....	20
4	SORPTION KINETICS	21
5	TYPES OF ADSORPTION AND THERMODYNAMIC ASPECTS....	22
6	SURFACE COMPLEXATION AND IONIC EXCHANGE.	24
6.1	FORMATION OF SURFACE COMPLEXES	25
6.2	IONIC EXCHANGE	26
7	SOLUBILITY AND PRECIPITATION.....	29
8	SURFACE COMPLEXATION MODELS, SCM.....	31
8.1	ELECTRICAL DOUBLE LAYER, EDL.....	32
8.2	REACTION CONSTANTS IN THE EDL	34
8.3	CONSTANT CAPACITY MODEL (CC)	36
8.4	DIFFUSE DOUBLE LAYER MODEL (DDL)	39
8.5	TRIPLE LAYER MODEL (TL)	40
8.6	OTHER MODELS.....	44
8.6.1	CD-MUSIC MODEL.....	44

8.6.2	<i>NON ELECTROSTATIC MODEL, NEM</i>	46
9	DETERMINATION OF PARAMETERS FOR THE APPLICATION OF SURFACE COMPLEXATION MODELS	47
9.1	SURFACE AREA AND SURFACE SITES	47
9.2	CATION EXCHANGE CAPACITY	49
9.3	SURFACE CHARGE AND POTENTIAL	50
9.3.1	<i>ELECTROPHORESIS: ζ-POTENTIAL</i>	50
9.3.2	<i>ACID BASE TITRATIONS: SURFACE CHARGE</i>	52
9.3.3	<i>ACID – BASE DISSOCIATION CONSTANTS</i>	55
9.3.4	<i>CAPACITANCES</i>	59
10	NUMERICAL ANALYSIS AND GEOCHEMICAL CODES.	60
11	ADSORPTION STUDIES IN COMPLEX MATERIALS	62
11.1	ANALYSIS OF THE AQUEOUS PHASES	62
11.2	ANALYSIS OF THE SOLID PHASES	68
11.3	DISPERSED AND CONSOLIDATED MATERIALS	70
12	FINAL CONSIDERATIONS	73
13	SIMBOLS AND CONSTANTS	75
14	BIBLIOGRAPHY	77

FIGURE INDEX

Figure 1.	Schematic of the main phases of a batch sorption experiment.....	5
Figure 2.	Adsorption edges (or adsorption tests as a function of pH), on solid materials with variable surface charge. The plot shows the examples for a generic cation (●) and anion (▲).....	7
Figure 3.	Example of sorption isotherms: adsorption of ^{137}Cs on a muscovite suspended in a granitic water. (a) Data expressed as C_{ADS} vs C_{LIQ} and (b) data expressed as K_d vs C_{LIQ} . In both cases data are expressed in a logarithmic form.	8
Figure 4.	Images of a natural fractured core of a crystalline rock.	10
Figure 5.	Typical set-up for a column experiment with crushed materials and a detail of the column filled by the adsorbent (right).	10
Figure 6.	Schematic of the adsorbate interactions with the adsorbent within the column in a saturation test and the corresponding breakthrough curve.	11
Figure 7.	Example of breakthrough curves for conservative tracer (HTO) and a non-conservative tracer (uranium) for the determination of the retardation factor, R_f	12
Figure 8.	(a) Sorption data that can be represented by a linear isotherm. The lineal regression indicates that the K_d is $2.91 \text{ mL}\cdot\text{g}^{-1}$. (b) Representation of the same data in a logarithmic form: the function is a straight line with a unitary slope.	15
Figure 9.	(a) Sorption data that can be represented by a Freundlich isotherm. (b) Data expressed in a logarithmic form. The slope of straight line is lower than 1 (0.502).	17
Figure 10.	(a) Sorption data that can be represented by a Langmuir isotherm. (b) Data plotted in the linearized form ($1/C_{\text{ADS}}$ vs $1/C_{\text{LIQ}}$).....	19
Figure 11.	Schematic of the interaction of a positive ion with the surface of a solid of variable charge, depending on the pH of the solution.	25
Figure 12.	Simplified sketch of the electrical double layer, EDL, at the solid – water interface.	33
Figure 13.	Electrical potential as a function of the distance from the solid surface in the constant capacitance, CC, model.....	37
Figure 14.	Electrical potential as a function of the distance from the solid surface in the diffuse double layer, DDL, model.....	38
Figure 15.	Electrical potential as a function of the distance from the solid surface in the Triple Layer Model	41
Figure 16.	Charge of the surface functional groups coordinated in a simple, double and triple way in a goethite, following Pauling's rules. Iron is coordinated in a octahedral form (Figure modified from Tadaniek & Eick, (2001)).....	44
Figure 17.	Electrified surface of the solid and the slipping plane. The ζ -potential is the electrical potential measured at this plane.....	51
Figure 18.	Examples of the ζ -potential of an oxide (alumina) and a clay (smectite) as a function of pH and $I=1\cdot 10^{-3} \text{ M}$ in NaClO_4	51

Figure 19.	Example of titration data of an oxide in a electrolyte (NaClO_4) at three different ionic strengths. $S=20 \text{ g}\cdot\text{L}^{-1}$; $N_s=10.8 \mu\text{mol}\cdot\text{m}^{-2}$ and $S_A=129 \text{ m}^2\cdot\text{g}^{-1}$	54
Figure 20.	Example of a titration curve of a solid ($S=10 \text{ g}\cdot\text{L}^{-1}$ and $N_s = 1.3\cdot 10^{-3} \text{ mol}\cdot\text{L}^{-1}$) suspended in NaNO_3 0.1 M.	56
Figure 21.	Estimation of (a) pK_{a1} and (b) pK_{a2} using the titration data of Figure 19 and the approximations indicated in Table 5.	58
Figure 22.	Speciation of the surface sites (neutral and negatively and positively charged) as a function of the pH, calculated with the DDL model and considering the data presented in Figure 18. Electrolyte: NaClO_4 0.1 M.	58
Figure 23.	Aqueous speciation of strontium ($[\text{Sr}]=1\cdot 10^{-6} \text{ M}$) as a function of the pH in (a) NaClO_4 0.1 M and (b) NaHCO_3 0.1 M.	63
Figure 24.	Example of the competence of the ions Ca, K and NH_4 in Cs ($[\text{Cs}]=1\cdot 10^{-8} \text{ M}$) adsorption in a clay material. The main background electrolyte is NaClO_4 $1\cdot 10^{-2} \text{ M}$. (From Missana et al., 2014b).....	64
Figure 25.	Aqueous speciation of the uranyl ($[\text{UO}_2^{2+}]=1\cdot 10^{-8} \text{ M}$) as a function of the pH in NaClO_4 0.1 M (a) without y (b) with EDTA ($1\cdot 10^{-6} \text{ M}$).	65
Figure 26.	Schematic diagram indicating which are the conditions to be fulfilled to assess the importance of colloids in radionuclides migration.	66
Figure 27.	Breakthrough curves of Eu(III) at different water flow rates, in the presence of smectite clay colloids. The elution of Eu without colloids was null at any flow. (Missana et al. 2008)	67
Figure 28.	Selenite sorption ($[\text{Se}]=4\cdot 10^{-10} \text{ M}$) as a function of in (a) Na-smectite; (b) Na-illite and (c) in mixed clays with different proportion of both clays. Data and model by Missana et al. (2009).	69
Figure 29.	Comparison between the distribution coefficients of Cs ($[\text{Cs}]=1\cdot 10^{-9} \text{ M}$) in granite obtained with powdered solid (red line) and in a small block of rock (blue points).	72

TABLE INDEX

Table 1.	Reactions and parameters needed to define the solid surface with the constant capacity, CC, model.	38
Table 2.	Reactions and parameters needed to define the solid surface with the diffuse double layer, DDL, model.	40
Table 3.	Reactions and parameters needed to define the solid surface with Triple Layer Model.....	43
Table 4.	Reactions and parameters needed to define the solid surface with the non-electrostatic, NE, model	45
Table 5.	Approximation for the calculation of the pK of protonation and deprotonation from the titration curves	56

1 INTRODUCTION

The control of hazardous substances is crucial to prevent their spreading to the biosphere and to preserve public health. Nowadays, heavy metals or radionuclides are amongst the most critical contaminants, together with different organic compounds or other “*emerging*” pollutants.

The World Health Organisation (WHO), points out the need of controlling in waters the presence of inorganic contaminants of high toxicity (WHO, 2018). These pollutants can be of natural origin (fluorine, arsenic, selenium, nitrate, iron, manganese, uranium) or anthropogenic (mercury, cadmium, zinc, copper, nickel, lead, chrome).

Heavy metals and radionuclides represent a very important risk because they are toxic at very low concentrations (Bradl, 2004; Sparks, 2005). Different experimental methodologies have been proposed to control the contamination by these elements and many studies are currently ongoing (Mulligan *et al.*, 2001; Bhattacharyya & Gupta, 2008; Barakat, 2011; Uddin, 2017).

Amongst the organic pollutants, pesticides (Kah & Brown, 2006) or dyes (Al-Ghouti *et al.* 2003; Gupta & Suhas, 2009; Hernandez-Montoya *et al.*, 2013; Yagub *et al.*, 2014; Anirudhan & Ramachandran, 2015; Hassaan & El Nemr, 2017; Cai *et al.*, 2017) represent a serious environmental problem. Dyes are widespread in modern industry (food, paper, textile, pharmaceutical, cosmetics etc., ...), have high molecular weight and quite complex structures, being of a persistent character.

In the last decades, the progressive increase of the “*emerging contaminant*” has caused a growing concern (Geissen *et al.*, 2015; Noguera-Oviedo & Aga, 2016; Gogoi *et al.*, 2018). These products can be of very different nature and even some widely used pharmaceuticals as antibiotics, analgesics, anti-inflammatories or hormones, are included in this group. Studies of the WHO warn that not negligible concentrations ($\text{ng}\cdot\text{L}^{-1}$ – $\mu\text{g}\cdot\text{L}^{-1}$) of different pharmaceuticals are often found in wastewaters and surface waters but also in drinking ones (WHO, 2012).

The presence of any contaminant in a (potentially) dangerous concentration can be natural or accidental; it may be caused by human activity or by the need of accumulating them for their isolation or disposal. In any case, it is very important to analyse in detail the scenario, where pollutants are present, to minimise the risks associated to their presence and to apply the most adequate prevention or remediation strategies.

Adsorption, which is defined as “*the process by which ions and/or molecules are accumulated in the interface between a solid and a fluid*”, is a very important process for the control of the migration of hazardous substances in the environment and a widely used technology for water treatment and purification.

Many different mechanisms can lead to adsorption of ions/molecules: van der Waals forces or electrostatic forces are involved in physical adsorption (physisorption) whereas in chemical

adsorption (chemisorption) a covalent or hydrogen bond is established between the ion/molecule of the solute and the solid surface. The bond energy in chemical adsorption is higher than in physical sorption and the complexes formed are stronger (Stumm, 1992).

In adsorption, the accumulation of ions at the solid surface is bidimensional. Additional processes as *absorption*, in which the element initially at the surface diffuses in the bulk material or *surface precipitation* in which 3-D structures are formed at the solid surface (Haworth, 1990; Ford *et al.*, 2001) may also contribute to the elimination of ions from the aqueous phase. The latter processes cannot be included in the term “adsorption” but are equally important to stabilize contaminants in the solid phases. The generic term including all the retention processes is “sorption” (Sparks, 2003).

In the context of retention processes, the solid in whose surface the ions/molecules are accumulated is called *adsorbent*, whereas the accumulated chemical specie is called *adsorbate*. To maximise contaminant retention, good adsorbents should have high specific surface areas in relation with their mass. A large number of different materials (clays, oxides, active carbon, zeolites and various organic materials), which can be natural or especially modified, have been analysed for the treatment of different types of contamination (Bonilla-Petriciolet *et al.*, 2017).

Adsorbent materials used in both conventional and radioactive waste disposals or employed for the containment of pollutant discharges are called *barrier* materials. These materials must have specific mechanical, thermal or chemical properties, according to the context of their use and, in particular, they must be *reactive*, i.e. be able to interact with the contaminants and retain them. All the barrier materials must be stable and durable, environmentally safe, available in large quantities and reasonably cheap. Amongst the most common barrier materials clayey rocks are found (Norris, 2014).

In some cases, barrier materials must be more permeable than the rest of the surrounding solids, to facilitate the contaminated water flow through the adsorbent. In this case, it is necessary to mix the reactive adsorbent with other materials to favour the increase of porosity and water permeability (Rötting *et al.*, 2008). In the frame of radioactive waste disposals, engineered barrier materials must have specific thermo-hydro-mechanical properties (AEN-NEA, 2002; Sellin & Leupin, 2014) and low permeability to ensure that radionuclide migration could eventually occur only by diffusion, to guarantee the safety of the system.

The in-depth analysis of adsorption processes is useful for the design of optimized sorbent materials. The materials must be adapted to the physicochemical characteristics of the contaminant and to the specific scenario. Only a deep comprehension of the system allows the development of materials (or barriers) with improved characteristics.

Furthermore, the knowledge of sorption mechanisms is necessary for the development of mechanistic models, which are essential for the prediction of contaminant migration, when the chemical conditions spatially and/or temporally change. The application of mechanistic models to real systems still represents a challenge that must be faced.

Many factors can affect contaminant speciation or contaminant/solid interactions and consequently be crucial for contaminant fate. The comprehensive analysis of all the processes potentially favouring contaminant mobility is needed to avoid or, at least, counteract them.

The objective of this document is to explain, in a simple way, the basics of adsorption processes, including the main experimental methodologies to tackle them, and the principal methods to analyse and interpret the experimental data.

The concept of electrical double layer and surface complexation models (SCMs), will be briefly explained. A short description of the methods for determining the SCMs' parameters (surface sites, surface charge, acid-base dissociation constants, etc) will be given. The possible approaches for the application of SCMs to complex systems will be discussed.

2 EXPERIMENTAL METHODS TO DETERMINE THE SOLID SORPTION CAPACITY.

During the adsorption process, the adsorbate is divided amongst the fluid and the adsorbent. If both the fluid and solid phases are kept in contact for enough time, the equilibrium is reached.

To establish the time needed to reach the equilibrium, sorption tests maintaining the adsorbent and the adsorbate in contact during different times (*kinetic tests*) must be carried out. Generally, ionic exchange processes are fast (hours), whereas the formation of other type of complex may last longer (days), depending on the type of the material and its particle size. If sorption tests are carried out with compacted or consolidated material, the contribution of diffusive processes may be relevant and the time needed to reach the sorption equilibrium can be significantly longer (weeks, months).

The main objective of adsorption tests is to determine how and how much the adsorbate is distributed between the solid and the liquid phases, under different experimental conditions. Amongst the variable of special interest, we can consider: the contact time, the temperature, the concentration of the contaminant or the adsorbent, pH, ionic strength of the liquid or the presence of ions or ligands that can favour or hinder retention.

There are two main types of tests: static (*batch*) tests or dynamic tests, the latter are carried out percolating the liquid with the adsorbing element through a column of solid material. Both methodologies present advantages and drawbacks, and their selection principally depends on the frame of the study and the type of material investigated.

2.1 STATIC SORPTION TESTS (BATCH)

Batch sorption experiments are the most frequently used tests for the analysis of the retention properties of solids, in powdered or crushed form, for their simplicity.

The methodology to carry out these experiments basically consists on suspending a mass (**m**) of the adsorbent in a volume (**V**) of liquid and adding a known quantity of adsorbate, of initial concentration C_{INI} ($\text{mol}\cdot\text{L}^{-1}$ or $\text{Bq}\cdot\text{L}^{-1}$). The suspension is maintained under stirring during a certain time (*t*), after which the solid and the liquid phases are separated, usually by filtration or (ultra)centrifugation.

After the separation process, the supernatant is analysed to determine the concentration of the contaminant remained in the liquid, C_{LIQ} . Obviously, the mass of the adsorbed contaminant is equal to the initial quantity minus the one remained in the liquid.

Figure 1 shows a simplified sketch of the main steps of a batch sorption test.

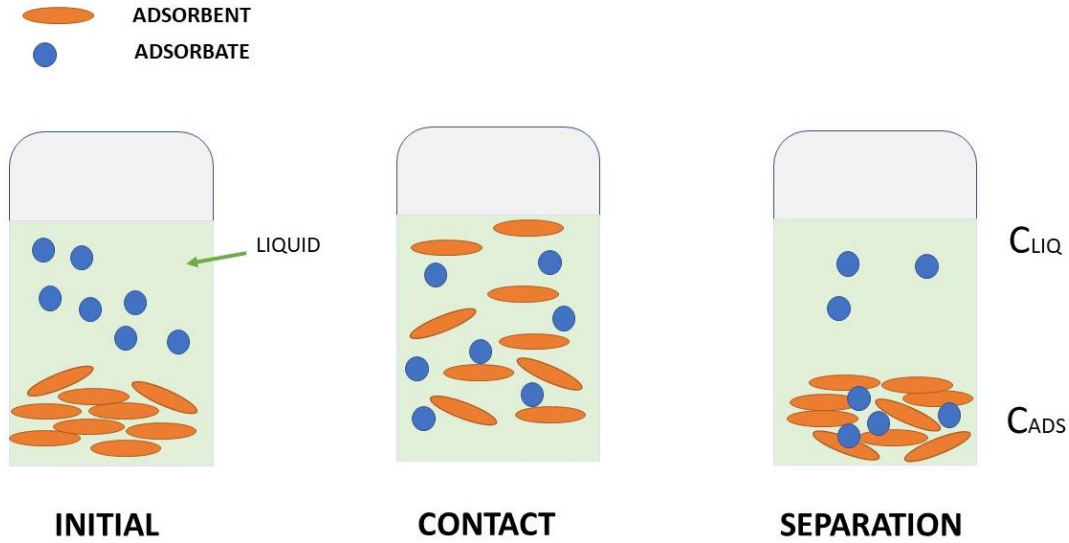


Figure 1. Schematic of the main phases of a batch sorption experiment.

If the volume of the liquid (V) and the mass of the adsorbent (m) are considered, the concentration of adsorbate C_{ADS} ($\text{mol}\cdot\text{g}^{-1}$) is:

$$C_{ADS} = \frac{V}{m} (C_{INI} - C_{LIQ}) + C_0 \quad \text{Equation 1}$$

C_0 is the quantity of adsorbate that might be naturally present in the solid. If this quantity is negligible in respect to the adsorbate concentration, this term can be obviated. In the same way, if in the liquid there are traces of the element whose sorption we are studying, or the solid lixiviates it, this should be accounted for in the C_{INI} term.

The relation between the adsorbed concentration of the contaminant (C_{ADS}) and the one remained in the liquid (C_{LIQ}) is defined as the *distribution coefficient* or K_d :

$$K_d = \frac{C_{ADS}}{C_{LIQ}} = \frac{C_{INI} - C_{LIQ}}{C_{LIQ}} \cdot \frac{V}{m} \quad \text{Equation 2}$$

The K_d is usually expressed in $[\text{L}\cdot\text{Kg}^{-1}]$ or $[\text{mL}\cdot\text{g}^{-1}]$ units, and it is the parameter used to represent the adsorptive capability of a solid (in the specific conditions of the experiment).

An alternative form of expressing sorption data is the percentage of adsorbed contaminant, in relation to the quantity initial added ($\%_{ads}$):

$$\%_{ads} = 100 \cdot \frac{C_{ADS}}{C_{INI}} \quad \text{Equation 3}$$

The numerical value of the distribution coefficient, or the adsorption percentage, depends on a number of factors, especially the chemical conditions. This means that K_d values cannot be extrapolated to conditions different from those of the experiment; therefore, to assess their dependence on various parameters of interest, it is necessary to perform multiple tests. To start the developing of mechanistic models for the interpretation of experimental data, it is

necessary to carry out the tests in the widest as possible range of experimental conditions of pH, ionic strength (I) and adsorbate concentration.

The (ir)reversibility of a sorption process depends on the type of material, on the type of adsorbent-adsorbate interactions and on the strength of the formed bond. To understand if sorption is or not reversible “desorption tests” must be carried out, after the conventional sorption experiments. Kinetic tests are especially relevant in this frame.

After having determined the “sorption K_d ”, the solid in which the adsorbate is retained has to be suspended again in a fresh liquid. The suspension is maintained under stirring during the selected contact time, and then, the solid and the liquid phase are separated and the “desorption K_d ”, $K_d(\text{des})$, determined as:

$$K_d(\text{des}) = \frac{C_{\text{ADS,S}} - C_{\text{LIQ,DES}}}{C_{\text{LIQ,DES}}} \cdot \frac{V}{m} \quad \text{Equation 2b}$$

$C_{\text{ADS,S}}$ is the quantity of contaminant in the solid after the sorption step and $C_{\text{LIQ,DES}}$ the concentration of the contaminant in the liquid phase upon the desorption step.

Sorption is considered “reversible” if K_d and $K_d(\text{des})$ coincide when the sorption and desorption times are the same. The hysteresis between sorption and desorption is quite common. In general, desorption process needs more time than adsorption to reach the equilibrium, above all when complexes with high bonding energy are formed. The non-complete reversibility of the sorption process may be caused by different causes, for example by the diffusion of the adsorbate within the bulk material or by the formation of precipitates whose equilibria are mainly controlled by their solubility.

2.1.1 SORPTION EDGES

The experiments aimed to analyse the dependence of the distribution coefficients on pH are called *sorption edges*, for the typical shape of these curves. An example of this type of tests is shown in Figure 2, where the percentage of adsorption (%) as a function of pH of an anion and a cation on a mineral oxide are shown. The observed dependence of sorption on pH, is related to the variable surface charge of the solid surface, produced by the existence of amphoteric sorption sites, which are positively charged under acidic conditions and negatively charged under and basic conditions. That is why, as shown in Figure 2, cations are better adsorbed at high pH and anions at low pH.

Nevertheless, in solids with permanent charge and when the main sorption mechanism is ionic exchange, the dependence of sorption on pH is not very relevant, whereas the ionic strength (I) is more influential.

To obtain the complete information adsorption edges should be repeated at different electrolyte concentrations and at different adsorbate concentrations.

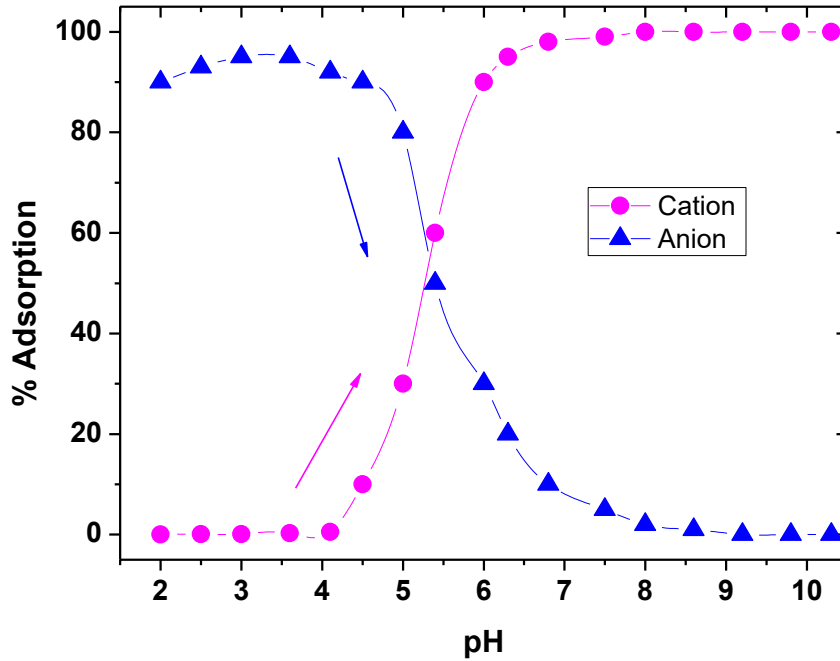


Figure 2. Adsorption edges (or adsorption tests as a function of pH), on solid materials with variable surface charge. The plot shows the examples for a generic cation (●) and anion (▲).

2.1.2 SORPTION ISOTHERMS

The set of batch experiment aimed to determine the dependence of the distribution coefficient on contaminant concentration are called *sorption isotherms*. In these tests, all the main parameters (temperature, pH, ionic strength) are fixed, and only the adsorbate concentration is varied. To obtain a more complete information, sorption isotherms should be repeated at different pH and ionic strengths.

In the classical representation of the sorption isotherms, the concentration of the adsorbed element, C_{ADS} , is plotted against the concentration of the adsorbate remained in solution at the equilibrium, C_{LIQ} . As the variation of the adsorbate concentration may vary several orders of magnitude, data are often expressed in a logarithmic form ($\text{Log}(C_{ADS})$ vs. $\text{Log}(C_{LIQ})$).

An example of this type of tests is shown in Figure 3, where the adsorption isotherm of Cs on a natural muscovite suspended in a low ionic strength water from a granitic rock is shown. Figure 3(a) shows the data $\text{Log}(C_{ADS})$ vs. $\text{Log}(C_{LIQ})$ and Figure 3(b) the data of $\log(K_d)$ vs. $\text{Log}(C_{LIQ})$. Both representations are very common and in each one different information can be evidenced.

Figure 3(a) indicates that as far as Cs concentration increases, the slope of the curve decreases, indicating a progressive decreasing of the sorption capability of the material. This is more clearly appreciated in Figure 3(b), where it can be seen as the distribution coefficient decreases (up to more than two orders of magnitude) when Cs concentration decreases.

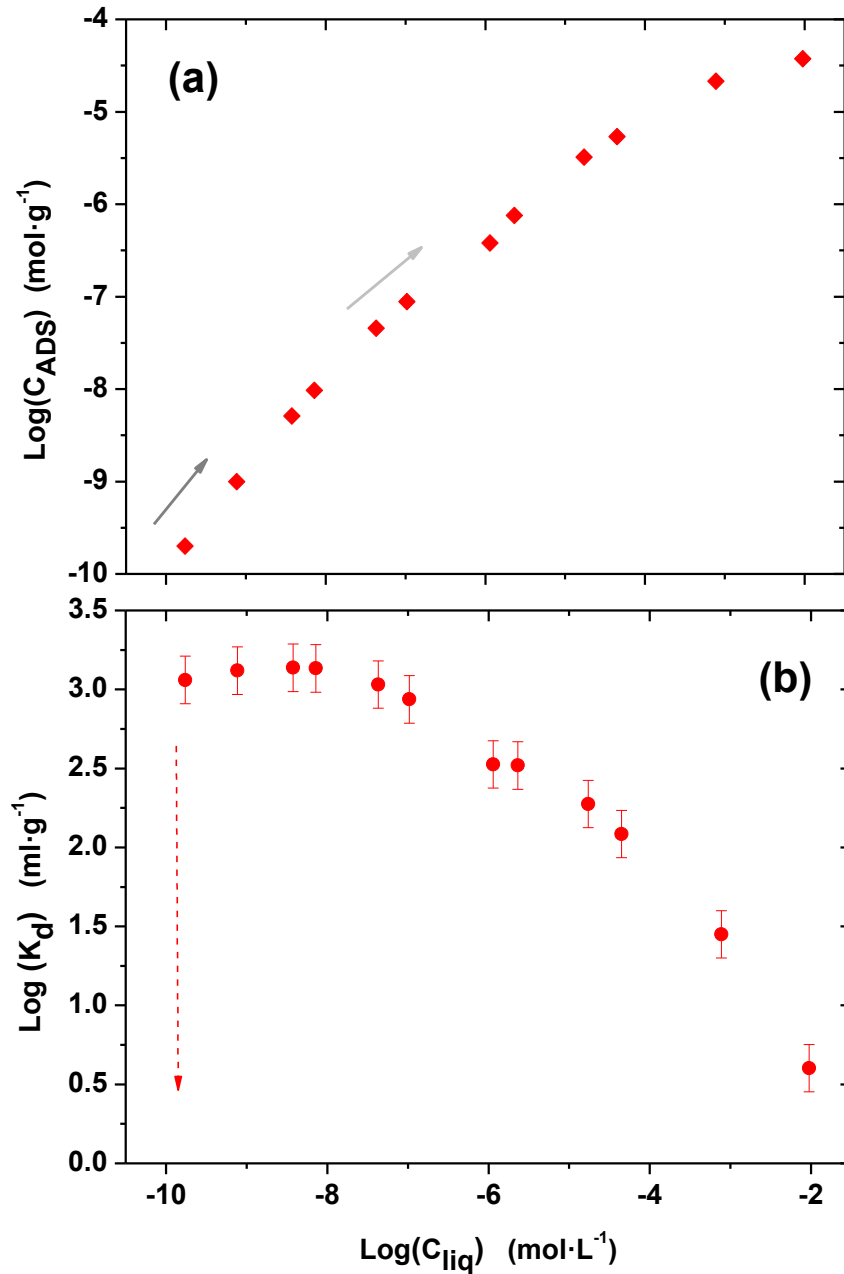


Figure 3. Example of sorption isotherms: adsorption of ^{137}Cs on a muscovite suspended in a granitic water. (a) Data expressed as C_{ADS} vs C_{LIQ} and (b) data expressed as K_d vs C_{liq} . In both cases data are expressed in a logarithmic form.

2.2 DYNAMIC SORPTION TESTS (COLUMN)

Batch tests are very useful to determine distribution coefficients for a contaminant under a wide range of experimental conditions and represent a very useful tool for the detailed analysis of sorption processes. However, it is often necessary to gather additional information, in respect to dynamic aspects, to correlate the adsorption properties of a solid and the migration of the contaminant in the presence of a water flow.

If an element dissolved in water does not suffer any interaction with the surrounding medium and is not adsorbed by the solid phases, it is defined as a *conservative* element. A conservative contaminant can migrate with the water flow experiencing *advection*, *diffusion* and *dispersion* processes.

Advection is the “dragging” of solutes by water; if this is the unique existing process, contaminants move as water does and with the same velocity.

Diffusion occurs as long as a concentration gradient is present, even if water flow is not present, and dispersion is produced by the heterogeneity of the porous medium, which lead to different fluid velocity within the transport paths.

When other interactions between the migrating contaminant and the medium exist, leading to adsorption, precipitation or other chemical reactions, the contaminant suffers a *retardation* in respect to water.

The retardation factor, R_f , expresses the velocity of the adsorbate in relation to water, being expressed by the ratio between the water velocity (\mathbf{v}) and contaminant velocity (\mathbf{v}_c): $R_f = \mathbf{v}/\mathbf{v}_c$.

The R_f mainly depends on the solid properties and on its sorption capability, and it can be written as:

$$R_f = 1 + \frac{\rho}{\theta} K_d \quad \text{Equation 4}$$

ρ represents the bulk density and θ the mean porosity of the solid material.

The water velocity is related to the water flow (\mathbf{Q}) by the following relation: $\mathbf{v} = \mathbf{Q}/\mathbf{A}$, where \mathbf{A} is the cross-section area of the channel where water is flowing.

A typical method to analyse sorption process under dynamic conditions is based on column tests, where an electrolyte with the dissolved adsorbate is passed through a column of adsorbent material.

In these tests, apart from the dynamic component derived from the existence of the water flow, the solid-to liquid ratio is much higher than in batch experiments.

The solid material used in column experiments can be porous, formed by crushed or powdered material, or fractured. The fractures in the column can be naturally present or be mechanically produced. Fractures represent the main paths for water movement and contaminant migration and the surface of the fracture and natural fracture filling materials are the main adsorbents of the system.

Figure 4 shows an example of a natural core from a granitic rock of the Grimsel Test Site (Switzerland), used at for several migration experiment in a natural fracture. Figure 5 shows the typical *set-up* of a column test with crushed material and, on the right part of the picture, a

detail of a column filled by the adsorbent, which is sometimes mixed with other inert materials to increase the permeability and to facilitate the passage of the liquid.



Figure 4. Images of a natural fractured core of a crystalline rock.



Figure 5. Typical set-up for a column experiment with crushed materials and a detail of the column filled by the adsorbent (right).

Before starting the experiment, the columns must be sealed to avoid spills; the liquid is then introduced in the material with a (peristaltic) pump. Before the injection of the adsorbate, the column must be completely hydrated and the solid-solution system chemically equilibrated.

The adsorbate with the initial concentration, C_0 , can be continuously injected in the column (saturation test) during the required time, or as a “pulse”. In this last option, only few millilitres of the solution with the adsorbate are injected (during a time t_i) and, afterwards the hydration follows with the clean electrolyte.

The adsorbate mass transfer to the solid is schematically represented in Figure 6.

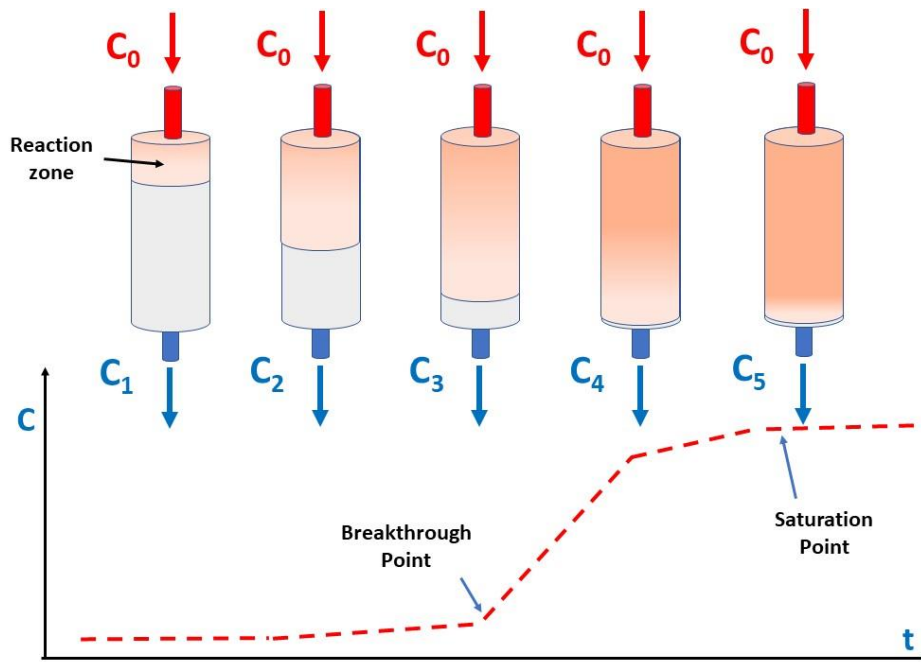


Figure 6. Schematic of the adsorbate interactions with the adsorbent within the column in a saturation test and the corresponding breakthrough curve.

The zone of interaction between the clean solid and the adsorbate moves along the length of the column. When the interaction front reaches the end of the column, the contaminant starts going out. From this moment on, the concentration of the contaminant in the eluted water can be measured to obtain the *breakthrough curve*. In the case of saturation experiments, the breakthrough curve has an S-shape (as that shown in Figure 6); in pulse tests the breakthrough curve resembles a peak function.

To define appropriately the breakthrough curves, the fractions of eluted water should be small enough, for example with a fraction collector as that shown in Figure 5; the limitations concerning the minimum volume to collect depends on the type of analytical technique that must be used to determine the adsorbate concentration.

Before carrying out the tests with any adsorbate, it is quite important determining the column transport parameters, as material porosity, and to make a hydrodynamic characterisation to understand how the water is moving in the system.

This is the necessary reference to determine the retardation suffered by different contaminants due to the presence of the solid adsorbent, in comparison with the water movement. To perform this previous characterisation, conservative tracers are used, for example tritiated water, HTO.

Figure 7 shows an example of two breakthrough curves obtained in the same column of crystalline rock material for a conservative tracer, HTO and a non-conservative one (uranium). The comparison of the two curves allows obtaining the retardation factor of uranium in respect to water, which is in this case about 5.6.

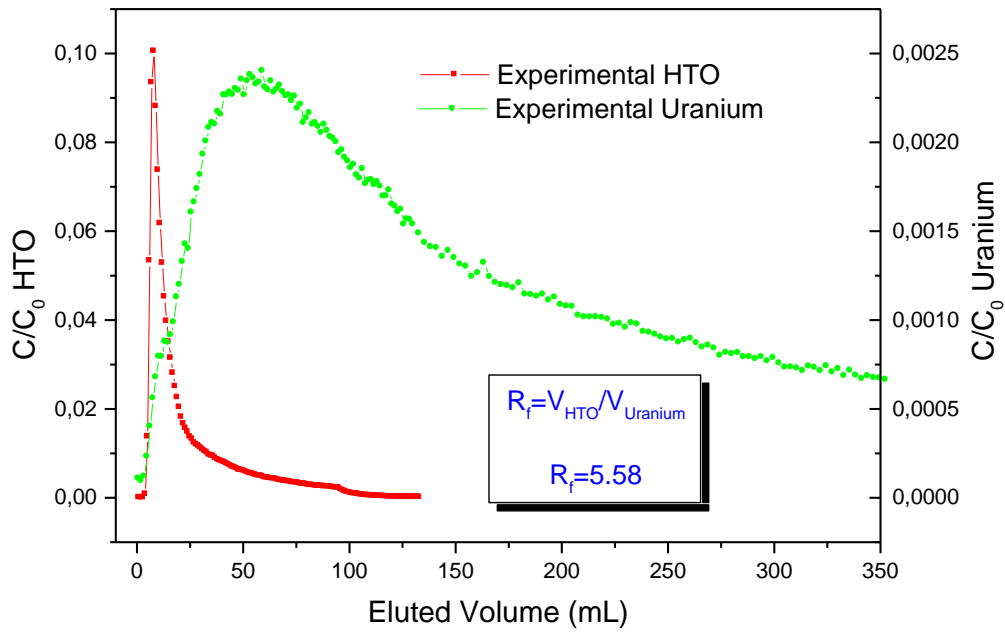


Figure 7. Example of breakthrough curves for conservative tracer (HTO) and a non-conservative tracer (uranium) for the determination of the retardation factor, R_f .

The full analysis of breakthrough curves is made considering the advection-diffusion theory. One-dimensional advective - dispersive transport of solutes is described by a partial differential equation. The main parameters used for the description of transport in a homogeneous medium are the dispersion coefficient (D) and the distribution coefficient (K_d), the latter accounting for sorption of the contaminant in the solid. The advection-dispersion equation for one-dimensional solutes transport subject to chemical adsorption in a homogeneous medium is:

$$\frac{\partial C_{LIQ}}{\partial t} + \frac{\rho}{\theta} \frac{\partial C_{ADS}}{\partial t} = D \frac{\partial^2 C_{LIQ}}{\partial x^2} - v \frac{\partial C_{LIQ}}{\partial x} \quad \text{Equation 5}$$

D is the dispersion coefficient and v the average pore-water velocity. If sorption is described as a lineal isotherm $C_{ADS} = K_d \cdot C_{LIQ}$ and steady state is assumed, the equation can be rewritten as:

$$R_f \cdot \frac{\partial C_{LIQ}}{\partial t} = D \frac{\partial^2 C_{LIQ}}{\partial x^2} - v \frac{\partial C_{LIQ}}{\partial x} \quad \text{Equation 5b}$$

The main parameters of this equations, that can be determined by numerical or analytical methods and simplified analysis of the breakthrough curves can be done with computer programmes as CXTFIT (Toride *et al.*, 1999) or STANMOD (van Genuchten *et al.*, 2012). More details on these methodologies can be found in García-Gutiérrez & Missana (2018).

When the tests are carried out with different flow velocities, different residence times for the contaminant within the column are obtained and, in consequence, a stronger or weaker interaction between adsorbate and adsorbent and a different overall adsorption. Furthermore,

the dispersive and advective contributions will be different, affecting the migration of the contaminant.

In many cases, it can be useful to determine the Peclet number (P_e), knowing D and v :

$$P_e = \frac{v \cdot x}{D}$$

This number indicates the relative contribution of advection and dispersion/diffusion in the system. $P_e < 0.4$ indicates that transport is diffusion controlled; $0.4 < P_e < 6$ indicated that both advection and diffusion are important, whereas $P_e > 6$ indicated that transport is controlled by advection (Fetter, 1999).

3 ANALYSIS OF SORPTION DATA: K_d AND SORPTION ISOTHERMS

As previously mentioned, the objective of a batch sorption test is to determine experimentally the distribution of a contaminant between the solid and the liquid phase thus, to measure the magnitudes C_{ADS} and C_{LIQ} .

For the analysis of sorption data, a number of different approximations with different degrees of complexity can be applied, depending on the pursued objectives and the nature of the experimental results.

As mentioned in 4.1, the functions which determine the relation between C_{ADS} and C_{LIQ} at different concentration of adsorbate are called *sorption isotherms*; the classic name of *isotherms* originates from the fact that temperature is a relevant parameter in adsorption processes and must be kept constant during the tests.

Adsorption isotherm models aim describing how pollutants react with the adsorbent surface and are defined by different starting hypotheses and parameters. The determination of these parameters is a support for the analysis of retention processes and give information, for example, on the maximum sorption capacity of the solid, or on other thermodynamic parameters, as for example the Gibb's free energy (Foo & Hamed; 2010).

The shape of the sorption isotherms may be indicative of different properties. One can infer if sorption is or not lineal, if precipitation may have occurred, etc. The non-lineal adsorption behaviour as a function of its concentration may indicate the existence of surface heterogeneity and/or multiple types of adsorption sites at the solid surface.

It is quite common to hear that minerals may have *strong* and *weak* sorption sites. Strong sites are those with low concentration but very high affinity for the adsorbate; K_d values measured in strong sites are higher than those measured in weak sites, which have much higher concentration but less affinity for the adsorbate (Dzombak & Morel, 1990; Missana *et al.*, 2014a).

3.1 LINEAR ISOTHERM MODEL AND DISTRIBUTION COEFFICIENT

The linear isotherm model is the easiest form to represent an adsorption process. As previously mentioned, the distribution coefficient, K_d is the ratio between the contaminant adsorbed concentration (C_{ADS} ,) and the contaminant concentration left in the liquid (C_{LIQ}): $K_d = \frac{C_{ADS}}{C_{LIQ}}$ therefore, the relation between C_{ADS} and C_{LIQ} is a straight line with the K_d as slope:

$$C_{ADS} = K_d \cdot C_{LIQ} \quad \text{Equation 6}$$

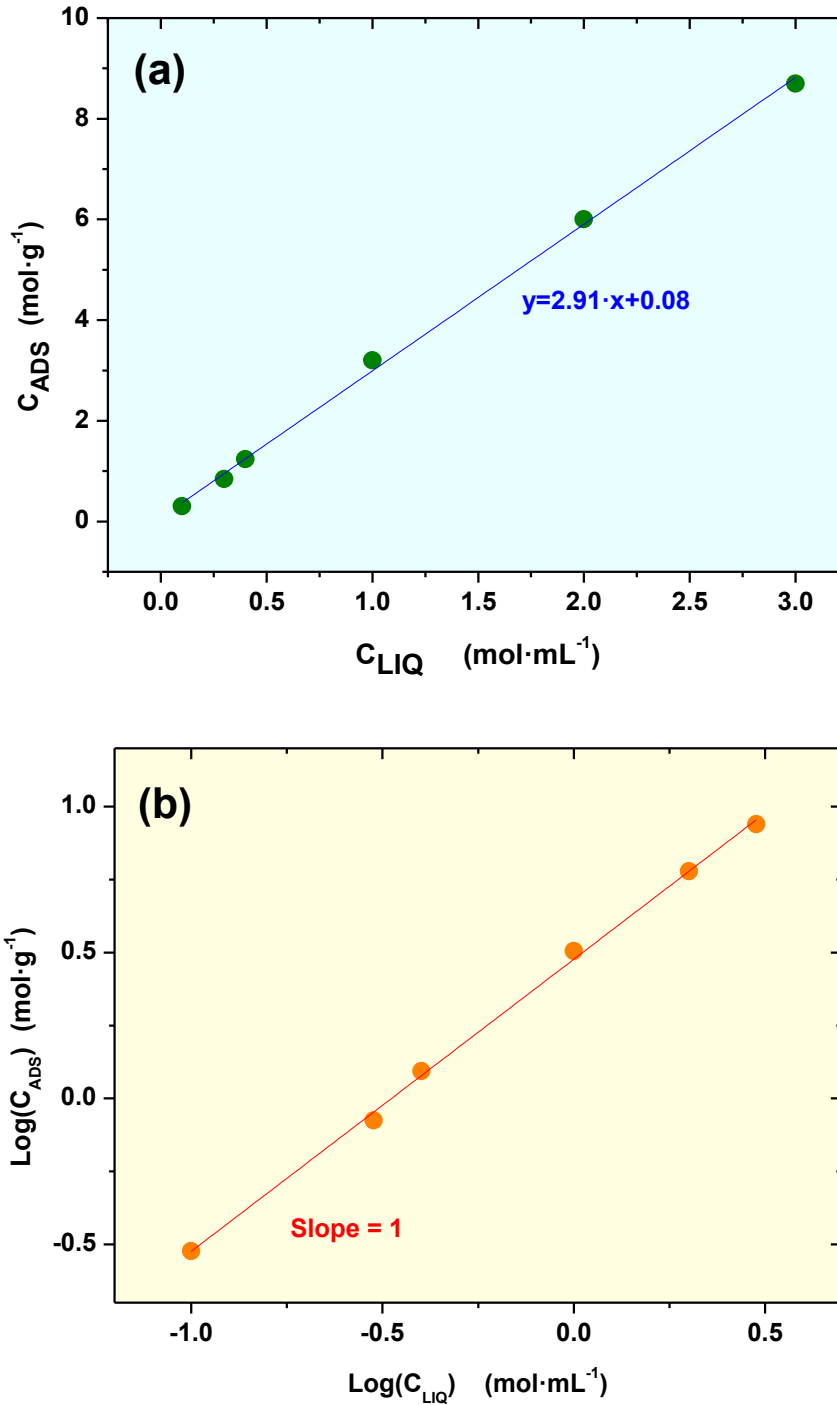


Figure 8. (a) Sorption data that can be represented by a linear isotherm. The linear regression indicates that the K_d is $2.91 \text{ mL}\cdot\text{g}^{-1}$. (b) Representation of the same data in a logarithmic form: the function is a straight line with a unitary slope.

This linear relation is defined also as “Henry’s Law”, for the analogy with the gas behaviour, where the quantity of adsorbate on the solid surface is proportional to the partial pressure of the gas ($X=K_H\cdot P$, where X is the quantity of adsorbate in the solid, P the partial pressure of the gas and K_H the Henry constant).

Figure 8 shows a set of data that can be represented by a lineal isotherm. In Figure 8(a) data are plotted as C_{ADS} vs C_{LIQ} . The linear regression gives slope for the straight line of $2.91 \text{ mg}\cdot\text{L}^{-1}$, value corresponding to the K_d .

In Figure 8(b), the same data are plotted in a logarithmic form:

$$\text{Log}(C_{ADS}) = 1 \cdot \text{Log}(C_{LIQ}) + \text{Log}(K_d) \quad \text{Equation 6b}$$

If the K_d or linear approximation is valid the data expressed in a logarithmic form are represented by a straight line with a unitary slope.

In general, the linear isotherm is valid at low adsorbate concentrations and in a small range of concentration.

3.2 FREUNDLICH ISOTHERM MODEL

In many sorption tests, non-linear adsorption is observed, thus the previously described K_d approximation cannot be applied. In 1906, Freundlich presented the first description which aimed describing non-linear adsorption processes.

The Freundlich isotherm can be written as:

$$C_{ADS} = K_f (C_{LIQ})^n \quad \text{Equation 7}$$

where K_f is a constant ($[\text{L}\cdot\text{Kg}^{-1}]$) and n is a number < 1 .

The parameter n represents the degree of heterogeneity of the adsorbent, the smaller is n the higher is the heterogeneity of the sample (Goldberg, 2005).

In a Freundlich isotherm, it can be observed that, as far as the concentration increases, the slope of the curve decreases. This means that the affinity between adsorbent and adsorbate decreases when the adsorbate concentration increases. In this sense, this approximation is considered useful to represent heterogeneous surfaces.

Figure 9 shows a set of data that can be represented by the Freundlich isotherm. Figure 9(a) shows the C_{ADS} vs. C_{LIQ} data. The values of the parameters of the isotherm K_f and n , obtained by fit of experimental data are 1.47 and 0.54, respectively.

In Figure 9(b) the same data are presented in a logarithmic form. In this way, the Freundlich is linearized:

$$\text{Log}(C_{ADS}) = n \cdot \text{Log}(C_{LIQ}) + \text{Log}(K_f) \quad \text{Equation 7b}$$

The straight line has a slope of value n (and less than 1).

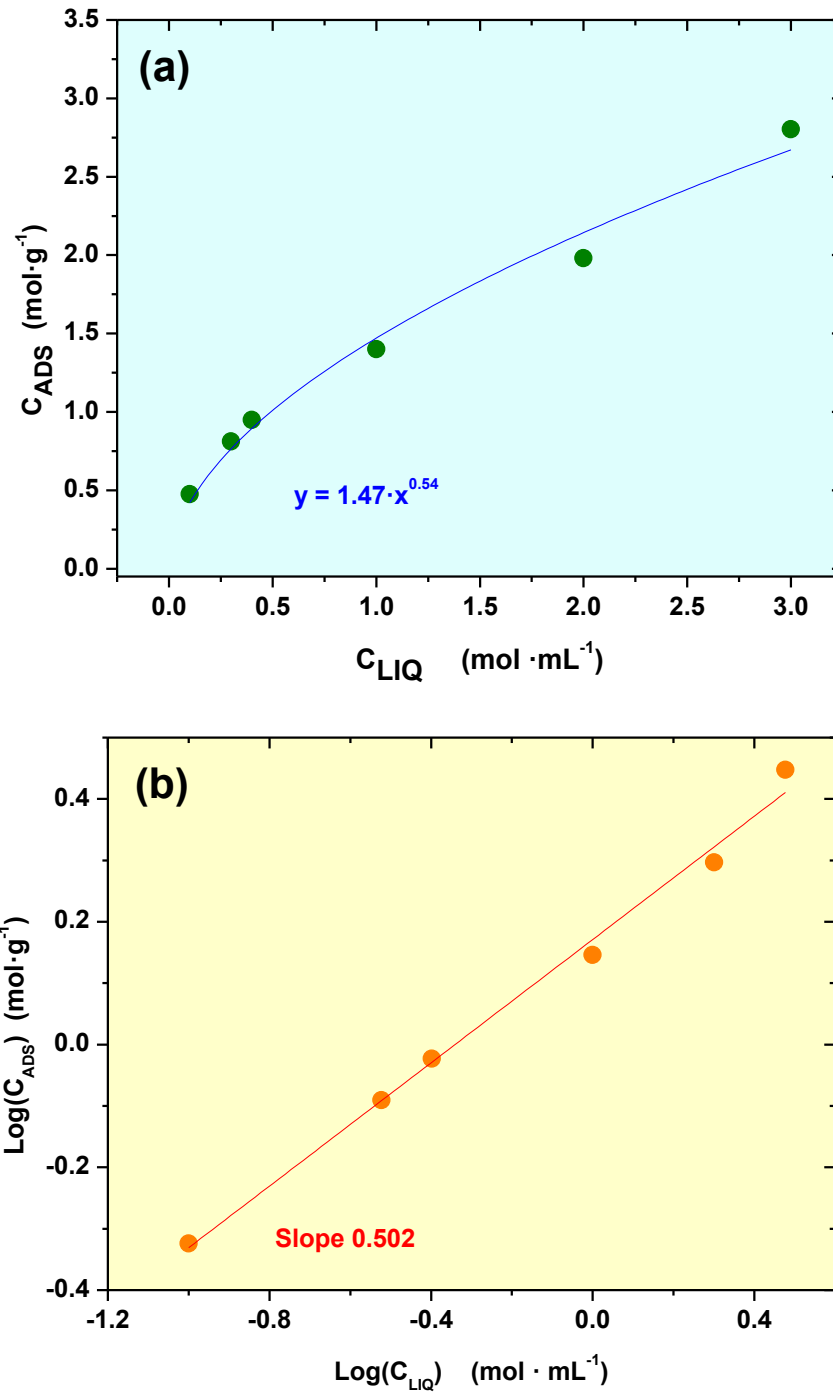


Figure 9. (a) Sorption data that can be represented by a Freundlich isotherm. (b) Data expressed in a logarithmic form. The slope of straight line is lower than 1 (0.502).

3.3 LANGMUIR ISOTHERM MODEL

In the two previously described formulations (linear and Freundlich isotherms), it is implicitly assumed that an infinite number of sorption sites are present in the surface of the solid. In reality, the adsorption capacity of any solid is limited; to account for this limitation, in 1918

Irvin Langmuir developed a mathematical description, similar to that used to describe monolayer gas adsorption on a solid surface.

In this approximation, Langmuir considered that the sorbent has a maximum adsorption capacity, is homogeneous (all the sorption sites are equivalent) and that the adsorption energy does not depend on the quantity of adsorbate already retained. In this model each atom/molecule is able to interact with only one site of adsorption and it is not possible to adsorb more than one monolayer of adsorbate at the surface.

The following reaction can be written to describe a generic (1:1) adsorption process onto a generic sorption site:



The equilibrium constant of the previous reaction, K_{Lang} , is:

$$K_{Lang} = \frac{[\text{Complexed Site}]}{[\text{Free site}][\text{Ion}]} = \frac{C_{ADS}}{C_{LIQ} \cdot C_{FR}} \quad \text{Equation 9}$$

C_{ADS} is the concentration of the adsorbed ion, C_{LIQ} is the concentration of the ion that remains in the liquid phase and C_{FR} is the concentration of un-complexed, free sites. This constant indicates the affinity between the adsorbate and the solid.

Considering that in the Langmuir's model the number of adsorption sites is limited and C_{MAX} is the maximum adsorbable concentration we assume that: $C_{ADS} + C_{FR} = C_{MAX}$.

Therefore, the equilibrium constant, K_{Lang} , can be rewritten as:

$$K_{Lang} = \frac{C_{ADS}}{C_{LIQ} \cdot (C_{MAX} - C_{ADS})} \quad \text{Equation 9b}$$

This constant represents the affinity of the adsorbate for the solid and it is related to the adsorption energy. This parameter can be used to estimate the standard free Gibb's energy ΔG^0 ($\text{J} \cdot \text{mol}^{-1}$) of the reactions, which depends on the equilibrium constants, K , in this way:

$$K = e^{\frac{-\Delta G^0}{RT}} \quad \text{Equation 10}$$

The classical form for the Langmuir isotherm (C_{ADS} vs C_{LIQ}), derived from Equation 9b is:

$$C_{ADS} = C_{MAX} \frac{K_{Lang} \cdot C_{LIQ}}{1 + K_{Lang} \cdot C_{LIQ}} \quad \text{Equation 11}$$

An alternative way to represent the data is the linearized form ($1/C_{ADS}$ vs $1/C_{LIQ}$):

$$\frac{1}{C_{ADS}} = \frac{1}{C_{MAX}} + \frac{1}{K_{Lang} \cdot C_{MAX}} \cdot \frac{1}{C_{LIQ}} \quad \text{Equation 11b}$$

This linearized form is frequently used to obtain C_{MAX} and K_{Lang} .

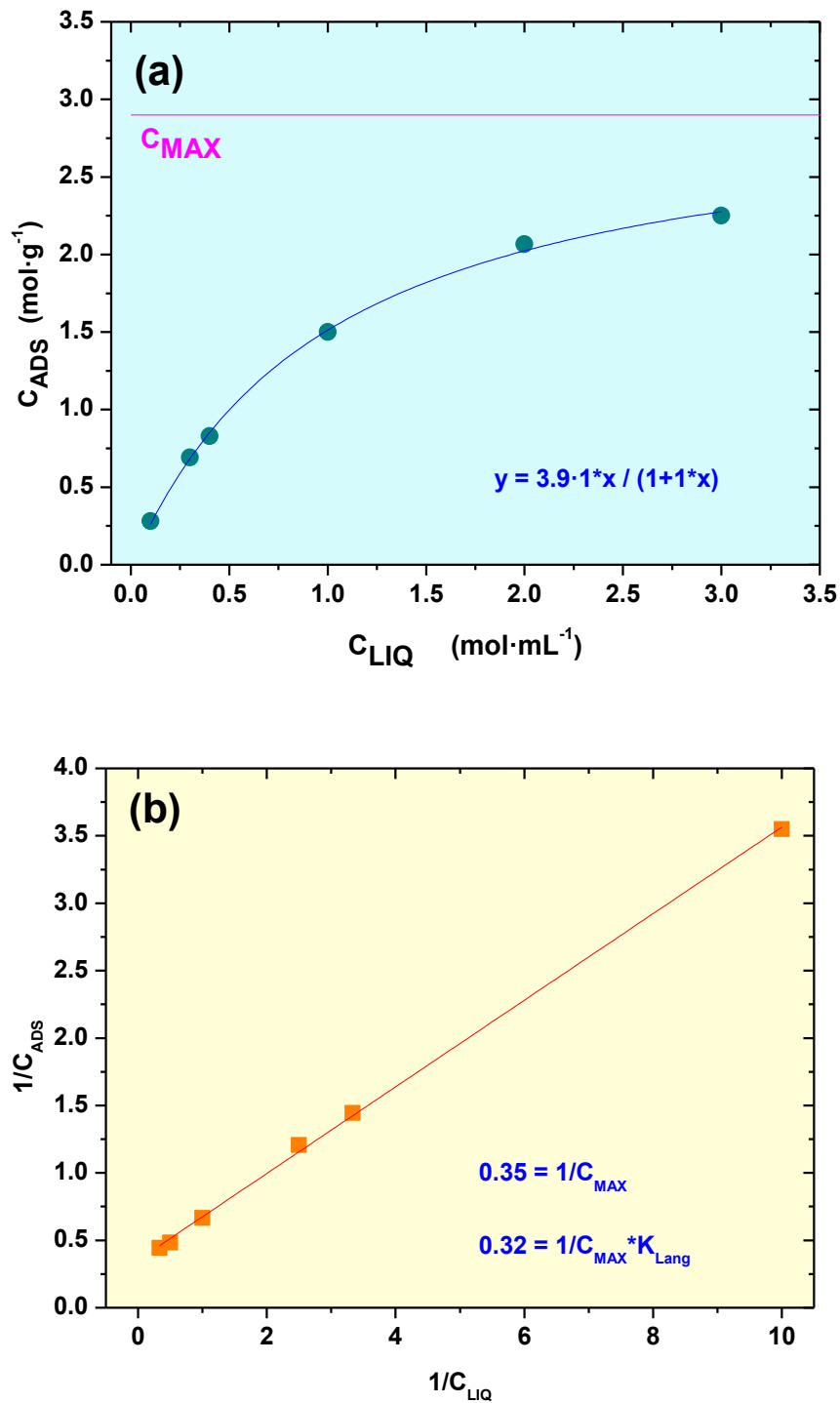


Figure 10. (a) Sorption data that can be represented by a Langmuir isotherm. (b) Data plotted in the linearized form ($1/C_{ADS}$ vs $1/C_{LIQ}$).

Figure 10 shows an example of data that can be adjusted by a Langmuir isotherm. In Figure 10(a) data are expressed as C_{ADS} vs C_{LIQ} ; in Figure 10(b) data are expressed in the linearized form. By the fit of experimental data, the C_{MAX} (2.86 mol·g⁻¹) can be determined, as well as the Langmuir constant K_{Lang} (1.09).

When the adsorbate concentration is very small, the Langmuir equation can be assimilated to a linear expression with $K_d = C_{MAX} \cdot K_{Lang}$. At high adsorbate concentration, the model predicts a constant adsorption equivalent to a monolayer of adsorbate (C_{MAX}). In this approximation, is impossible to adsorb more than an adsorbate monolayer on the solid surface.

3.4 MODIFIED LANGMUIR ISOTHERM

The Langmuir's isotherm is widely used in the literature to fit experimental sorption data; however sometimes data linearization does not give rise to straight lines but to convex curves. This is most probably due to the fact that the hypothesis on which the Langmuir model is based are not fulfilled.

For example: the Langmuir's description considers that the bond energy between sorbent and adsorbate does not vary with the degree of site occupancy and this fact may not be true in reality. Similarly, the solid surface might not be homogeneous and multiple adsorption sites with different reactivity exist.

To incorporate into the model the possible existence of multiple sorption sites, a generalised form for the Langmuir equation can be written. This is based on the summation of n equation for the n different adsorption sites:

$$C_{ADS} = \sum_{i=1}^n C_{MAX,i} \frac{K_{Lang,i} \cdot C_{Liq,i}}{1 + C_{Liq,i}} \quad \text{Equation 12}$$

With this equation, the fit of the experimental data usually significantly improves, even if a better adjust does not always means a better knowledge of the system, as the number of fit parameters has increased too (Goldberg, 2005).

Another possible element that can be considered, in a modified form of the Langmuir equation, is the presence of ions different from the adsorbate in the aqueous phase that can be competitive for sorption sites. This is quite common in natural waters.

In this case, the Langmuir isotherm, which considers the adsorption of a ion I, in the presence of competitive ions j, can be rewritten as (Limousin *et al.*, 2007):

$$C_{ADS,I} = C_{MAX,I} \frac{K_{Lang,I} \cdot C_{LIQ,I}}{1 + \sum_{j=1}^q K_{Lang,j} \cdot C_{LIQ,j}} \quad \text{Equation 13}$$

This formula implies that the maximum capacity of adsorption of the solid is not affected by the competence of different species.

4 SORPTION KINETICS

Sorption tests as a function of time (*kinetic tests*) allow evaluating the time needed to establish the equilibrium of the adsorbate between the solid and the liquid phase. These tests should be carried out first than any other, to make sure that the rest of tests are performed at the equilibrium. Experimentally, one can consider that the equilibrium is reached when the final adsorbate concentration in the liquid remains constant with time (within a variation of 5%). Kinetic tests are useful also to achieve additional information on the type of interactions occurring at the interface.

The most used approximations to represent batch sorption data as a function of time (t) are the pseudo-first order and the pseudo-second order equations (Azizian, 2004; Largitte & Pasquier, 2016).

The kinetic equation of pseudo-first order (in its linearized form) is the following:

$$\ln(C_e - C_t) = \ln(C_e) - k_1 \cdot t \quad \text{Equation 14}$$

C_e and C_t are the quantity of contaminant adsorbed at the equilibrium and at time t, respectively and k_1 (s^{-1}) is the velocity constant of pseudo-first order.

The kinetic equation of pseudo-second order (in its linearized form) is the following:

$$\frac{1}{C_t} = \frac{1}{k_2 \cdot C_e^2} + \frac{1}{C_e} \cdot t \quad \text{Equation 15}$$

k_2 is the velocity constant of pseudo-second order.

If a diffusive process is also involved in sorption, a temporal dependence of the contaminant may depend on the time square root. The kinetic equation is the following:

$$q_t = k_i \sqrt{t} + c \quad \text{Equation 16}$$

where k_i is the intra-particle diffusion constant.

5 TYPES OF ADSORPTION AND THERMODYNAMIC ASPECTS.

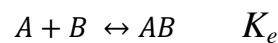
Sorption can be classified depending on the type of interactions occurring between adsorbent and adsorbate and the different resulting bonding energies. The *chemical adsorption, or chemisorption*, implies the transference of an electron between the adsorbent and the adsorbate, for example through the formation of a covalent bond (Langmuir, 1997). In chemisorption, the bonding energy may vary between 40 and 800 kJ·mol⁻¹; the higher the bond energy, the more difficult are desorption processes. In chemisorption, is not possible to form more than a monolayer of the adsorbate in the solid surface.

When electron exchange between the adsorbent and adsorbate does not exist, the adsorption process will be *physical adsorption, or physisorption*. Physisorption can be produced by van der Waals force, dipole-dipole or electrostatic interactions. The adsorption energy will be significantly less than in a chemical adsorption process (5 to 40 kJ/mol). For this reason, desorption processes will be significantly easier, in general physical adsorption is reversible, and the formation of adsorbate multilayer on the surface will be possible.

The estimation of thermodynamic parameters in adsorption processes is very important. In particular, to determine the standard Gibb's free energy (ΔG^0), enthalpy (ΔH^0) and entropy (ΔS^0) is of interest.

These parameters may help understanding if the adsorption (under the conditions of the experiment) is a process favourable or spontaneous, exothermic or endothermic. Besides, it is possible to infer the nature of the process (physisorption or chemisorption).

Let's consider a generic reaction between the adsorbent (A) and adsorbate (B), forming a complex AB with and equilibrium constant K_e .



When the reaction is at the equilibrium, the chemical potential in the liquid (μ_{LIQ}) and at the interface (μ_{INT}) are equal and the variation of the Gibb's free energy tends to zero:

$$\Delta G = \mu_{LIQ} - \mu_{INT} = 0 = \Delta G^0 + R \cdot T \cdot \log(K_e).$$

This implies that:

$$\Delta G^0 = - R \cdot T \cdot \log(K_e) = \Delta H^0 - T \cdot \Delta S^0$$

and:

$$\text{Log}(K_e) = \frac{-\Delta H^0}{RT} + \frac{\Delta S^0}{R} \quad \text{Equation 10b}$$

This equation (as well as Eq.11) indicates that the determination of equilibrium constant is an important point to study the thermodynamic of sorption processes.

Following Equation 10b, $\log(K_e)$ data can be plotted vs. $1/T$ (Van't Hoff plots) to estimate ΔH^0 and ΔS^0 values.

Negative values of ΔG^0 indicate that the process is spontaneous and favourable. The larger ΔG^0 value, the more favourable is the reaction. If ΔG^0 is negative and ΔH^0 contributes more than $T \cdot \Delta S^0$, the reaction is controlled by the enthalpy, otherwise it is controlled by entropy.

Negative values of ΔH^0 indicates an exothermic process, positive an endothermic one. The magnitude of ΔH^0 may give a hint on the adsorbent/adsorbate interactions: in physical adsorption the enthalpy is generally lower than 20 kJ/mol; electrostatic interactions may give values between 20 and 80 kJ/mol, whereas in chemical adsorption values between 80 and 450 kJ/mol can be reached (Bonilla-Petriciolet *et al.*, 2017).

Negative values of ΔS^0 indicates that upon the adsorption the disorder at the interface decreases. On the other hand, positive values suggest the existence of structural changes or surface re-adjustment caused by the formation of the adsorbent/adsorbate complexes.

6 SURFACE COMPLEXATION AND IONIC EXCHANGE.

The most relevant mechanisms that causes contaminant adsorption in solids are *surface complexation* and *ionic exchange*. The principal characteristics of these mechanisms will be briefly described below.

In adsorption processes, the solid surface charge is a critical parameter, because the affinity of an ion for a solid depends also on the sign and magnitude of the surface charge and on the resulting electrical potential.

In most common natural solids, two different types of charge exist: the variable and the permanent. The variable charge is typical in oxide minerals but can be also present in organic complexes with phenolic, alcoholic (=OH) or carboxylic (=COOH) functional groups.

In the oxide surface, functional groups (>S-, where the S indicates that they are on the solid surface) exist; they can be neutral or positively or negatively charged, depending on the electrolyte chemistry and fundamentally on its pH.

These surface sites (or surface functional groups) are able to adsorb/desorb protons and in a similar way they can form surface complexes with anions or cations. The ions that determines the surface charge in a solid are defined as *potential determining ions, PDI*. In variable charge solids, the surface charge is generated by a mechanism implying stoichiometric reactions between the surface functional groups (>SOH), with (OH⁻) and (H⁺) ions, which are the PDI.

The surface sites with negative charge are indicated as >SO⁻ and those with positive charge >SOH₂⁺. The reactions of protonation and deprotonation of the >SOH, are expressed in this form:



with the respective equilibrium constant, as will be detailed later.

The point of zero charge (**PZC**) is the pH in which the charge produced by the ions determining the potential is null (OH⁻=H⁺). This condition can be reached if none of the surface sites is ionized or when the positive and negative charge are compensated. The solid surface has a positive charge if pH<PZC and negative if pH>PZC. The PCZ is an important parameter to be experimentally determined.

The chemical conditions can modify the sign and magnitude of the surface charge and, in consequence, affect the interactions between solute ions and the solids.

Figure 11 shows the schematic of the interaction of a positively charged ion with the surface of a solid with variable charge.

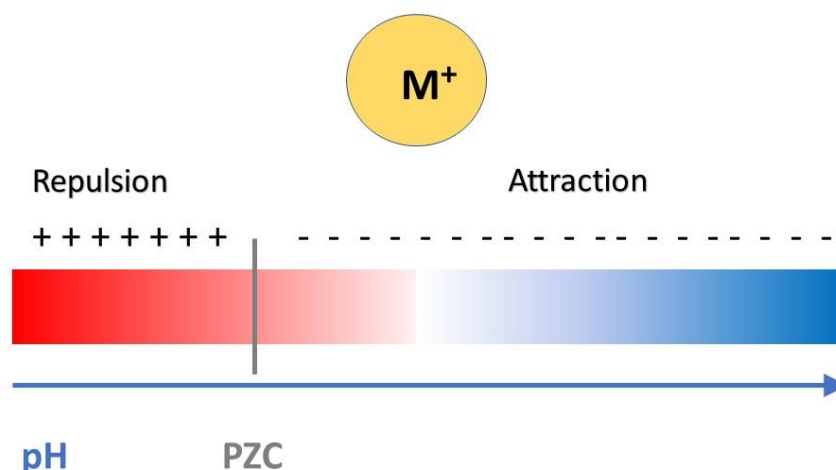


Figure 11. Schematic of the interaction of a positive ion with the surface of a solid of variable charge, depending on the pH of the solution.

For any pH before the PZC, the interaction between the cation and the surface will be hindered as both have positive charge and repulsion is expected; on the other hand, after the PZC the electrostatic attraction will favour the interaction and therefore the adsorption, as previously seen in Figure 2.

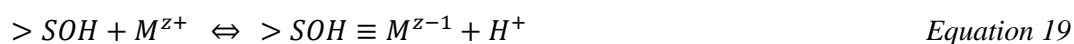
The permanent charge is a typical characteristic of the clays; it is produced by isomorphic substitutions in their layer structure (for example, in tetrahedral layers Si^{4+} is substituted by Al^{3+} and in octahedral layers Al^{3+} is substituted by divalent ions as Mg^{2+} or Fe^{2+}), which give rise to an excess of negative charge.

To compensate this excess of charge, in the solution nearest to the clay, surface positive ions are accumulated. These ions are easily exchangeable with other ions present in solution and the *cation exchange capacity*, CEC, of the solid represents the quantity of “sorbed” and exchangeable ions per unit mass of the solid and is usually expressed in $[\text{eq}\cdot\text{Kg}^{-1}]$ or $[\text{meq}/100\text{g}]$.

6.1 FORMATION OF SURFACE COMPLEXES

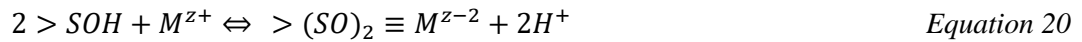
The surface functional groups ($>\text{SOH}$), apart from reacting with the IDP, are able to interact with other ions present in the solution. The chemical bonds between the adsorbable species present in solution and the surface sites lead to the formation of *surface complexes*.

In a very simplified form, we can consider that a cationic ion of valence z , M^{z+} , can form a surface complex by the displacement of the proton, following a reaction of the type:

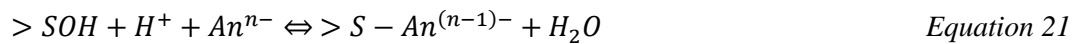


The equilibrium of the reaction, is determined by the *complexation constant*, K_M . The definition of the equilibrium constants in the frame of the surface complexation modelling will be detailed later.

The complex described by Eq.19, is of (1:1) type and is called *monodentate* surface complex. If the adsorption reaction occurs implying two surface sites (2:1) the complex will be defined as *bidentate* and the reaction will be expressed as:



If the adsorbate is an anion or any other ligand with negative charge (An^{n-}) the complexation reaction can be expressed as:



A surface complex can be an *inner sphere complex* if the adsorbate is directly bonded with the surface, in this case, we can suppose the existence of covalent chemical bonds and therefore *specific* adsorption.

An *outer sphere complex* is a complex where, at least, a water molecule is interposed between the solid surface and the ion. Outer sphere complexation has a character predominantly electrostatic and can be defined as *no specific*.

It is sometimes possible to identify the type of complex by spectroscopic techniques or obtain information by the analysis of macroscopic data (Manning *et al.*, 1998; Goldberg *et al.*, 2008; Sun *et al.*, 2014; Ding *et al.*, 2016). In batch experiments, the dependence of sorption with the ionic strength, can be an indication of inner/outer sphere complexation. In general, the ionic strength is important in outer sphere complexes and less relevant for inner sphere ones.

6.2 IONIC EXCHANGE

Ionic exchange is a very important adsorption mechanism and many technologies adopted it for the elimination of unwanted substances from the water. In this process, the ions present in the liquid phase are substituted by other existing in the solid surface, maintaining the same charge. Ionic exchange reactions are stoichiometric, rapid and reversible.

In industrial processes, different materials as ionic exchange resins are used. Ion exchange resins are polymeric materials with different surface functional groups that can be both anionic or cationic (sulphonic, $=SO_3^-$; carboxylic, $=COO^-$; amine, $=N(CH_3)_3^+$). These groups are initially neutralised with counter ions as H^+ , OH^- , Na^+ or Cl^- . When the resin is contacted with the solution with the adsorbate, the initial counterions are exchanged with those that must be eliminated.

Cationic exchange is the main mechanism of sorption in clays, which mainly present a permanent charge. Sorption by cation exchange does not present a dependence with pH, but significant dependence on ionic strength.

To facilitate the mechanistic studies of sorption in clays, these are initially exchanged with a monovalent ion, generally Na, to transform them in a homoionic form (Na-clay).

The ionic exchange reaction between a cation B, with valence z_B , present in the solution and the cation A, with valence z_A , on the solid surface ($\equiv S$) is defined by:



Using the mass law equation, it is possible to express the ion Exchange relation in terms of selectivity coefficient, K_{SEL} . According to Gaines and Thomas (1953), the selectivity coefficient between cations A and B is defined as:

$${}^B_A K_{SEL} = \frac{(N_B)^{z_A}}{(N_A)^{z_B}} \cdot \frac{(a_A)^{z_B}}{(a_B)^{z_A}} \quad \text{Equation 23}$$

where a_A y a_B are the activities of cations A and B, and N_A and N_B the fractions sites in the solid occupied by A and B, respectively.

The equivalent fraction occupied by a certain ion Y, N_Y , is the number of adsorbed equivalents per gram of solid, divided by the CEC of the solid: $N_Y = \frac{eq_{ads}/g_{solid}}{CEC}$

Selectivity coefficients can be determined through batch experiments, when the ionic exchange is the main sorption mechanisms.

Reminding the definition of distribution coefficient, it can be written as:

$$K_d = \frac{\text{adsorbed moles of B} / g_{solid}}{\text{moles of B in solution} / V} \text{ equivalent to } K_d = \frac{N_B(CEC)}{z_B} \frac{1}{(B)}$$

where (B) is the concentration of the cation B in mol per volume units. If B is present in trace concentration, the main electrolyte ion (A) will occupy practically all the sorption sites $N_A \approx 1$. Therefore:

$${}^B_A K_{SEL} = \frac{(N_B)^{z_A}}{(1)^{z_B}} \frac{(a_A)^{z_B}}{(a_B)^{z_A}} = \left(\frac{K_D z_B (B)}{CEC} \right)^{z_A} \frac{\gamma_A^{z_B}}{\gamma_B^{z_A}} \frac{(A)^{z_B}}{(B)^{z_B}} \quad \text{Equation 24}$$

where γ_A and γ_B are the activity coefficients. This equation simplified is:

$${}^B_A K_{SEL} = \left(\frac{K_D z_B}{CEC} \right)^{z_A} \frac{\gamma_A^{z_B}}{\gamma_B^{z_A}} (A)^{z_B} \quad \text{Equation 24b}$$

It has been mentioned that in an ionic exchange process the ionic strength plays an important role on retention. In fact, it is possible to show that the K_d of a cation B, in an electrolyte A, depend on A concentration according to this relation:

$$z_A \cdot \text{Log}(K_d) = -z_B \cdot \text{Log}(A) + \text{Log} \left(\frac{{}^B_A K_{SEL} \cdot (CEC)^{z_A} \cdot \gamma_B^{z_A}}{z_B^{z_A} \cdot \gamma_A^{z_B}} \right) \quad \text{Equation 25}$$

If the charge of the adsorbate ion, B, and the electrolyte ion, A, is the same, then $\text{Log}(K_d)$ depends linearly the logarithm of the concentration of A, $\text{Log}(A)$, and the slope of the straight line is -1.

If the ions that are exchanged have different charge, then the slope of the line is $-z_B/z_A$.

7 SOLUBILITY AND PRECIPITATION.

The *solubility* of contaminant species is one of the most important characteristics to consider for retention/migration studies. The solubility represents the capacity of a mineral of dissolving and defines the maximum possible concentration in the aqueous phase of the element composing it.

Let's consider a mineral AB, composed by the chemical element A and B and the respective activities, expressed as a_{AB} , a_A and a_B .

The constant of solubility product, K_{sp} , of the relation ($AB \leftrightarrow A+B$) at the equilibrium, is defined as:

$$K_{sp} = \frac{a_A \cdot a_B}{a_{AB}} \quad \text{Equation 26}$$

The smallest is the value of K_{sp} , the less soluble the mineral is. For example, barite ($BaSO_4$), which is a barely soluble mineral, has a constant of solubility products of $1.1 \cdot 10^{-10}$, whereas the K_{sp} of gypsum ($CaSO_4$), significantly more soluble, is $2.4 \cdot 10^{-5}$.

The K_{sp} is needed to know whether, in a certain solution, a mineral is precipitating or dissolving. In an aqueous phase the activities (not necessarily at the equilibrium) a_A , a_B and a_{AB} can be measured to calculate the ionic activity product, **IAP**, which is formally defined exactly as Equation 26.

The saturation index, **SI**, is the logarithm of the ratio between the ionic activity product and the constant of solubility product ($SI = \log(IAP/K_{sp})$); this parameter indicates if a mineral to reach the equilibrium will precipitate or dissolve.

Basically, if $SI=0$, the system is in equilibrium, nothing precipitates or dissolves; if $SI<0$ the system is under-saturated, and the mineral is dissolving; if $SI>0$ the system is over-saturated, and precipitation is occurring.

In general, the precipitation of a contaminant within a solid (non-colloidal) phase is favourable from an environmental point of view, because limits the occurrence in the aqueous phase and its transport.

The solubility limit is a very important parameter for the safety assessment of radioactive waste repositories. The chemical conditions provided by the engineered barriers must favour the conditions in which radionuclides have minimum solubility. Cementitious materials for example, generates hyperalkaline conditions which favour the precipitation of contaminants and their overall retention.

Surface precipitation or co-precipitation processes may occur at the solid-solution interface (Ford *et al.*, 2001). These may represent a very effective retention process, often not reversible.

Surface precipitation can be produced or favoured by mechanisms of different nature. The properties of the adsorbate may suffer changes induced by the characteristics of the surface (for example redox effects) which facilitate retention; it is also possible that the aqueous phase nearest to the surface is different from that of the *bulk* solution and that this different chemistry influences the solubility of some species. Finally, because of the existence of unpaired ions, in the proximity of the surface, an excess of free energy may exist which can cause a local decreasing of solubility limits.

All these mechanisms may coexist, and their relative importance depends on the electrostatic properties of the systems, the stability of the solid surface and the physicochemical properties of the adsorbate.

Sometimes, it is not easy to distinguish sorption from processes like surface precipitation; some hint may be derived from macroscopic evidences, as for example the change on electrophoretic properties, caused by the formation of new solid species at the surface, or the sharp changes in the slope of adsorption isotherms.

In particular, in the isotherms expressed in their Log-Log form, slopes higher than 1 can be the indication of precipitation. Furthermore, if the formation of a solid solution or precipitate occurs at the solid surface, is possible to obtain quantity of adsorbed material (apparently) higher than the maximum capacity of the solid.

The use of spectroscopic technique is recommended to analyse the speciation of the contaminant and differentiate surface precipitates from adsorbed species (Roberts *et al.*, 2017).

Precipitation process must be included in the geochemical modelling for the overall estimation of retention.

8 SURFACE COMPLEXATION MODELS, SCM

The study of the adsorption based only on semi-empirical parameters, like the distribution coefficients or sorption isotherms models, often is not enough to gather a real knowledge of the processes occurring at the solid/solution interface.

The exclusive application of this type of approximations does not allow describing sorption processes in natural materials, where the chemistry is complex and where different types of sorption sites or sorption mechanisms may exist, as well as spatial and temporal variability. The distribution coefficient or the parameters obtained from the isotherms are valid only for the conditions in which the specific test has been performed, and they cannot be extrapolated to others being predictive.

A possible alternative for the analysis of sorption data, is the mechanistic approach through the application of *surface complexation models, SCMs*.

SCMs were proposed at the beginning of the '70s and their main objective was to analyse sorption process through a chemical, physical and thermodynamic description of the liquid / solid interface, based on the theory of the *electrical double layer EDL*.

The main advantage of SCMs is that they may be able to predict contaminant behaviour in the system if the characteristic of the medium (pH, ionic strength or solute species) vary. A SCM explicitly accounts for the surface charge in the solid, including protonation and deprotonation reactions (Equations 17 and 18) and charge and mass balances. To describe sorption in a SCM a set of chemical reactions is established, with the corresponding equilibrium constants describing the complexes between ions and the surface.

Despite their limitations and some criticisable aspects, SCMs represent a significant improvement over the empirical sorption models, as the complexation constants derived are less system dependent than K_d values or the parameters obtained from sorption isotherms.

Different types of SCMs have been proposed during the years and the main differences between them arise on the initial description of solid liquid interface, the EDL, with specific constraints and consequently on the electrostatic corrections to be applied.

All the models are built on the following principles:

- At the surface of the solids, functional groups that can react with the ionic species of the solution exist. These groups can form surface complex in an analogue way to the formation of aqueous complexes.
- The surface charge is determined by all the possible reactions occurring with the surface groups (protonation/deprotonation; ion-pair formation; complex formation).

- The equilibria of the surface complexation reactions are described through mass action laws and applying the appropriate electrostatic corrections, based on the double layer theory.
- The apparent complexation constants are empirical parameters, related to the thermodynamic constants through the activity of surface species.

The selection of a model or another for the description of the experimental data is arbitrary. Westall & Hohl (1980) showed that it is possible to find a set of parameters able to fit reasonably well the experimental data, using any of the surface complexation model.

The determined parameters are different, depending on the model adopted for the fit and the direct comparison of results obtained by different authors might lead to incorrect conclusions. Apart from the final adjustment of data and its (apparent) precision, it is always necessary to evaluate the physical meaning of the results of the modelling.

The mathematic problem may have more than one possible solution and dependence on the initial parameters that should be evaluated by an expert judgement.

The hypotheses on the surface complexes must be reasonable; to increase the number of equations (and consequently the parameters of adjustment), may improve the fit, but not necessarily provide a more correct and realistic description of the involved processes. In any step of the modelling process the decisions taken must be defensible and documented (Payne et al, 2013).

Finally, it is important to place in value the experimental work. It is impossible to develop a good model on scarce or imprecise experimental data. Feedback should always exist between experiment and modelling and both activities should never be considered as independent tasks.

Anytime that doubts arise, or new hypotheses are posed, additional tests should be done to confute o refuse them. Furthermore, the application of models and the use of geochemical code may help designing experimental tests in optimal conditions.

In the next paragraph, the basic concepts of the electrical double layer will be briefly summarised as well as the most important complexation models based on this theory.

8.1 ELECTRICAL DOUBLE LAYER, EDL

As already mentioned, most of the solids dispersed in a liquid phase (clays, oxy-hydroxides, carbonates, ...) present electrically charged surfaces. To counterbalance the surface charge, ions of opposite sign (counter-ions) tend to accumulate in the liquid nearest the surface.

For this reason, the interface between the solid and the bulk fluid is called *electrical double layer*, EDL. A simplified sketch of the EDL is shown in Figure 12. The first description of the

EDL comes from Gouy (1910) and Chapman (1913), but it has been modified and corrected over the years, with a special contribution by Stern and Grahame.

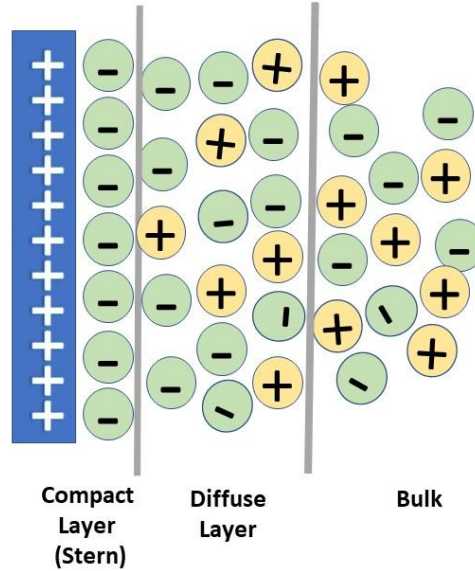


Figure 12: Simplified sketch of the electrical double layer, EDL, at the solid – water interface.

As can be seen in Figure 12, the counterion concentration near the solid surface is very high, and these form a quite compact layer. This region is called Stern layer (or inner Helmholtz layer) where the ions are relatively immobile.

In the external layer (or diffuse layer), ions suffer electrostatic interaction with the surface, but they can still shift by thermal movement. Within this layer, the excess of counterions decreases with the distance from the charged surface in an exponential way, following a Maxwell-Boltzmann distribution. In the bulk of the solution, the concentration of negative and positive ions is equivalent.

The relation between the density of charge in the diffuse layer (σ_d , $C \cdot m^{-2}$) and the potential (Ψ_d , V), is obtained by solving the Poisson-Boltzmann equation, with the appropriate boundary conditions:

$$\nabla^2 \Psi = \frac{-\rho}{\epsilon_r \epsilon_0} \quad \text{Equation 27}$$

where ρ is the volumetric density of charge ($C \cdot m^{-3}$), ϵ_r is the relative permittivity of the solution, and ϵ_0 the permittivity of the free space.

The solution of Equation 27 for a monovalent electrolyte of a ionic strength I ($mol \cdot L^{-1}$) is:

$$\sigma_d = -\sqrt{8\epsilon\epsilon_0RTI} \cdot \sinh\left(\frac{F\Psi_d}{2RT}\right) = -\sqrt{8\epsilon\epsilon_0RTI} \cdot \sinh\left(\frac{e\Psi_d}{2k_B T}\right) \quad \text{Equation 28}$$

where e is the electron charge k_B the Boltzmann constant, T the absolute temperature, F the Faraday constant and R the gas constant.

In an aqueous solution at 25 °C, the term $\sqrt{8\varepsilon\varepsilon_0RTI}$ can be simplified to $0.1174\sqrt{I}$ being the surface charge density expressed in $C\cdot m^{-2}$.

The general equation for an electrolyte at 25 °C is:

$$\sigma_0 = -\sigma_d = 0.1174\sqrt{I} \cdot \sinh\left(\frac{zF\Psi_d}{2RT}\right) \quad \text{Equation 28b}$$

Another interesting parameter for the description of the solid-liquid interface is the thickness of the double layer ($1/\kappa$), or *Debye length*, that can be expressed as:

$$\kappa^{-1} = \sqrt{\frac{\varepsilon_0\varepsilon_r k_B T}{2 \cdot 1000 \cdot N_A \cdot e^2 \cdot I}} \quad \text{Equation 29}$$

For a symmetrical monovalent electrolyte, Equation 29 is: $\kappa^{-1} = \sqrt{\frac{\varepsilon_0\varepsilon_r R \cdot T}{2 \cdot 1000 \cdot F^2 \cdot I}}$. This formula, can be simplified for an aqueous solution at a 25 °C being:

$$\kappa^{-1}(nm) = \frac{0.304}{\sqrt{I}} \quad \text{Equation 29b}$$

Equation 29 indicates that the ionic strength of the electrolyte plays an important role on the double layer structure. The thickness of the double layer and therefore the space affected by the presence of an electrical potential depends, in fact, on the ionic strength.

8.2 REACTION CONSTANTS IN THE EDL

If the interactions of the ions with the solid are influenced only by electrostatic forces, which maintains the counterions near the surface, these interactions can be defined as *non-specific*. The ions interacting with the solid surface only by electrostatic forces are called *inert*.

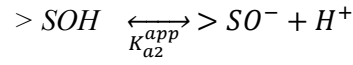
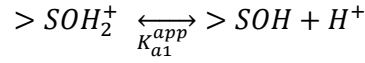
Nevertheless, in adsorption processes, apart from the electrostatic forces, chemical forces can be present. These lead to the formation of surface complexes between aqueous ions/molecules and the surface functional groups. In that case the interactions can be defined *specific* and the ions as *specifically adsorbable*.

In surface complexation reactions, the equilibria are described with law mass reactions similarly to complex formation in the aqueous phase; however, the existence of an electrical potential, which influences the solid/solution interface, implies corrections to these equations.

The concentration of any ion n (with charge, z) in any point x of the interface is determined by the Maxwell-Boltzmann distribution, then:

$$n(x) = n_{bulk} \cdot \exp\left(\frac{-zF\Psi(x)}{RT}\right) = n_{bulk} \cdot \exp\left(\frac{-ze\Psi(x)}{k_B T}\right) \quad \text{Equation 30}$$

Considering the basic equations to define the surface charge of the solid (Eq. 17 and 18):



their reaction quotients or *apparent* reaction constant will be K_{a1}^{app} y K_{a2}^{app} :

$$K_{a1}^{app} = \frac{[>SOH][H^+]}{[>SOH_2^+]} \quad \text{Equation 17b}$$

$$K_{a2}^{app} = \frac{[>SO^-][H^+]}{[>SOH]} \quad \text{Equation 18b}$$

Accounting for Equation 31, the concentration of protons in the interface is not always equal to that of the bulk solution (where pH is measured) because, in fact, any ion in the solute presents a Maxwell-Boltzmann distribution.

Thus, the expression for proton concentration in the interface is:

$$[H^+]_x = [H^+]_{bulk} \cdot \exp\left(\frac{-F\Psi(x)}{RT}\right) = [H^+]_{bulk} \cdot \exp\left(\frac{-e\Psi(x)}{kT}\right) \quad \text{Equation 30b}$$

This means that in the EDL, the apparent constants include a Coulombic term, which accounts for the effects produced by the surface potential.

For any constant we will have:

$$K^{app} = K^{int} \cdot \exp\left(\frac{e\Psi}{k_{BT}}\right) \quad \text{or} \quad K^{int} = K^{app} \cdot \exp\left(-\frac{e\Psi}{k_{BT}}\right) \quad \text{Equation 31}$$

The exponential term represents the conversion factor between the concentration in the solution and the concentration in the interface, supposing that the ion distribution obeys the Maxwell-Boltzmann statistics and that the free energy of the ions only depends on the electrical potential Ψ .

In the general case of a surface complexation reaction, considering as an example the Equation 19:



The complexation constant K_M , can be written as:

$$K_M(app) = \frac{\{>SO \equiv M^{z-1}\}[H^+]}{\{SOH\}[M^{z+}]} \exp\left(\frac{(z-1) \cdot e \cdot \Psi}{k_B \cdot T}\right) \quad \text{Equation 19b}$$

This basically means that in an adsorption process, the total free energy $\Delta G^0 = -R T \ln K$ takes into account two parts: the first one corresponding to the chemical contribution (ΔG_{INT}^0) and the second one accounting for the effects of the surface potential (ΔG_{COUL}^0). Therefore:

$$\Delta G_{APP}^0 = \Delta G_{INT}^0 + \Delta G_{COUL}^0 \quad \text{and} \quad -RT \ln K_{APP} = -RT \ln K_{INT} + z F \Psi_0$$

The models that considers this term of electrostatic correction, are called electrostatic models. Nevertheless, *non-electrostatic* models also exist, where this correction is neglected.

Neglecting the Coulombic term, means that the chemical contribution to the free energy is dominant in relation to the electrical contribution. These models have been widely used in the literature for the analysis of sorption data, due to their simplicity (Bradbury and Baeyens, 1997; Missana *et al.*, 2009).

Different types of SCMs, based in the EDL exist: the most used are the constant capacitance (CC) model; the diffuse double layer (DDL) model and the triple layer (TL) model. The main difference between the different models lies on the description of the EDL, the location of adsorbed ions and the equations describing the potential.

In all the cases, the surface potential is assumed to be null in the bulk solution. The ions determining the potential as H^+ and OH^- , are adsorbed at the solid surface (plane 0).

8.3 CONSTANT CAPACITY MODEL (CC)

The constant capacity (CC) model (Hohl & Stumm, 1976; Sposito, 1983), is based on the simplest description of the solid-solution interface.

Figure 13 shows the schematic of the interface described in the CC model and the behaviour of the electrical potential as a function of the distance from the solid surface.

In the CC model, the double layer is assimilated to a flat capacitor and the constant of proportionality between the charge and the potential is the capacitance of the double layer (C), thus the relation between the surface electrical potential Ψ_0 and the surface charge σ_0 is:

$$\Psi_0 = \frac{\sigma_0}{C} \quad \text{Equation 32}$$

If d is assumed as the distances between the two capacitor plates, C can be expressed as:

$$C = \frac{\varepsilon_0 \cdot \varepsilon_r}{d} \text{ or, considering the thickness of the double layer, } C = \varepsilon_0 \cdot \varepsilon_r \cdot \kappa.$$

In the CC model, all the formed complexes are inner sphere (only exist the possibility of forming complexes at the plane of the surface, plane 0) and all the ions are subject to the same potential. The ions of the electrolyte are considered as inert.

The main drawback of this model is that is not able to account for the variation that may occur with the ionic strength. If different data sets are collected for different ionic strengths, the model parameters must be calculated for any ionic strength. Furthermore, this model can be applied only at ionic strengths high enough (≥ 0.1 M), which is the condition needed to assume that the electrical potential is linear in the interface.

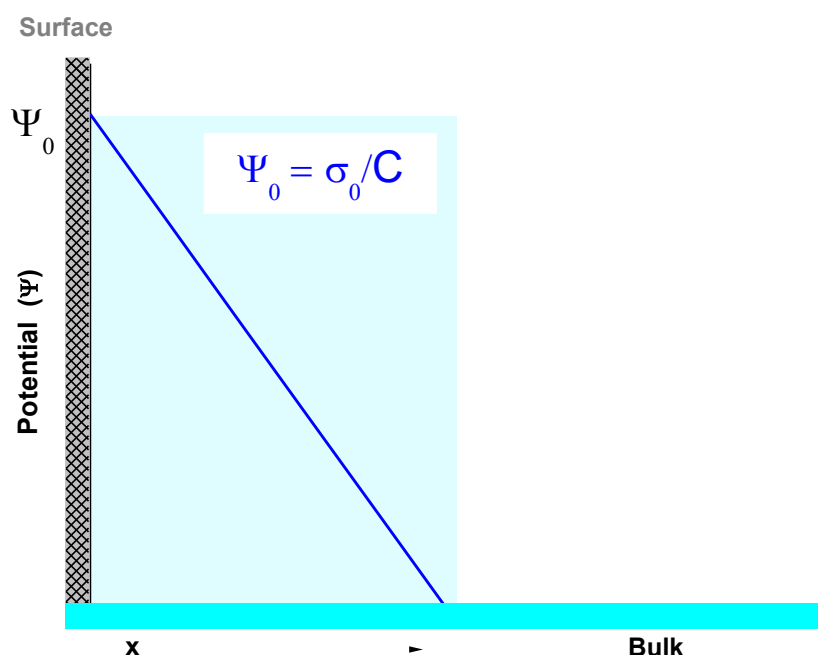


Figure 13. Electrical potential as a function of the distance from the solid surface in the constant capacitance, CC, model.

The main reactions and parameters needed to describe the surface of a solid, for the CC model are summarised in

Table 1. This model has four adjustable parameters. It is necessary to determine the protonation and deprotonation constants K_{a1} and K_{a2} that can be determined by potentiometric titration experiments with the surface charge, σ_0 .

The net charge of the solid is represented by the difference between positively and negatively charged sites. In a titration experiment the charge is initially expressed in $\text{mol}\cdot\text{L}^{-1}$:

$$\sigma_0^* = [\text{SOH}_2^+] - [\text{SO}^-] \quad \text{Equation 33}$$

The conversion factor, B, between $[\text{mol}\cdot\text{L}^{-1}]$ and $[\text{C}\cdot\text{m}^{-2}]$ to obtain the surface charge density σ_0 , is: $B = \frac{F}{S \cdot S_A}$.

The third parameter that must be determined is the quantity of surface sites, N_s , which is the sum of the neutral surface functional groups and the positively/negatively charged:

$$N_s = [\text{SOH}] + [\text{SOH}_2^+] + [\text{SO}^-]. \quad \text{Equation 34}$$

The number (o density) of surface sites, represents an intrinsic characteristic of the solid and can be experimentally measured; it can be expressed in different units ($[\text{sites}]$, $[\text{mol}\cdot\text{L}^{-1}]$, $[\text{mol}\cdot\text{g}^{-1}]$, $[\text{mol}\cdot\text{m}^{-2}]$), using the appropriate conversion factors.

Reaction	K(app)	K(intr)
$SOH_2^+ \leftrightarrow SOH + H^+$	$K_{a1} = \frac{\{SOH\}[H^+]}{\{SOH_2^+\}}$	$K_{a1}^{intr} = K_{a1} \cdot \exp\left(-\frac{e \cdot \Psi_0}{k_B \cdot T}\right)$
$SOH \leftrightarrow SO^- + H^+$	$K_{a2} = \frac{\{SO^-\}[H^+]}{\{SOH\}}$	$K_{a2}^{intr} = K_{a2} \cdot \exp\left(-\frac{e \cdot \Psi_0}{k_B \cdot T}\right)$
Charge in the plane 0, σ_0	$\sigma_0 = B \cdot ([SOH_2^+] - [SO^-])$	
Charge-Potential relation	$\Psi_0 = \frac{\sigma_0}{C}$	
Capacitance, C	$C = \frac{\sigma_0}{\Psi_0}$	
Surface sites balance	$N_s = [SOH] + [SO^-] + [SOH_2^+]$	
Fit parameters	K_{a1}, K_{a2}, N_s, C	
Comments	The application of the model is limited to ionic strength relatively high (0.1 M). For any of the studied ionic strengths the corresponding parameters will be calculated.	

Table 1. Reactions and parameters needed to define the solid surface with the constant capacity, CC, model.

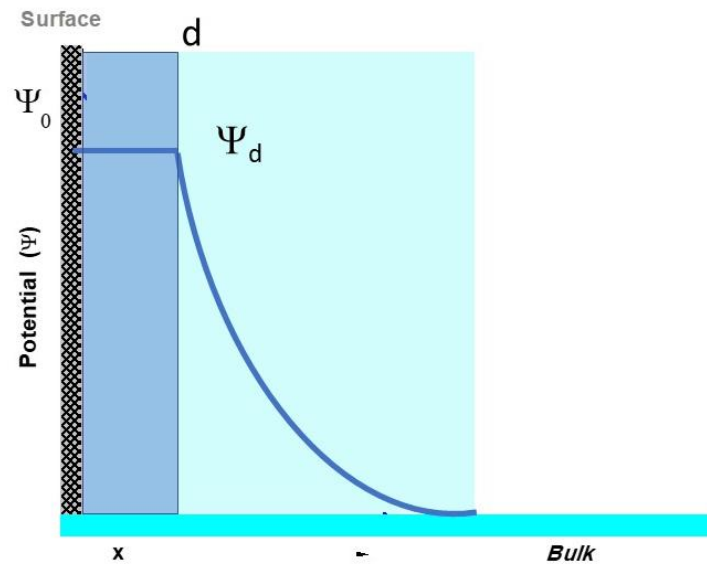


Figure 14. Electrical potential as a function of the distance from the solid surface in the diffuse double layer, DDL, model.

The last parameter needed to describe the solid-solution interface with the CC model is the capacitance, C. In most cases, this parameter is considered as a fit parameter, because the its experimental determination is not straightforward.

Finally, all the equation related to the surface complex formation (Equations 19, 20, and 21) will give rise to the *complexation constants*. In practices, these constants are also determined as fit parameters.

Despite this is a very simplified model, it has been widely used in the determination of Surface complexation constants of metals at a trace concentration in different solids (Goldberg & Sposito, 1984).

8.4 DIFFUSE DOUBLE LAYER MODEL (DDL)

The diffuse double layer, DDL, model (Stumm *et al.*, 1976; Huang & Stumm, 1973), is most probably the most used SCM. A very relevant book on the application of DDL on iron oxides is the one written by Dzombak and Morel (1990).

Figure 14 represents the interface described by the DDL model indicating the behaviour of the electrical potential as a function of the distance from the solid surface. This model supposes the existence of a compact region near the surface (it can be formally considered equivalent to the Stern layer) where the electrical potential is constant. This region is delimited by the plane 0 and the plane *d*, where adsorption occur. The potential in the plane *d*, Ψ_d , where the diffuse layer starts is equal to the surface potential Ψ_0 .

In the region external to the plane *d*, the potential decreases exponentially. The relation charge – potential is described by the Gouy Chapman theory (Equation 29):

$$\sigma_d = -\sqrt{8\varepsilon\varepsilon_0RTI} \cdot \sinh\left(\frac{F\Psi_d}{2RT}\right).$$

To maintain the electroneutrality of the system the condition $\sigma_0 + \sigma_d = 0$ must be valid;

thus: $\sigma_0 = -\sigma_d$.

The main reactions and parameters needed to describe the solid surface with the DDL model are summarised in Table 2. This model has three adjustable parameters, K_{a1} , K_{a2} and N_s .

As in the CC model, the total number of surface sites, N_s , is the sum of the neutral surface functional groups and the positively/negatively charged ones.

In the DDL model, as in CC model, all the surface complexes are inner sphere complexes and all the ions are adsorbed at the plane (*d*). The rest of the ions remain in the diffuse layer.

The CC model is a special case of the DDL model. Both consider a single adsorption plane, and in both cases the electrolyte ions cannot be specifically adsorbed. At high ionic strengths (when CC model can be applied), the electrical double layer is shrunk, and the electrical potential can be approximated to a linear function

Reactions	K(app)	K(intr)
$SOH_2^+ \leftrightarrow SOH + H^+$	$K_{a1} = \frac{\{SOH\}[H^+]}{\{SOH_2^+\}}$	$K_{a1}^{intr} = K_{a1} \cdot \exp\left(-\frac{e \cdot \Psi_0}{k_B \cdot T}\right)$
$SOH \leftrightarrow SO^- + H^+$	$K_{a2} = \frac{\{SO^-\}[H^+]}{\{SOH\}}$	$K_{a2}^{intr} = K_{a2} \cdot \exp\left(-\frac{e \cdot \Psi_0}{k_B \cdot T}\right)$
Charge in the plane 0, σ_0	$\sigma_0 = B \cdot ([SOH_2^+] - [SO^-])$	
Charge-Potential relation	$\sigma_d = -\sqrt{8\varepsilon\varepsilon_0RTI} \cdot \sinh\left(\frac{F \Psi_d}{2RT}\right)$	
Electroneutrality	$\sigma_0 + \sigma_d = 0$	
Surface sites balance	$N_s = [SOH] + [SO^-] + [SOH_2^+]$	
Fit parameters	K_{a1}, K_{a2}, N_s	

Table 2. Reactions and parameters needed to define the solid surface with the diffuse double layer, DDL, model.

In the DDL model, the dependence of sorption with the ionic strength should be accounted for by the surface charge dependence on (I), as indicated by the Gouy-Chapman equation. In principle, no restrictions for the ionic strength, must be considered. Therefore, a single set of parameters should be valid for any considered ionic strength.

8.5 TRIPLE LAYER MODEL (TL)

The previously described models consider the existence of a unique adsorption plane and the formed complexes can be only inner-sphere complexes.

If only a single adsorption plane exists all the ions are subject to the same potential, thus according to this description, is not possible differentiating complexes having different bond strength. Furthermore, both in CC and in DDL models, the ions of the electrolyte are considered as inert.

For these reasons, more complex models were developed to describe the solid-solution interface (Davis & Leckie, 1978 a, b; Davis *et al.*, 1978; Blesa & Kallay, 1988; Hayes & Leckie, 1987).

In its description of the solid-solution interface, the triple layer, TL, model, includes two additional planes where adsorption can take place. In this model, the adsorption of the electrolyte ions can be considered and, in consequence, possible difference in adsorption processes caused by the background electrolyte can be evidenced (Yates & Healy, 1980).

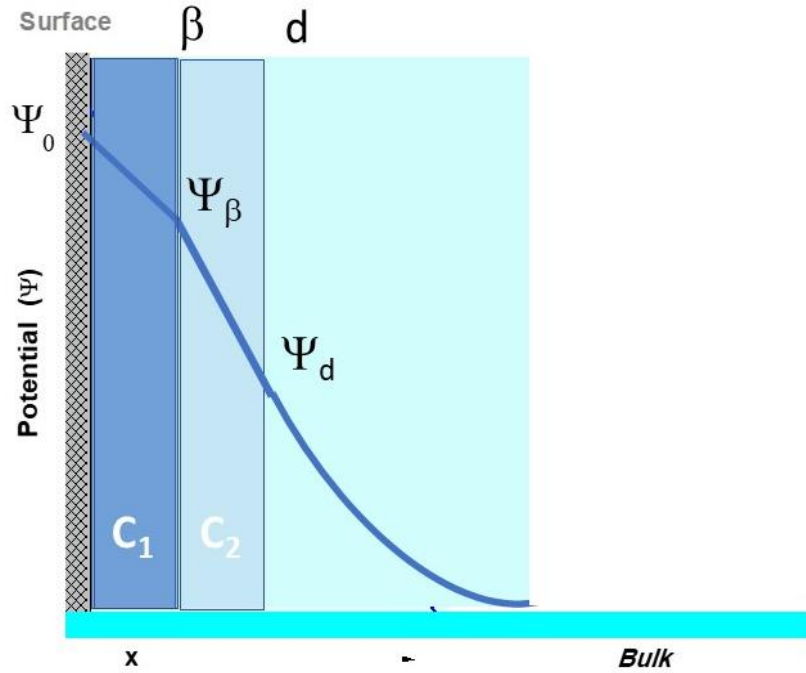


Figure 15. Electrical potential as a function of the distance from the solid surface in the Triple Layer Model

In Figure 15, the structure of the interface according to the TL model and the behaviour of the potential as a function of the distance from the solid surface, can be seen. Three different planes can be distinguished: plane (0) corresponding to the solid surface and two other planes, plane β and plane d , where the diffuse layer starts.

In the TL model, the different ions present in the solution can have different locations in the interface. The ions H^+ and OH^- (IDP) form inner sphere complexes in the plane 0, but the adsorption of any other ion can lead to inner or outer sphere complexation in the plane 0 or β , respectively. Likewise, the electrolyte ions (for example, $NaClO_4$) can be adsorbed in the plane β at a potential Ψ_β .

The surface interactions depend on both the potential Ψ_0 and Ψ_β , being the electrostatic correction dependent on the adsorption plane.

For the ions adsorbed in the plane 0, for example protons, we will have:

$$[H^+]_0 = [H^+]_{bulk} \cdot \exp\left(\frac{-e\Psi_0}{kT}\right)$$

and for other ions adsorbed in the plane β :

$$[Y^+]_0 = [Y^+]_{bulk} \cdot \exp\left(\frac{-e\Psi_\beta}{kT}\right)$$

Between the plane 0 and the plane β (inner Helmholtz layer) and between the plane β and the plane d (outer Helmholtz layer), the difference of the electrical potential depends linearly on

the distance from the surface. This is equivalent to two capacitors with capacitances of C_1 and C_2 , respectively.

The main reactions and parameters needed to describe the solid surface by the TL model are summarised in Table 3. This model is more complex than the previous ones, and this implies a higher number of adjustable parameters (7): K_{a1} , K_{a2} , K_{Y+} , K_{X-} , N_s , C_1 , C_2 .

Unlike the CC and DDL models, for the TL model, to determine the surface charge it is necessary to consider positively and negatively charged surface sites and those coordinated with the electrolyte ions:

$$\sigma_0 = B \cdot ([SOH_2^+] + [SOH_2X] - [SO^-] - [SOY]) \quad \text{Equation 35}$$

In the plane β , the charge is determined by the difference between surface sites coordinated with the positive and negative ions of the electrolyte (Table 3):

$$\sigma_\beta = B \cdot ([SOY] - [SOH_2X]) \quad \text{Equation 36}$$

Finally, in the TL model, the number of sites is:

$$N_s = [SOH] + [SO^-] + [SOH_2^+] + [SOY] + [SOH_2X] \quad \text{Equation 37}$$

Specific parameters for this model are the two capacitance C_1 and C_2 and K_{Y+} , K_{X-} ,

It is not straightforward to experimentally determine the values of the capacitances, which are often considered as fit parameters, even if it is generally accepted that the capacitance C_2 takes the value of $0.2 \text{ F}\cdot\text{m}^{-2}$.

To determine K_{Y+} , K_{X-} , numerical methods are frequently used even if in the past, double graphical extrapolations (Righetto *et al.*, 1995) were described. In any case, the unique use of potentiometric titrations to derive all the model parameters may lead to problems (Koopal *et al.*, 1987).

The TC model gives a more detailed representation of the solid -liquid interface with respect to the previously described models, with a unique adsorption plane, but its main drawback is the high number of parameters, many of them are often determined by numerical optimisation. Unfortunately, sometimes it is difficult to affirm that the improvement observed in data fit is due to the better physical description or to the increased fit parameters. In this sense, the need of encountering additional information, to decrease the number of fit parameters or defending the selection of parameters, opens a very interesting research field.

Sahai and Sverjensky (1996, 1997 a and b) proposed estimating the parameters of the TL model using independent information and analysed a large quantity of data of different solids, suspended in various electrolytes. They suggested to measure the quantity of surface sites, N_s , by the tritium exchange technique and not using the potentiometric titrations. From the potentiometric titrations they used only the value for the point of zero charge, whereas for the determination of $\Delta pK_{a1,2}$, they used a method based on the Born solvation theory previously

proposed by James and Healy (1972) and the electrostatic theory by Parks (1965). Finally, they suggested fixing the capacitance of the external layer, C_2 in $0.2 \text{ F}\cdot\text{m}^{-2}$. With this methodology, they obtain a reduction of the number of fit parameters to three (C_1 , K_{X^-} y K_{Y^+}) improving the reliability of determination of parameters from numerical optimisation.

Reactions	K(app)	K(intr)
$SOH_2^+ \leftrightarrow SOH + H^+$	$K_{a1} = \frac{\{SOH\}[H^+]}{\{SOH_2^+\}}$	$K_{a1}^{intr} = K_{a1} \cdot \exp\left(-\frac{e \cdot \Psi_0}{k_B \cdot T}\right)$
$SOH \leftrightarrow SO^- + H^+$	$K_{a2} = \frac{\{SO^-\}[H^+]}{\{SOH\}}$	$K_{a2}^{intr} = K_{a2} \cdot \exp\left(-\frac{e \cdot \Psi_0}{k_B \cdot T}\right)$
$SOH_2X \leftrightarrow SOH + H^+ + X^-$	$K_{X^-} = \frac{\{SOH\}[X^-][H^+]}{\{SOH_2X\}}$	$K_{X^-}^{intr} = K_{X^-} \cdot \exp\left(-\frac{e \cdot (\Psi_\beta - \Psi_0)}{k_B \cdot T}\right)$
$SOH + Y^+ \leftrightarrow SOY + H^+$	$K_{Y^+} = \frac{\{SOY\}[H^+]}{\{SOH\}[Y^+]}$	$K_{Y^+}^{intr} = K_{Y^+} \cdot \exp\left(-\frac{e \cdot (\Psi_\beta - \Psi_0)}{k_B \cdot T}\right)$
Charge in plane 0, σ_0	$\sigma_0 = B \cdot ([SOH_2^+] + [SOH_2X] - [SO^-] - [SOY])$	
Charge in plane β, σ_β	$\sigma_\beta = B \cdot ([SOY] - [SOH_2X])$	
Charge in the diffuse layer	$\sigma_d = -\sqrt{8\varepsilon\varepsilon_0RTI} \cdot \sinh\left(\frac{F \Psi_d}{2RT}\right)$	
Electroneutrality	$\sigma_0 + \sigma_\beta + \sigma_d = 0$	
Capacitance (between plane 0 y β), C_1	$C_1 = \frac{\sigma_0}{\Psi_0 - \Psi_\beta}$	
Capacitance (between plane β y d), C_2	$C_2 = \frac{\sigma_d}{\Psi_d - \Psi_\beta}$	
Surface sites balance	$N_s = [SOH] + [SO^-] + [SOH_2^+] + [SOY] + [SOH_2X]$	
Fit Parameters	$K_{a1}, K_{a2}, K_{Y^+}, K_{X^-}, N_s, C_1, C_2$	
Comments	The value of the C_2 capacitance is often fixed to $0.2 \text{ F}\cdot\text{m}^{-2}$	

Table 3. Reactions and parameters needed to define the solid surface with Triple Layer Model

The TL model has often been applied for the analysis of sorption studies in several different types of minerals (Hsi & Langmuir, 1985; Zachara *et al.*, 1987; Zhang & Sparks, 1990; Villalobos & Leckie, 2001; Zhang *et al.*, 2004; Goldberg, 2013; Sun *et al.*, 2014). James and Parks (1982) analysed the application of the TL model to clayey materials. The TC model has been recently used to describe the surface properties of smectites (Leroy & Revil (2004); Leroy *et al.*, 2015).

8.6 OTHER MODELS

8.6.1 CD-MUSIC MODEL

The CD-MUSIC model (Hiemstra *et al.*, 1989 a and b, Hiemstra & van Riemsdijk, 1996) represents an alternative approximation to the classic surface complexation models and combines the thermodynamic and electrostatic description with structural and crystallographic information.

The model is based in a description of the electrical double layer with three planes, similar to that of TL model: the plane of the surface (0 plane), plane 1 and plane 2 which delimitate the Helmholtz layers and the diffuse layer.

However, important differences to the previously described models exist, especially in respect to the definition of the acid base properties of surface sites, the location of ions and the charge distribution (Tadanier & Eick, 2002).

The reactivity of surface sites can be determined, starting from mineralogical and spectroscopic analyses. Their reactivity varies depending the crystalline structure of the minerals and on the surrounding ions, that establish the coordination environment. In the specific case of a goethite, sketched in Figure 16, the hydroxyls groups, can be coordinated with iron (Fe^{3+}) through their oxygen in three different ways: by single, double or triple coordination.

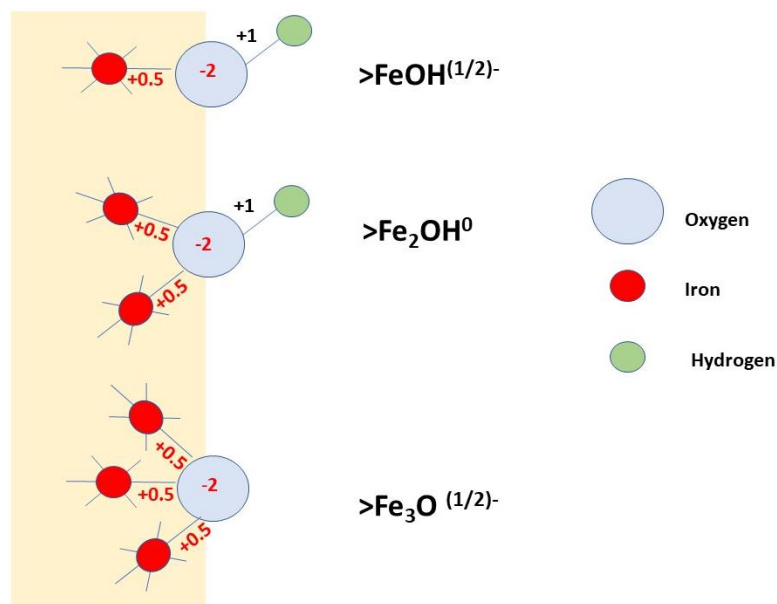


Figure 16. Charge of the surface functional groups coordinated in a simple, double and triple way in a goethite, following Pauling's rules. Iron is coordinated in a octahedral form (Figure modified from Tadaniek & Eick, (2001)

To maintain the electroneutrality of the system it is necessary that the charge of the cation (Fe) is balanced by the oxygens. Applying the Pauling's rules to the structure of the goethite, surface site may result with a non-entire charge.

In fact, three different groups can exist: $>FeOH^{1/2-}$ (simple coordination); $>Fe_2OH^0$ (double coordination) and $>Fe_3OH^{1/2-}$ (triple coordination). An example of these surface functional groups can be seen in Figure 16.

These functional groups have a different affinity for protons, and this implies a different way to determine the acid-base properties of the solid. The MUSIC model (Hiemstra *et al.*, 1996) allows calculating these affinities. From this model, is obtained that the doubly coordinated site ($>Fe_2OH^0$) can be considered as inert, whereas the reactions of protonation of the other two sites ($>FeOH^{1/2-}$ -y $>Fe_3OH^{1/2-}$) have a constant ($\log K_a$) of 9.2 (Tadanier & Eick, 2002).

This model may account for the complexation of the electrolyte ions and for inner sphere and outer sphere complexes. Protonated oxygens are in the plane of the surface; the specifically adsorbed ions are located between the plane 1 and 2; electrolyte and other not specifically adsorbed ions are located in plane 2.

Furthermore, in this model the ions are not considered as punctual charges, but they produce a distribution of spatial charge which is different for inner sphere or outer sphere complexes.

The CD-MUSIC model takes advantage by minerals crystallographic information also to determine the quantity of adsorption sites. The contribution of a surface functional group depends on the crystallographic plane in which is located (Tadanier & Eick, 2002).

Reaction	K(app)
$SOH_2^+ \leftrightarrow SOH + H^+$	$K_{a1} = \frac{\{SOH\}[H^+]}{\{SOH_2^+\}}$
$SOH \leftrightarrow SO^- + H^+$	$K_{a2} = \frac{\{SO^-\}[H^+]}{\{SOH\}}$
Surface charge σ_0	$\sigma_0 = B \cdot ([SOH_2^+] - [SO^-])$
Surface sites balance	$N_s = [SOH] + [SO^-] + [SOH_2^+]$
Fit parameters	K_{a1}, K_{a2}, N_s

Table 4. Reactions and parameters needed to define the solid surface with the non-electrostatic, NE, model

Due to its structure, the contribution of the (110) plane to the overall surface of the particle is about a 90 % in contrast to the (021) plane which contributes only a 10 %. The location is expected to affect not only the quantity of sites, but also the affinity for the adsorbate.

This model has been used for the analysis of sorption data in different minerals and different contaminants (Antelo *et al.*, 2010; Iglesias *et al.*, 2010; Tian *et al.*, 2017; Goli *et al.*, 2011; Nie *et al.*, 2017; Mayordomo *et al.*, 2018).

8.6.2 NON ELECTROSTATIC MODEL, NEM

The non-electrostatic model, NEM, has been widely used for the analysis of sorption processes, for this reason it is worth to be mentioned. In this model is implicitly considered that the electrostatic contribution is negligible compared to the chemical one, and no electrostatic correction due to the electrical interface potential is needed.

The surface charge can be still be represented by the difference in positively and negatively ionized surface sites and the number of surface site is equal to that already described for CC and DDL models. The number of fit parameters is only three as in the DDL model.

The main reactions and parameters needed to describe the solid surface by the NEM are summarised in Table 4.

9 DETERMINATION OF PARAMETERS FOR THE APPLICATION OF SURFACE COMPLEXATION MODELS

In the previous paragraphs, it has been shown as the description of the solid -liquid interface through the SCM needs the determination of several parameters; the equations defining the interactions between the solute and surface functional groups, leading to adsorption, will provide additional constants (the *complexation constants*, see 8.1) that must be determined. The more complex and detailed the model is, the greater the number of parameters to be determined.

It is certainly appropriate, when it is possible, to obtain experimental supporting information, to decrease the number of parameters obtained by numerical fit and to strengthen the validity of the numerical procedure to determine the rest of parameters.

Some of the magnitudes that appears in models' description can be experimentally measured other can be estimated by theoretical analyses. In all the models, necessary parameters are the number of surface sites, N_s , (or their density which is function of the sorbent surface area, S_A), and the protonation/deprotonation constants (K_{a1} and K_{a2}). The solid surface area σ_0 is a fundamental magnitude, whose variation as a function of the pH and ionic strength should be studied before starting any adsorption study.

In the following sections, the most classical methodologies to derive the parameters needed for most SCMs will be briefly mentioned.

9.1 SURFACE AREA AND SURFACE SITES

The adsorption capacity of a solid is directly related the number of surface sites (or coordination points, N_s) and to its specific surface area. The knowledge of these parameters is basic for the application of SCMs.

The specific surface area (S_A) represents the area on the adsorbent surface por mass of material and is expressed in [$m^2 \cdot g^{-1}$]; the knowledge of its value is important because it allows normalizing and comparing data from different materials and/or sources.

The particle size of the adsorbent is an important parameter for the surface area. Assuming spherical particles of a diameter, d [nm], and being their density ρ [$g \cdot cm^{-3}$], the geometrical surface area ($m^2 \cdot g^{-1}$) can be approximated to the value given by the following formula:

$$S_A(\text{geom}) = \frac{6000}{\rho d} \quad \text{Equation 38}$$

In general, the geometrical value is lower than the real one because it does not account for the porosity of the material and possible defects.

In the literature many methods were proposed for the determination of solids surface area and, depending on the applied methodology, the obtained values may vary even one order of magnitude. The most known method for specific surface area determination is that proposed by Brunauer, Emmett y Teller, BET, consisting of the analysis of a gas sorption isotherm (normally N₂) obtained with a dried solid.

In a clay material, however, this technique can only give the value for the “external surface” area (Kaufhold *et al.*, 2010) because the N₂ molecule is too big to enter in the interlaminal regions (Sparks, 2003).

The total surface area can be determined also with other “wet” techniques, based on the adsorption of well-characterised organic molecules. A quite common method to determine clay surface area is the ethylene-glycol-monoethyl-ether (EGME) adsorption; the methylene blue can be also used. If the section of the adsorbate molecule and the maximum capacity of the solid are known, the surface area can be calculated. In the case of methylene blue, for example, the molecule can be approximated to a rectangular parallelepiped of 17.0 x 7.6 x 3.3 Å; thus the projected area on the solid is approximately 130 - 135 Å²; value of area used to carry out calculations, considering that the maximum adsorption is reached with a monolayer of adsorbate.

The concentration of surface sites can be obtained by potentiometric titrations, but also by crystallographic or spectroscopic techniques.

In acid – base titration experiments, under extreme pH conditions, it can be assumed that all the sites are ionised, thus the maximum value of proton (hydroxyl) adsorption can be determined. In these regions the log(K_{a1,a2}) are mostly independent on the quantities of a added acid/base and this allows determining N_s. One problem related to this methodology, which gives only approximated estimations, is that the calculated valued may be biased by the ionic strength of supporting electrolyte and that the values obtained under acidic and basic conditions are not always the same.

A recommended method for N_s determination in oxides is the tritium exchange a technique proposed since the middle sixties (Berubé *et al.*, 1967; Onoda & de Bruyn, 1966; Yates and Healy, 1975). The technique basically consists on the exchange of the hydrogen of the surface functional groups >SOH, with that of the radioactive tritiated water, HTO.

The coordination sites can be expressed in different units, but the most useful is to normalise them to the solid surface area [sites·nm⁻²].

The change of units from sites·nm⁻² to mol·L⁻¹ is made knowing S_A and the concentration of solid C_s (g·L⁻¹):

$$N_s \left(\frac{\text{mol}}{\text{L}} \right) = \frac{N_s \left(\frac{\text{sites}}{\text{nm}^2} \right)}{N_A \left(\frac{\text{sites}}{\text{mol}} \right)} \cdot 10^{18} \left(\frac{\text{nm}^2}{\text{m}^2} \right) \cdot S_A \left(\frac{\text{m}^2}{\text{g}} \right) \cdot C_s \left(\frac{\text{g}}{\text{L}} \right).$$

To favour the comparison of sorption data and complexation constants obtained from different source (and materials) it has been suggested to use a unique value for the adsorption site density.

Dzombak and Morel (1990) and Davis and Kent (1990) suggested the value of $2.31 \text{ sites}\cdot\text{nm}^{-2}$ ($3.84 \mu\text{mol}\cdot\text{m}^{-2}$), for most of natural materials.

Kulik (2002) introduced the definition of a standard state for a surface specie, to describe the reference for comparison of different authors data. To this scope also defined a reference value for N_s ($12.05 \text{ sites}\cdot\text{nm}^{-2}$) and the conversion between the constants conventionally obtained and the reference state is given by (Richter *et al.*, 2005):

$$\text{Log}K_{REF} = \text{Log}K + \text{Log} \frac{N_s}{N_{s(ref)}}$$

In many cases, it is considered that the surface functional groups are homogeneous (all of the same type) and in this case the models will consider only one adsorption site (*1-site model*).

In 1-site models, the possible differences in the reactivity are averaged when the surface complexation constants are determined. In the reality, in the same material, it is probable that different adsorption sites exist. In multi-sites models, the characteristics of each adsorption site must be investigated and for each of them different complexation reactions can be established. It is very frequent the use of two-sites models.

In two-sites models, the contribution of sites with low capacity and high affinity (strong sites) and others with high capacity and lower affinity (weak) sites is usually defined. The total number of sites is then: $N_S = N_{S,weak} + N_{S,strong}$.

9.2 CATION EXCHANGE CAPACITY

The cation exchange capacity, CEC, is the maximum capacity of a solid to adsorb ions by the cationic exchange mechanism. This is a very important parameters for clayey materials and in all those materials for which the main adsorption mechanism is the cationic exchange.

The CEC of a mineral can be determined by adsorbing, up to the saturation of sorption sites, a highly selective (index) cation and then to displace it with another cation to determine the maximum adsorbed quantity. Some of the product used to apply this methodology are ammonium acetate, barium chloride or cesium nitrate.

Alternative techniques based on dye or copper complexes as, for example $[\text{Cu}(\text{trien})]^{2+}$, by using photometric techniques were also proposed (Meier y Kahr, 1999; Amman *et al.*, 2005).

The results obtained by different technique may give rise to different values, for this reason it is very important to fix the initial conditions (for example pH), and to evaluate for each mineral all the occurrences that could bias experimental data, for example the presence of soluble minerals (Dohrmann, 2006).

9.3 SURFACE CHARGE AND POTENTIAL

The measurement of the surface charge of a dispersed solid is determined mainly by two techniques the *potentiometric titrations* and the *electrophoresis*. The surface charge, σ_0 , is measured by potentiometric titration whereas the ζ -potential (zetapotential) is calculated upon the measurement of the electrophoretic mobility (Hunter, 1981).

It is useful to determine the surface charge as a function of the pH and ionic strength of the aqueous media, to measure the point of zero charge, PZC, of the solid and the constants of the acid-base equilibria, needed for the application of the SCM.

9.3.1 ELECTROPHORESIS: ζ -POTENTIAL

Electrophoretic measurements are based on the fact that the charged particles suspended in a fluid, under an electric field, move in a direction or another depending on their surface charge. Positively charged particles move towards the negative pole and negatively charged ones towards the positive pole. Additionally, the velocity reached by the particles in an electric field, E , may be estimated considering the Stokes' Law:

$$v = \frac{q \cdot E}{6 \cdot \pi \cdot a \cdot \eta} \quad \text{Equation 39}$$

The velocity, v , depends on the properties of the particles charge, q , and radius, a , assuming that they are spherical and also by the viscosity of the fluid, η .

In the electrophoretic tests the experimental magnitude to be measured is the electrophoretic mobility of the particles (μ) defined as the velocity reached for unity of applied electric field: $\mu = v/E$, parameter that obviously depends on size and charge of the particles.

As schematically shown in Figure 17, the charge of the particles generates an electrical potential at the interface, which can be estimated in an approximate way.

The particles moving in a fluid are surrounded by a layer of fluid bond to the surface which also move together with the particles (Figure 17). The ideal plane that limits the part of the fluid moving with the particle is called *slipping plane*. The ζ -potential, is defined as the potential in correspondence to the slipping plane.

To determine the ζ -potential from the electrokinetic mobility the following relation (Hückel equation):

$$\mu = \frac{2}{3} \frac{\epsilon_0 \epsilon_r}{\eta} \cdot \zeta \cdot f(\kappa a) \quad \text{Equation 40}$$

being $1/\kappa$ the Debye length defined in Eq.30.

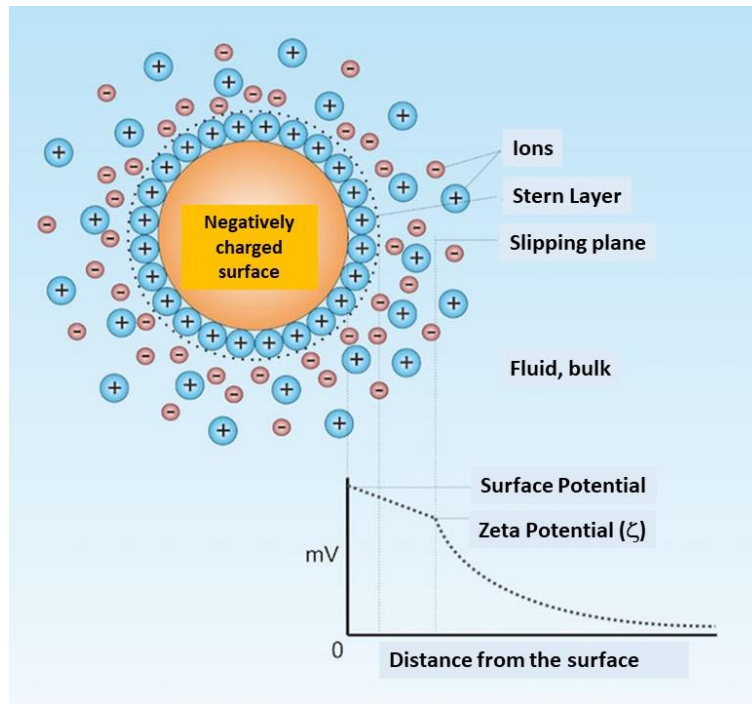


Figure 17. Electrified surface of the solid and the slipping plane. The ζ -potential is the electrical potential measured at this plane.

The function $f(\kappa a)$, or Hückel function, depends on the characteristics of the fluid and its ionic strength and on the size of the particles. Its value ranges from 1 to 1.5.

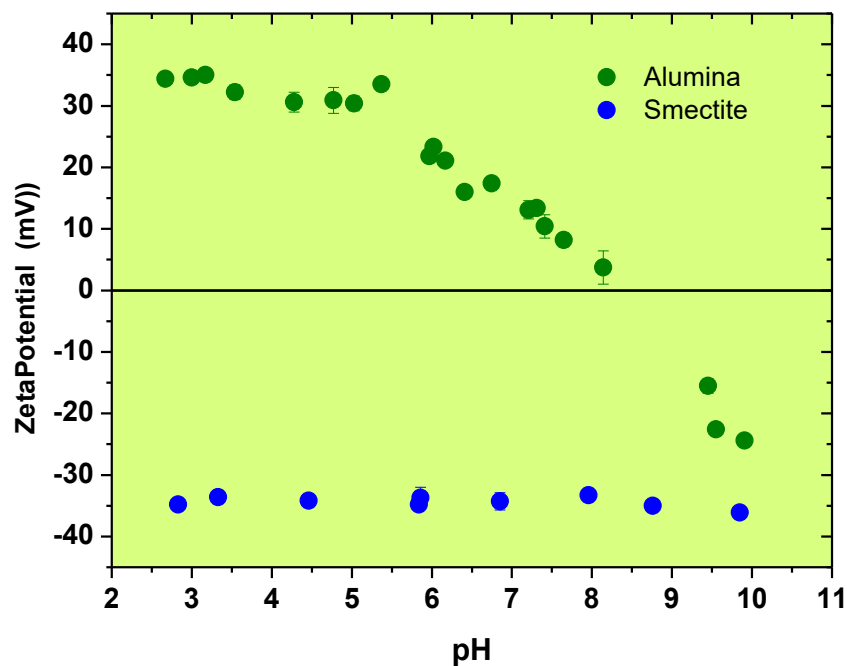


Figure 18. Examples of the ζ -potential of an oxide (alumina) and a clay (smectite) as a function of pH and $I=1 \cdot 10^{-3}$ M in NaClO_4 .

Most of the measurements with natural particles are carried out in aqueous media with a medium-low ionic strength. In this case, the value of $f(\kappa a)$, can be taken as 1.5, that represents the Smoluchowski approximation (Delgado *et al.*, 2007). The value of ζ -potential is approximated because $f(\kappa a)$ is not always measurable and because the dielectric constant or the fluid viscosity in the vicinity of the particle surface are not well known.

In addition, as the position of the slipping plane is not known, the ζ -potential is not necessarily equivalent to the surface potential Ψ_0 or the diffuse potential Ψ_d . Nevertheless, for the DDL model the potential Ψ_d is often assimilated to the ζ -potential (Sprycha and Szczypa, 1984; Sprycha, 1989; Delgado *et al.*, 2007).

ζ -potential measurements are very useful to determine the *isoelectric point*, *IEP*, of the solids. The IEP is the pH in which the ζ -potential is null. At this pH, the particles which have no charge are not perturbed by the presence of an electric field.

As the ζ -potential is measured at the slipping plane, which is located in a region more external in respect to the Surface (plane 0), the IEP represents the condition in which the charge from H^+ and OH^- (IDP) plus all the ions adsorbed in the region between the plane 0 and the slipping plane is null. If specific adsorption exists, the IEP changes. If an anion is adsorbed the PIE will be lower (more acidic pH) whereas if a cation is adsorbed it is necessary to adsorb more OH^- , thus a more elevated pH to balance the additional positive charge.

Figure 18 shows an example of ζ -potential measurements for an oxide (alumina) and a smectite clay (smectite) as a function of pH in $NaClO_4$ at $I=1 \cdot 10^{-1}$ M. It can be clearly observed that the potential of the oxide decreases with increasing the pH and its signs varies according to the protonation / deprotonation of surface sites. The IEP of this oxide is approximately pH= 8-8.5.

The smectite clay has a predominating structural negative charge and its potential is negative and approximately constant in the entire range of pH.

9.3.2 ACID BASE TITRATIONS: SURFACE CHARGE

Acid -base titration are very useful for the determination of the surface charge, the point of zero charge, PZC, and the protonation/deprotonation constants for the minerals having variable charge. Titration experiments are relatively easy, that's why, is recommendable performing them before adsorption tests, for a better adsorbent characterisation. The combination of potentiometric and electrokinetic data reinforces the basis for the selection of the parameters of surface complexation models.

In the literature, data bases with the PZC of many minerals exist (Komulski, 2018), including the information on the methods for their determination. Sverjensky (1994) proposed a methodology to determine the points of zero charge starting from crystallographic data and solvation theory.

Different methods based on potentiometric acid-base titration are available, and they are selected depending on the material to be evaluated (Schulthess & Sparks, 1986).

“*Rapid*” and continuous titrations are carried out by adding to a solid, suspended in a electrolyte, known amounts of acid or base at intervals of few minutes and measuring the obtained pH. Before starting the titrations, the solid should be washed with acid/ base and deionised water (DW), trying to get rid of eventual impurities (Davies *et al.*, 1978). The solid should be then freeze-dried and stored in absence of CO₂. All the steps of titration experiments should be carried out in absence of CO₂, for example, in a glove box or bubbling N₂, because the adsorption of carbonates, affects the surface properties of some solids.

To start with the rapid titrations, the solids are suspended in CO₂-free water. Secondly, an (inert) electrolyte is added, for example NaClO₄ of analytical grade, to adjust the ionic strength to the minimum value of interest (for example, I=1·10⁻³ M). Then a known quantity of the acid is added to shift the pH to an arbitrary low value (for example, 3, or at least 2 unit less than the expected PZC). From this point, small quantities of the base are added, waiting from 2 and 5 minutes from an addition to another. When the highest pH is reached, an inverse titration is carried out to come back to the initial pH value. To minimize the dissolution of the solid, the more extreme values of pH should not to be <3 or >11. Once the initial pH is reached, it is possible to add new electrolyte and to repeat the experiment at a high ionic strength.

To correctly evaluate the titration curves is necessary to repeat the test at least at three different ionic strengths. The pH of the solution is varied with acids (HCl, HClO₄) or bases (NaOH) at a relatively high concentration (≥ 0.1 M) to decrease the added volume and not to vary the solid concentration or the ionic strength appreciably.

The results of acid-base titrations consist of curves of pH as a function of the acid-base added concentrations.

These curves can be explained consider the electroneutrality principle that must be valid at any point of the titration. The sum of the negative and positive charges must be always equal:

$$([OH^-] + [ClO_4^-] + (\sigma_0^{*-})) = ([H^+] + [Na^+] + (\sigma_0^{*+})) \quad \text{Equation 41}$$

In Equation 42, ($\sigma_0^{*\pm}$) represents the positive or negative surface charge expressed in mol·L⁻¹.

The presence of sodium or perchlorate ions depends on the ionic strength of the electrolyte or the acid/base additions:

$$[ClO_4^-] = (NaClO_4)_{added} + (HClO_4)_{added} \quad \text{and} \quad [Na^+] = (NaClO_4)_{added} + (NaOH)_{added}.$$

Knowing that the net charge, σ_0^* , is the difference between the positive and negative charge:

$$\sigma_0^* = [OH^-] - [H^+] + [ClO_4^-] - [Na^+] = [OH^-] - [H^+] + [HClO_4]_{added} - [NaOH]_{added}.$$

The formula can be generalised considering C_A and C_B as the concentration of the generic added acid and base concentration and then:

$$\sigma_0^* (\text{mol}\cdot\text{L}^{-1}) = [\text{OH}^-] - [\text{H}^+] + C_A - C_B \quad \text{Equation 42}$$

When the adsorbent concentration (S in $\text{g}\cdot\text{L}^{-1}$) is known the surface charge can be expressed in $[\text{mol}\cdot\text{kg}^{-1}]$ (Q) using the relation: $Q = \sigma_0^* \cdot S^{-1}$.

Figure 19 shows the example of a potentiometric titration of an oxide suspended in NaClO_4 at three different ionic strengths.

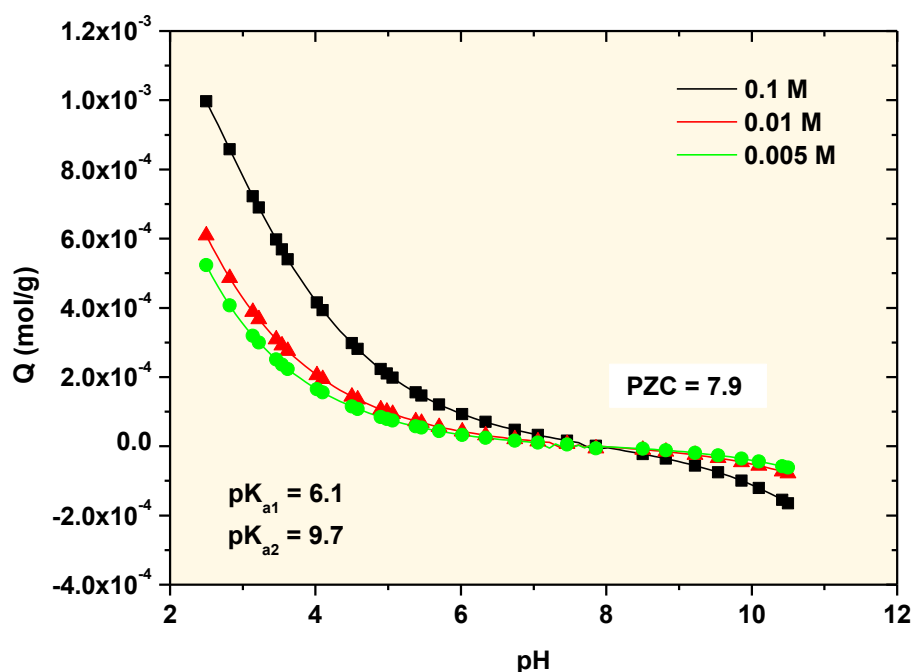


Figure 19. Example of titration data of an oxide in a electrolyte (NaClO_4) at three different ionic strengths. $S=20 \text{ g}\cdot\text{L}^{-1}$; $N_s=10.8 \mu\text{mol}\cdot\text{m}^{-2}$ and $S_A=129 \text{ m}^2\cdot\text{g}^{-1}$.

The PZC of the solid is obtained measuring the relative surface charge as a function of the pH at different concentrations of an inert electrolyte. If the curves show a common intersection point this can be identified as the PZC, and the relative charge can be converted in absolute making the origin of the charge to coincide with the PZC (Schulthess and Sparks, 1986). From the data of Figure 19, the determined PZC is around pH 8.

When a solid is suspended in various electrolytes and the same intersection point is obtained, it means that the electrolytes are effectively inert and that this intersection point is indeed the PZC (Liklema, 1984). If specific adsorption exists, the common intersection point is lower than the PZC in the case of cation adsorption, and higher than the PZC in the case of the adsorption of an anion. In fact, when a cation is specifically adsorbed, OH^- adsorption is favoured and to establish the equilibrium of the PZC ($\text{OH}^- = \text{H}^+$) a lower pH is necessary.

The PZC and IEP of a solid might not be exactly the same, because in fact the first is representative of the charge at the surface, whereas the latter of the charge at the slipping plane; nevertheless, in the absence of specific adsorption, they should be very similar.

Rapid titrations provide reliable results for most oxyhydroxides, but in the case of complex materials (mineral mixture) as sediments or soils, may not be adequate. Above all when soluble trace minerals are present (as for example calcite or other carbonate) or when the kinetic to reach the solid-liquid equilibrium is slow, is difficult to interpret the curves obtained from these tests.

The use of rapid titration implicitly assumes that the only mechanism generating consumption or liberation of H^+ y OH^- are the protonation/ deprotonation reactions (Eq.17 and 18).

In the case of more complex systems, other causes of H^+ y OH^- consumption, as for example dissolution processes, must be considered, above all at extreme pH. For these cases, alternative methods to rapid titrations were proposed.

A technique which is useful for clayey materials is the “*batch*” titration followed by a “*back-titration*” (Schulthess and Sparks, 1986; Baeyens & Bradbury, 1995; Tournassat *et al.*, 2004).

In the batch-back titration different samples are prepared, each at one different pH, adding the needed quantities of acid or base. After the equilibration time (hours or days), in all the samples, the solid and the supernatant are separated. The liquid phase is the reference of the original suspension at each pH (not the single electrolyte).

The back titration is carried out with the supernatant to establish the exact quantity of acid/base needed to return to the initial pH. The difference between the quantity initially added and the quantity added in the back titration gives the net value of acid/base consumed by the solid to generate the surface charge (ΔH^+).

9.3.3 ACID – BASE DISSOCIATION CONSTANTS

Potentiometric titrations are used also for the determination of the acid – base dissociation constants needed for calculating site speciation and the application of SCMs. These parameters can be obtained by the best fit of the titration curves. With the data presented in Figure 19, and using the DDL model, the best fit was obtained with the values for K_{a1} and K_{a2} of $10^{-6.1}$ y $10^{-9.7}$ respectively. The number of sorption sites ($10.8 \mu\text{mol}\cdot\text{m}^{-2}$) was known. The theoretical curve is plotted as a continuous line. Once the pKs are obtained (6.1 y 9.7) it is possible determining the theoretical point of zero charge from the relation: $pH_{PZC} = \frac{pK_{a1} + pK_{a2}}{2}$. The obtained value is 7.9, in perfect agreement with the experimental data.

Numerical methods are suitable for determining these parameters from potentiometric titrations, however simplified methods must be mentioned, because they are important for the first analysis of experimental data.

Figure 20 shows the data of a titration experiment, performed with a solid ($10 \text{ g}\cdot\text{L}^{-1}$) suspended in NaNO_3 , at a unique ionic strength (0.1 M). The concentration of surface sites of this solid is $1.3\cdot 10^{-3} \text{ mol}\cdot\text{L}^{-1}$. As shown in the Figure, the PCZ is between pH 6 and 7.

As observed in the previous sections, the solid surface charge, Q ($\text{mol}\cdot\text{g}^{-1}$), is the difference between the positively and negatively charged sites $Q = \{\text{SOH}_2^+\} - \{\text{SO}^-\}$.

Q can be expressed as: $Q = \frac{c_A - c_B + [\text{OH}^-] - [\text{H}^+]}{m}$ with c_A and c_B the concentration of added acid/base ($\text{mol}\cdot\text{L}^{-1}$) and m the solid concentration ($\text{g}\cdot\text{L}^{-1}$).

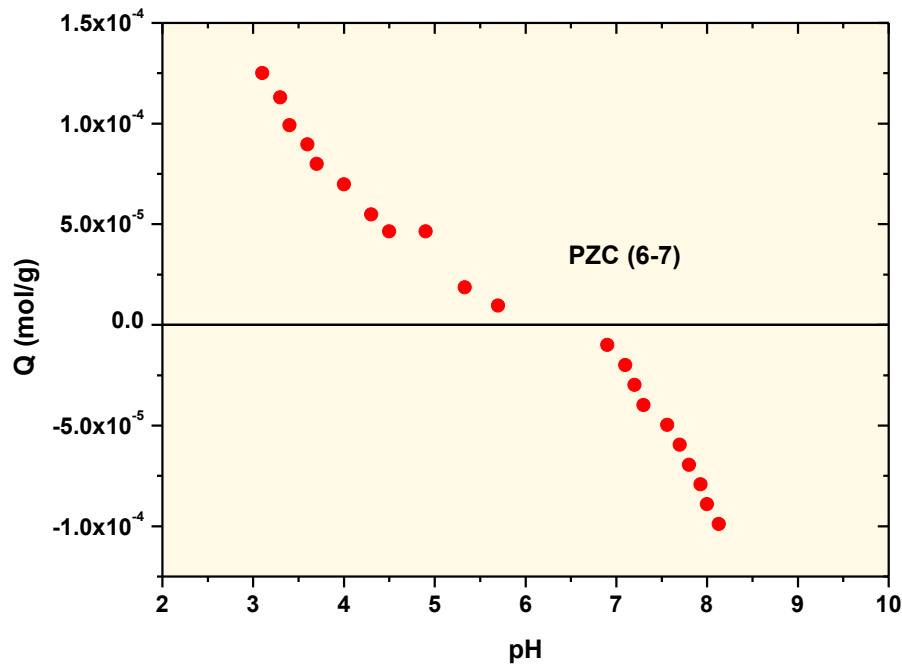


Figure 20. Example of a titration curve of a solid ($S=10 \text{ g}\cdot\text{L}^{-1}$ and $N_s = 1.3\cdot 10^{-3} \text{ mol}\cdot\text{L}^{-1}$) suspended in NaNO_3 0.1 M .

Reaction	Apparent equilibrium constant	Approximation
$\text{SOH}_2^+ \leftrightarrow \text{SOH} + \text{H}^+$	$K_{a1} = \frac{\{\text{SOH}\}[\text{H}^+]}{\{\text{SOH}_2^+\}}$	$K_{a1} = \frac{(N_s - Q)[\text{H}^+]}{Q}$
$\text{SOH} \leftrightarrow \text{SO}^- + \text{H}^+$	$K_{a2} = \frac{\{\text{SO}^-\}[\text{H}^+]}{\{\text{SOH}\}}$	$K_{a2} = \frac{[\text{H}^+] \cdot Q}{N_s - Q}$

Table 5. Approximation for the calculation of the pK of protonation and deprotonation from the titration curves

The simplification is based on the relations summarised in

Table 5, for titration data far enough from the PZC. In fact:

- 1) If **pH is** $\ll \text{pH}_{\text{PZC}}$, the charge is basically determined by $\{\text{SOH}_2^+\}$ and surface sites can be written as: $N_s = \{\text{SOH}_2^+\} + \{\text{SOH}\}$
- 2) If **pH is** $\gg \text{pH}_{\text{PCC}}$ the charge is basically determined by $\{\text{SO}^-\}$ and surface sites can be written as: $N_s = \{\text{SO}^-\} + \{\text{SOH}\}$.
- 3) In the acid region the charge can be expressed as $Q = \frac{c_A - [\text{H}^+]}{s}$ and in the basic region as $Q = \frac{[\text{OH}^-] - c_B}{s}$.

The equilibrium constant can be also simplified as indicated in Table 5. In these expressions, Q must always be taken as absolute value. The intrinsic constants of the protonation/deprotonation reactions can be obtained plotting pK_{a1} y pK_{a2} as a function of the surface charge Q , and extrapolating the values at null charge.

Using titrations data of Figure 20 and simplifying the equation as indicated in Table 5, the plots of $\text{pK}_{a1,a2}$ as a function of Q can be obtained, as shown in Figure 21 (a and b).

The relation between the $\text{pK}_{a1,2}$ and Q is a straight line, and it is straightforward to determine the intrinsic pK_a value corresponding to null charge.

In this case, the obtained values are $\text{pK}_{a1} = 4.66$ and $\text{pK}_{a2} = 8.01$. From the relation

$$\text{pH}_{\text{PZC}} = \frac{\text{pK}_{a1} + \text{pK}_{a2}}{2}, \text{ the theoretical PCZ is } \text{pH} = 6.34, \text{ which agrees with the data in Figure 20.}$$

The DDL model has three parameters: the $\text{pK}_{a1,2}$ and the number of surface sites, N_s . The knowledge of these three parameters, allows determining the basic information to fully characterise the surface of the adsorbent. In particular, it is of interest the determination of surface sites speciation, as a function of the main chemical variables.

Figure 22 shows the concentration of surface sites (neutral and positively and negatively charged) as a function of pH , of the solid which titration curves were presented in Figure 19, calculated by the DDL model.

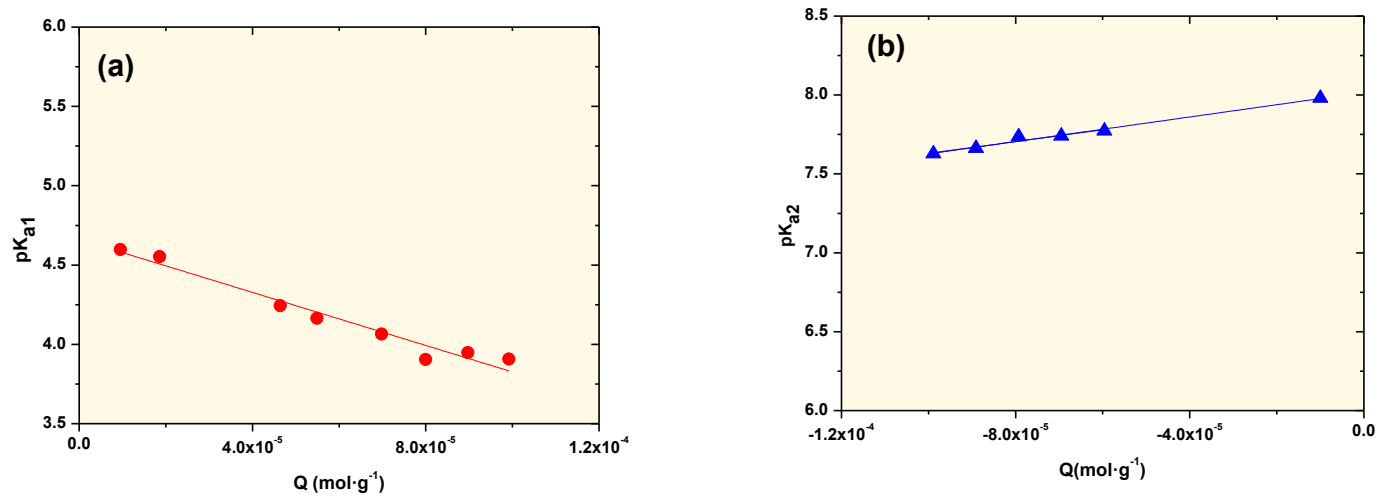


Figure 21. Estimation of (a) pK_{a1} and (b) pK_{a2} using the titration data of Figure 19 and the approximations indicated in Table 5.

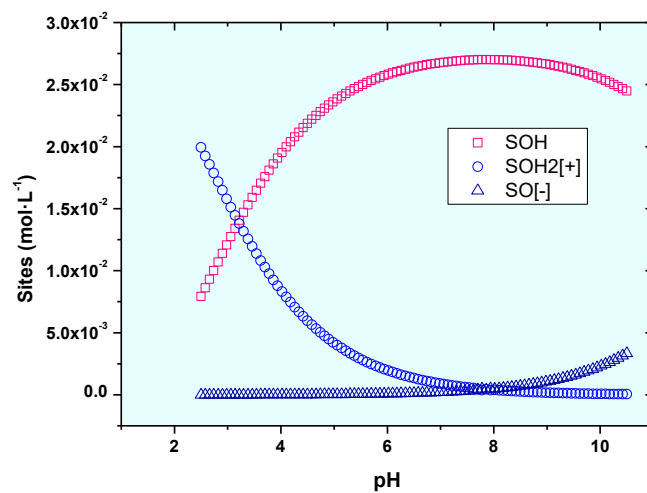


Figure 22. Speciation of the surface sites (neutral and negatively and positively charged) as a function of the pH, calculated with the DDL model and considering the data presented in Figure 18. Electrolyte: NaClO_4 0.1 M

9.3.4 CAPACITANCES

In the CC and TL model description of the solid-solution interface, electric capacitances are defined. In the CC model, the electrical double layer is represented as a flat capacitor with a capacity C , which represents the proportionality factor between the charge and the potential.

In the TC model, in the inner and outer Helmholtz layers, the charge-potential relation is also linear, and two different capacitances C_1 and C_2 , must be considered.

Many uncertainties exist on the determination and selection of these capacitances (Westall and Hohl, 1980; Lützenkirchen, 1998, 1999) because the capacitances of the solid-solution interface cannot be directly measured. Recent studies indicate that techniques based on atomic force microscopy, electrochemical or colloid probe might be very promising for the experimental determination of the electrical double layer parameters (Nishimura *et al.*, 2002; Smith *et al.*, 2018).

Due to these uncertainties and experimental limitations, the values of the capacitances have often been considered as adjustable parameters.

For the application of the CC model in aluminium oxides Westall and Hohl (1980) recommended a value for C of $1.06 \text{ F}\cdot\text{m}^{-2}$. This value has been used in many studies and also for the application of the CC to clayey soils (Goldberg *et al.*, 2000).

In the TC model, the value of the capacitance of the external layer, C_2 , is often taken as $0.2 \text{ F}\cdot\text{m}^{-2}$, on the basis of the experience obtained with Hg and AgI systems (Pieper and Vooyo, 1974; Stumm *et al.*, 1970) and because this value provided a good agreement with electrokinetic (ζ -potential) data.

In the absence of additional available data, Hayes *et al.* (1991) suggested for C_1 , a value of $0.8 \text{ F}\cdot\text{m}^{-2}$. It can be considered that the inner capacitance is related to the distance between the plane 0 and the plane β i.e. $C_1 = \frac{\varepsilon_0 \cdot \varepsilon_r}{\beta}$.

Given physically acceptable values for ε_r in the double layer (6-50) and considering that β , corresponds to the distance of closest approach of hydrated ions (2.3 - 4.3 Å), C_1 should not be outside the range of 0.1 to $2 \text{ F}\cdot\text{m}^{-2}$ (Hayes *et al.*, 1991). This should be accounted for when the capacitance values are obtained by numerical fit.

Sahai and Sverjenski (1997a,b) and Sverjenski (2001) observed that the capacitances depend on the size of the electrolyte ion and that it is possible to determine a theoretical relation between the capacitance, the type of solid and the electrolyte. The application of these theoretical principles to the selection of C_1 , significantly contributed to the applicability of the TL model and to the reduction of the number of its adjustable parameters.

10 NUMERICAL ANALYSIS AND GEOCHEMICAL CODES.

For the analysis of the experimental sorption data, different approaches can be used, from simply quantitative, to the application of sorption isotherms or mechanistic models. In the case of the use of sorption isotherm models, one or more parameter must be determined. In most cases, the equations of the adsorption isotherms can be linearized, and their parameters found by simple linear regression. When this is not feasible, it is necessary to determine the unknown magnitude by adjusting the theoretical (calculated) curve to the experimental one by numerical methods. The same occurs for the parameters of surface complexation models.

To apply numerical procedure for data adjustment, different error functions can be used; they must be minimised to make sure that the “best fit” of the data is obtained.

Amongst these error functions, the most used is the sum of squared differences between the measured quantity (x_{me}) and the calculated one (x_{cal}):

$$\sum_{i=1}^n (x_{me} - x_{cal})_i^2 \quad \text{Equation 43}$$

Another common test to evaluate the goodness of a fit is the Chi-Square test (χ^2).

$$\sum_{i=1}^n \frac{(x_{i,cal} - x_{i,me})^2}{x_{i,me}} \quad \text{Equation 44}$$

No more details will be given on the methodologies to obtain the best adjust of experimental data, as all these calculations can be automatically carried out in common programs as EXCEL or ORIGIN.

In an analogous manner, numerical optimisation can be used for the obtention of the complexation constants obtained with SCMs (Dzombak and Morel, 1990; Hayes *et al.*, 1991). Some geochemical codes (p.e. MINEQL, MINTEQA6, FITEQL) incorporate routines for the numerical optimisation of SMC adjustable parameters.

Many other geochemical codes as *Phreeqc* (Parkhurst & Appelo, 2013), *CHESS* (van der Lee & de Windt, 2002) or *Geochemist's Workbench* (Betke & Yeakel, 2014) exist. Some do not have algorithms for the numerical optimisation; nevertheless, they allow calculating the main important magnitude of the SCM (surface charge, concentration of retained and aqueous species, solubility products, saturation indexes, etc.). The calculated values can be compared with the experimental ones in a reiterative form, changing model parameters to find the best data fit.

In these trial and error procedures, Equations 43 and 44 or similar, are adequate to minimize the error in the parameter estimations. Furthermore, it is very important to carry out sensitivity analyses for all the parameters to be determined.

The main advantage of the geochemical codes is that they can incorporate thermodynamic databases for all the elements of interest and include the chemical equilibria of different

species accounting for the complete chemistry of the system. This is a quite appreciable advantage and facilitates the analysis of sorption processes within more chemically complex systems.

Indeed, geochemical and thermodynamic modelling is a very powerful tool, but its validity depends on many factors, amongst which the accuracy of the thermodynamic data bases employed for calculations. These databases are under continuous evolution, to support modelling in many contexts of application.

The OECD-NEA, through different phases of the project *Thermochemical Database*, TDB, Project, encouraged the creation of thermodynamic databases for radioactive elements, which is of special interest within the frame of radioactive waste disposals.

Many of the most important agencies for the radioactive waste management and associated research groups have carried out specific studies to provide reliable and coherent data for the compilation of these databases (Grivé *et al.*, 2014; Giffaut *et al.*, 2014).

11 ADSORPTION STUDIES IN COMPLEX MATERIALS

Many studies have been published in the past on the application of SCMs on pure minerals of different nature and considering relatively simple chemical conditions. Nevertheless, mechanistic studies to understand retention processes in complex systems are still rare.

Payne *et al.* (2013) published a very interesting paper on the guidelines for the application of SCMs to complex systems, focusing their attention on the context of radioactive waste disposals. The possible radionuclide migration in these systems represents a critical safety problem and the associated risks must be evaluated in detail.

In performance assessment of waste disposals, the principal magnitudes used to account for migration/retention are solubility products, effective diffusion coefficients and distribution coefficients of the radionuclides. The values used as input data for transport codes, are usually obtained under site-specific conditions. As already mentioned, a calculation based on a single value (o range of values) cannot not predictive of the system behaviour under different conditions. To provide more strength to performance assessment evaluations, Payne *et al.* (2013) recommended to implement mechanistic approximations. The application of thermodynamic models can be very useful to improve these evaluations, providing the knowledge for the (justified) selection of the input values range and evidencing gaps existing in the understanding of underlying phenomena or in databases and providing the theoretical basis for the selection of transport parameters used as an input of performance assessment calculations.

For the interpretation of contaminant retention/migration processes in real systems, it is necessary to develop models with a reasonable level of complexity, making the unavoidable simplifications, when needed but always properly justified. The main model objectives must be well-defined, and all the most relevant decisions must be perfectly documented and supported by experiments.

The application of SCM to *real* systems implies a large experimental effort, to obtain all the complementary information needed. The detailed comprehension of the water chemistry in contact with the solid and of the adsorbent characteristic is necessary, as well as figuring out how to deal with their heterogeneity and variability with time.

11.1 ANALYSIS OF THE AQUEOUS PHASES

The knowledge of the aqueous chemistry is necessary to analyse the *speciation of the contaminant*, determinant in adsorption processes.

As a simple example, Figure 23 shows the speciation of strontium ($[Sr]=1 \cdot 10^{-6}$ M) as a function of the pH in two solutions at the same ionic strength ($I=0.1$ M): NaClO₄ (Figure 23 a) and NaHCO₃ (Figure 23b). In NaClO₄, the predominant species of Sr is always the divalent cation Sr²⁺; the formation of the specie Sr(OH)⁺, is appreciable only under alkaline pH.

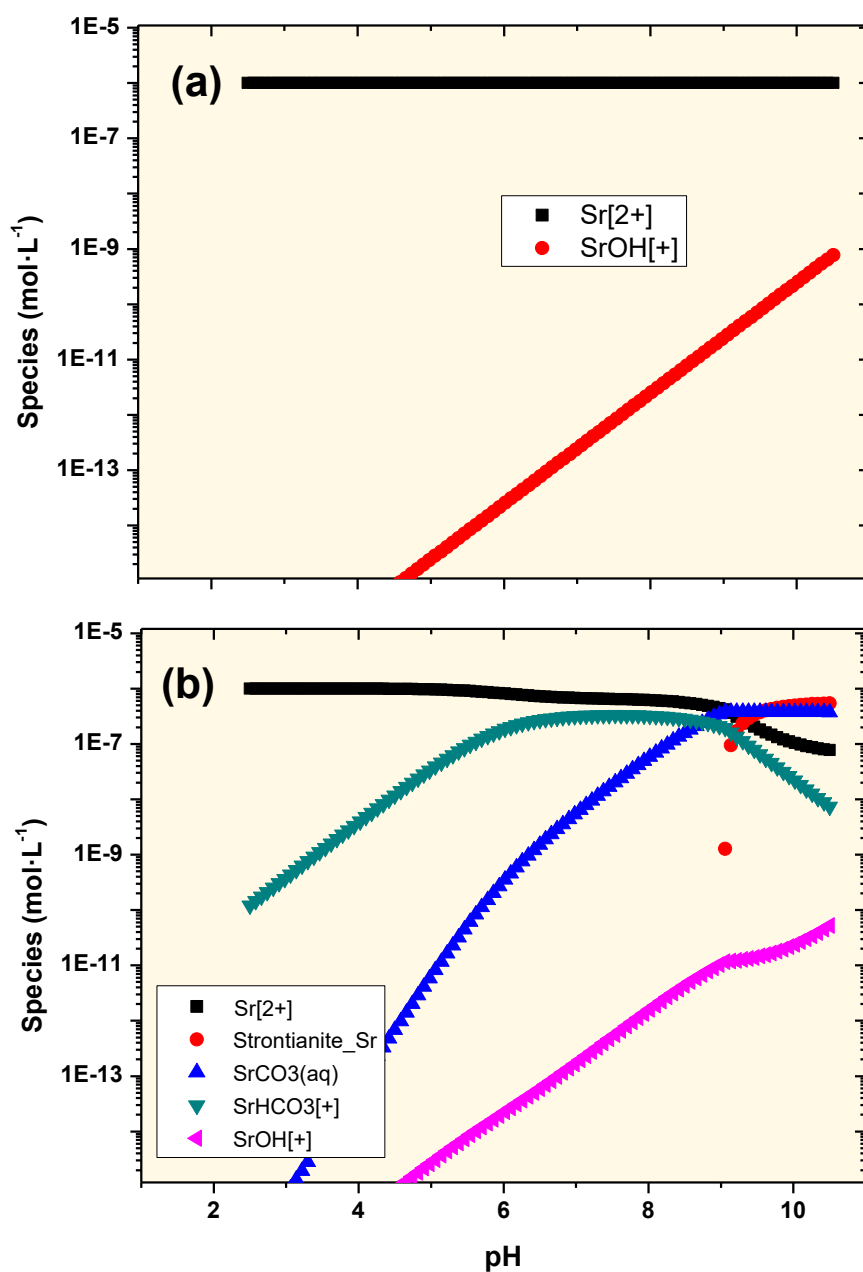


Figure 23. Aqueous speciation of strontium ($[Sr]=1 \cdot 10^{-6} M$) as a function of the pH in (a) $NaClO_4$ 0.1 M and (b) $NaHCO_3$ 0.1 M.

In $NaHCO_3$, the Sr^{2+} is still the predominant specie up to pH 9, but under neutral alkaline conditions, the carbonate-Sr species cannot be neglected. After pH 9, the precipitation of the solid strontianite ($SrCO_3$) is observed; this is relevant as precipitation may affect the overall retention of Sr. It is evident that a different aqueous speciation will have a role on the formation of Sr surface complexes.

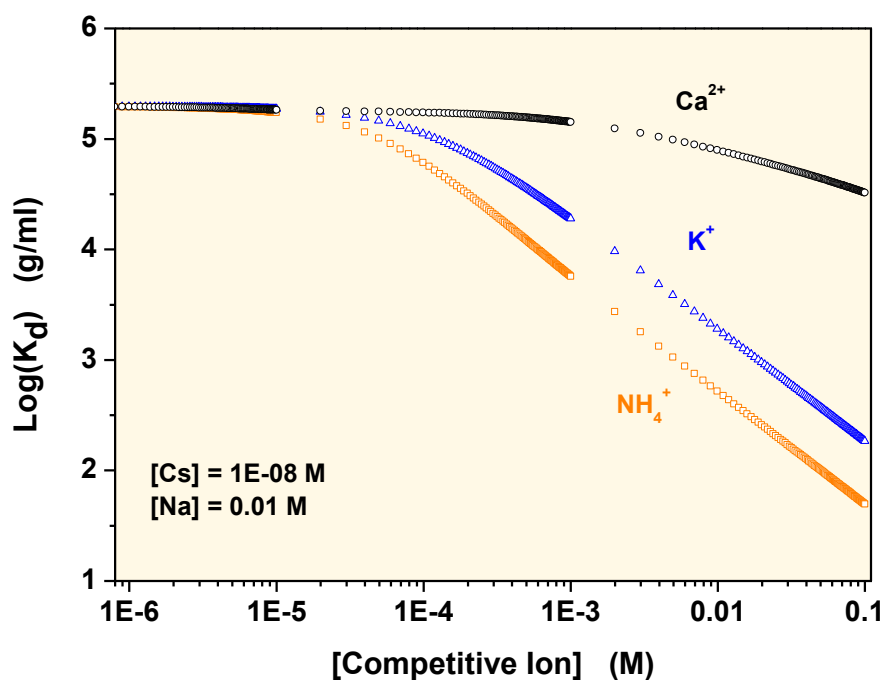


Figure 24. Example of the competence of the ions Ca, K and NH_4 in Cs ($[\text{Cs}] = 1 \cdot 10^{-8} \text{ M}$) adsorption in a clay material. The main background electrolyte is $\text{NaClO}_4 1 \cdot 10^{-2} \text{ M}$. (From Missana et al., 2014b)

The presence of different ions in the electrolyte may not only affect the speciation of the adsorbate, but directly its retention, through *competitive* phenomena. Some ions in solution can be competitive with the contaminants for the same adsorption sites, and the resulting effect is in general a decreasing of contaminant retention.

Figure 24 shows the effect produced by the ions Ca, K y NH_4 on Cs adsorption in a clay (mixed smectite-illite). As far as the concentration of the competitive ion increases, the distribution coefficient of Cs decreases. In particular, in this system that the effect produced by potassium and ammonium is more pronounced than that induced by calcium. The competitive effects are specific for each contaminant, depend on the chemistry of the system and must be analysed in an independent form.

The detailed study of the aqueous phase has as main objective to evaluate any possible factor increasing pollutant mobility in the environment. Amongst the undisputed items that can be detrimental for contaminant retention organics and colloids can be found.

Natural and/or anthropogenic *organic* compounds can form very strong aqueous complex with the contaminant stabilising them in the aqueous phase or interacts with the solid surfaces and affecting the overall distribution of the pollutant between the solid and the liquid phase (Tipping, 2002; Keith-Roach, 2008; Felipe-Sotelo et al., 2015).

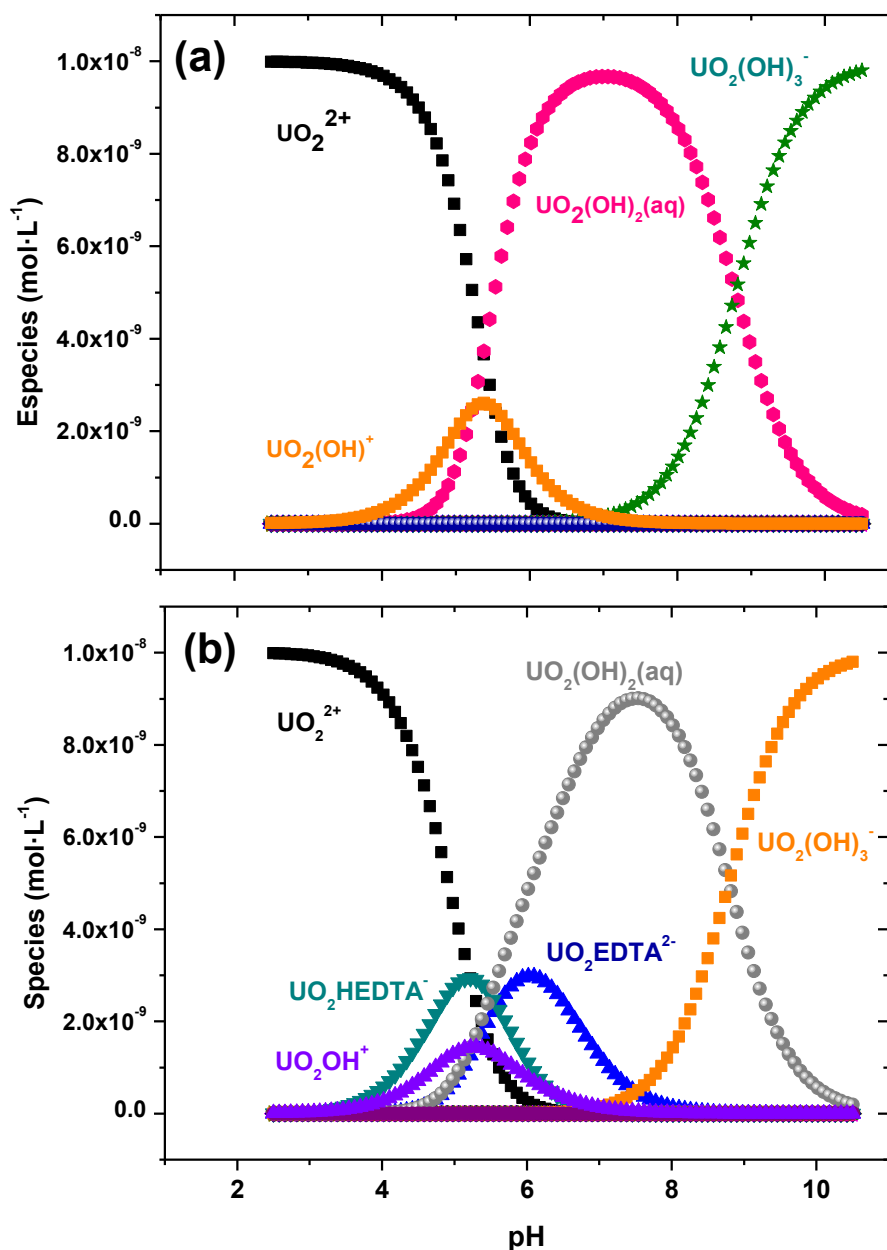


Figure 25. Aqueous speciation of the uranyl ($[UO_2^{2+}] = 1 \cdot 10^{-8} M$) as a function of the pH in $NaClO_4$ 0.1 M (a) without y (b) with EDTA ($1 \cdot 10^{-6} M$).

Figure 25 shows a simple example of the aqueous speciation of uranium (VI) ion in a solution of $NaClO_4$ (0.1 M) in absence (Figure 25a) and in the presence (Figure 25b) of the ethylenediamine-tetraacetic acid, EDTA ($1 \cdot 10^{-6} M$). The EDTA is a very effective chelant and it is widely used in decontamination processes, including nuclear installations. Figure 25 shows that the presence of the EDTA has a role on UO_2^{2+} speciation, especially in the region between pH 4 and 8, where two aqueous species in which EDTA and uranium are coordinated exist.

To understand the overall role of the organic on the uranium retention is necessary to study the thermodynamic characteristics of the organic-contaminant species and their capacity of interacting with the solid surface. The importance of developing detailed thermodynamic database for organic and RN (or other pollutant) complexes must be pointed out.

The importance of organic ligands on radionuclide migration will depend on the source of the organic (type and concentration) and on the type of surrounding materials, that will provide the physicochemical conditions of the environment (pH, ionic strength, type of solute ions). This means that the results are site-specific and for this reason, a mechanistic comprehension is necessary that can be extrapolated to any scenario.

Another issue worth to be mentioned for its role on contaminant migration, is the presence of colloidal particles. *Colloids* are particle with a size lower than 1 μm , suspended in a fluid, having a very large surface area in respect to their mass, surface phenomena predominate and control their behaviour. They have a surface charge controlling their stability, their deposition in surrounding media and their sorption capability. Colloid can constitute a mobile or immobile phase depending on their nature and the specific chemical environment, but if colloids are mobile, the contaminants adsorbed on them are also mobiles.

Basically, colloid can be important, as additional migration mechanism, only if several conditions, schematically represented in Figure 26 are fulfilled.

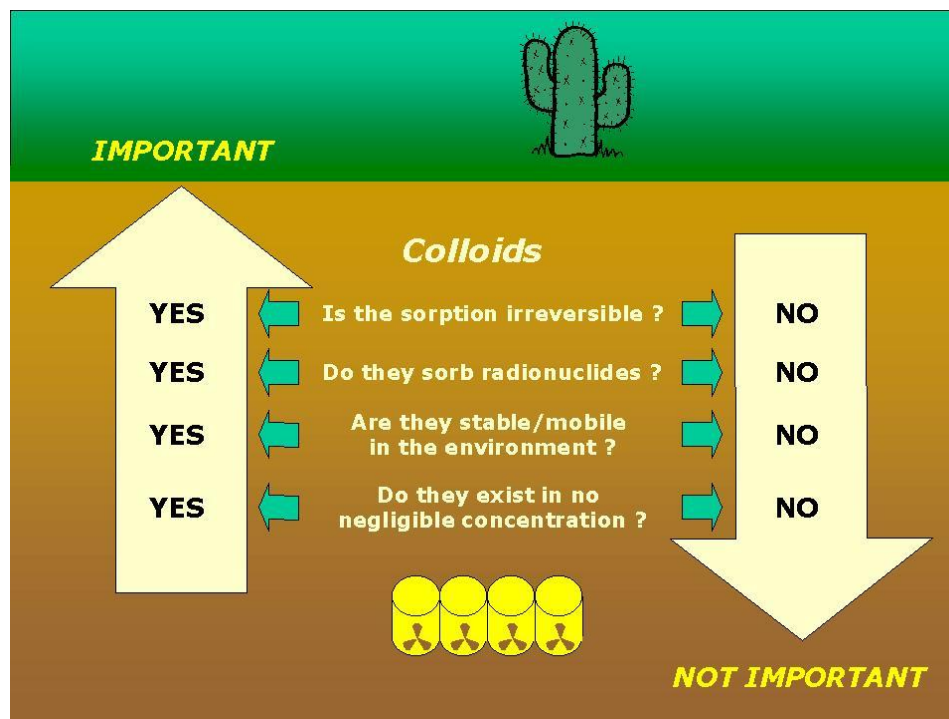


Figure 26. Schematic diagram indicating which are the conditions to be fulfilled to assess the importance of colloids in radionuclides migration.

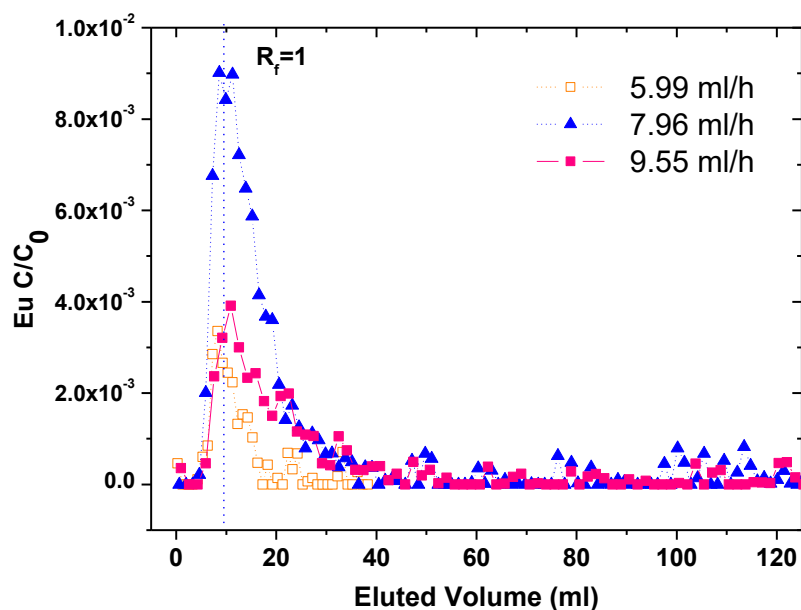


Figure 27. Breakthrough curves of Eu(III) at different water flow rates, in the presence of smectite clay colloids. The elution of Eu without colloids was null at any flow. (Missana *et al.* 2008)

As can be seen in Figure 26, the *existence*, *stability* and *mobility* of the colloids are the first issues to be evaluated. Following the schematic of Figure 26, the *sorption* and the *irreversibility* of the sorption of radionuclides onto colloids have to be studied in order to verify the real importance in the radionuclide transport of these particles in a given environment. This means that it is necessary to evaluate the colloid concentration in the aqueous phase, to characterise their main properties (size and surface charge) and their variation chemistry varies. Additionally, it is necessary measure the sorption capability of the particles, in relation to the contaminant of interest, and to know if it is irreversible or not. If all the conditions specified in Figure 26 are fulfilled, colloids will be important in radionuclide migration, otherwise their importance may be negligible.

Colloid-driven contaminant transport is a mechanism potentially very relevant for those elements that are barely mobile, as tri- and tetravalent actinides, as it was shown in the famous study carried out in the Nevada Test Site by Kersting *et al.*, (1999).

An example of the effect of colloid on contaminant migration is shown in Figure 27, where the breakthrough curve of europium within a granite column in the presence of smectite colloids is shown. Trivalent europium is a highly sorbing element, thus, when injected alone in the column its sorption onto the rock is so high that its elution cannot be observed at any water flow rate. Nevertheless, a small quantity of Eu come out from the column, in the presence of smectite colloids and at the same velocity as water. Smectite colloids were shown to be mobile in this system under high flow rates (Missana *et al.*, 2008) and this is the reason why, part of the europium adsorbed onto these colloids eluted with them.

Not only colloids naturally present in the water may be potential vectors for contaminant migration, but also those that can be generated within the waste disposals. In the case or

radioactive waste, colloids that can be formed by the alteration of the engineered barriers must be considered. As a consequence, the study of geochemical processes that can modify the properties of these materials and jeopardize the integrity of the system at a long-term is needed. Amongst these processes the corrosion of metallic containers, cement degradation and bentonite barriers erosion should be considered (Missana *et al.*, 2011; Alonso *et al.* 2018; Missana *et al.*, 2018).

The exhaustive characterisation of the colloid properties, of the colloid-colloid, colloid-contaminant and colloid-solid interactions is an essential topic of research and parallel to sorption studies, to evaluate contaminant migration in real systems.

11.2 ANALYSIS OF THE SOLID PHASES

For the global analysis of contaminant retention/migration, the possible relevance of the heterogeneity of sorbing materials must be considered; in fact, natural materials may provide a large variety of surface sites with different characteristics and reactivity.

To account for the heterogeneity, for the application of surface complexation models to complex systems, Davis *et al.* (1998) described two different types of approaches: *additive* and *generalized composite* approach.

The first approximation considers that a complex solid is formed by different minerals, each one with different sorption properties, and that the overall adsorption in the solid depends in an additive way on the contribution of each single mineral. The second approximation assumes that the complex material can be characterised in general terms, without going in depth on its real nature.

For the application of SCMs, it is necessary to know some important parameter of the solid as, for instance, the quantity of surface functional groups or the surface area. Depending on the selected approach (additive or generalised composite), the determination of the parameters is done in a different manner. In the additive approach, the solid has to be exhaustively characterised, determining which are the main adsorptive minerals, their quantity and to analyse the physicochemical characteristics of each one. In the case of generalised composite approach, the mean properties of the (unique) material will be considered. The choice of one approximation or another also implies different way of defining the surface functional groups. In the additive approach, all the identified minerals have their own sites and sorption mechanism; in the generalised composite, generic sites where complexation occur will be defined. Several authors suggested to use the value of $3.84 \mu\text{mol}\cdot\text{m}^{-2}$ ($2.31 \text{ sites}\cdot\text{nm}^{-2}$) for representing the site density of many natural materials.

The main advantage of the generalised composite is that requires little information on the sorbent materials, however, even this methodology can be sometimes useful to obtain a general information of the studied system, this still remains an empirical methodology.

The additive approach needs much more experimental information, but the sorption properties of the systems are analysed in depth through the analysis of any single mineral component. This clearly favours the application of SCMs and the mechanistic interpretation of data.

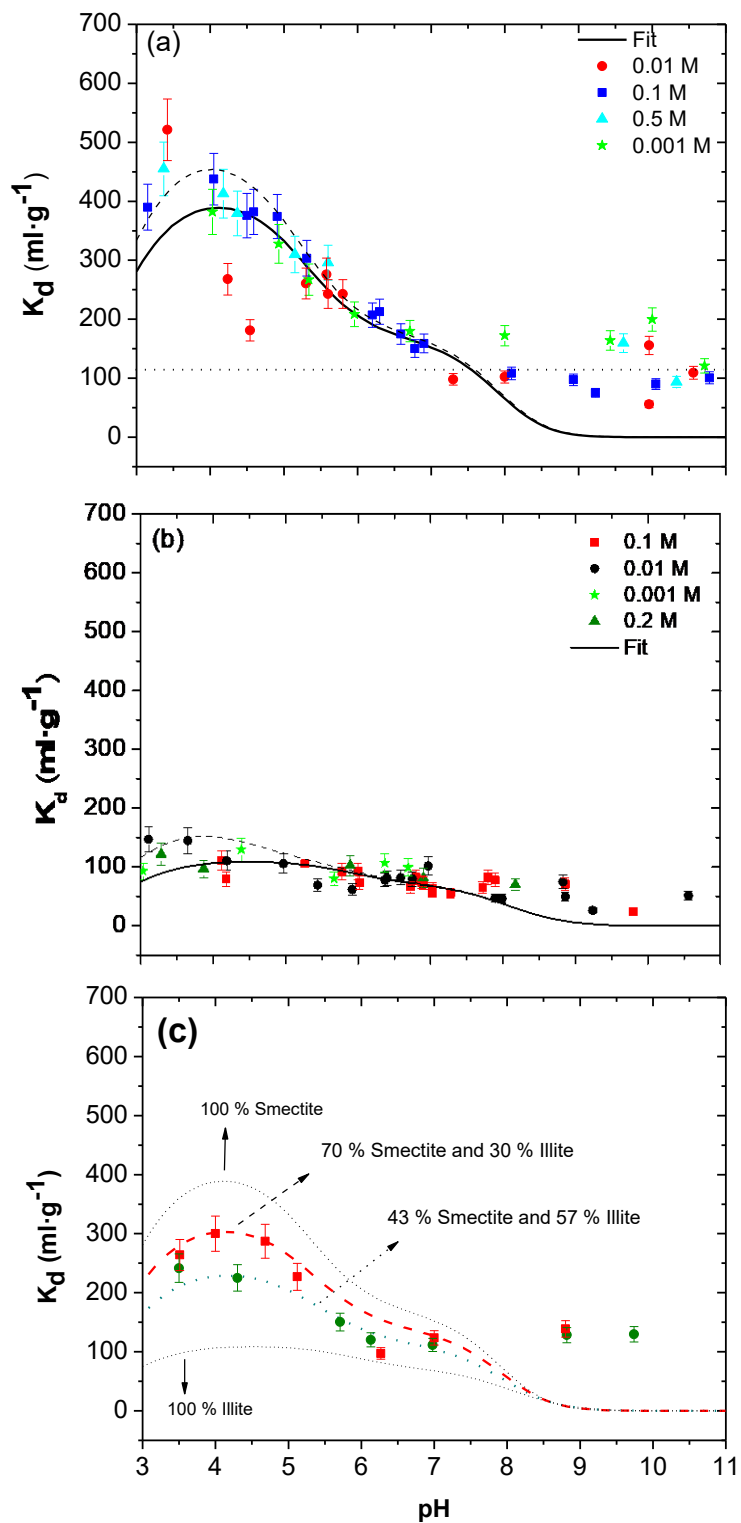


Figure 28. Selenite sorption ($[\text{Se}]=4\cdot 10^{-10}$ M) as a function of in (a) Na-smectite; (b) Na-illite and (c) in mixed clays with different proportion of both clays. Data and model by Missana et al. (2009).

These two above-described methodologies can be compared to the concepts of top *top-down* and *bottom-up* for the description of complex systems. Basically, in the first one, a general first description of the system is done, which is eventually refined until obtaining a reasonable fit of the experimental data. The bottom-up concept needs the previous knowledge of the main variables influencing the behaviour of the system: all the different individual elements are identified and linked together until the experimental data are adequately described. The bottom-up concept is more adequate for the development of predictive models, because entails the knowledge of all the involved actors. The most delicate work in this direction is precisely the identification of the essential elements and decision-making on the possible simplifications.

A simple application of the bottom-up approach for the modelling of selenite adsorption in clayey materials is shown in Figure 28 (Missana *et al.*, 2009). Figure 28(a) shows data for the selenite adsorption as a function of pH in Na-smectite suspended in NaClO₄ at different ionic strengths and the best fit of the data obtained using a non-electrostatic model. Figure 28(b) shows data and modelling for selenite adsorption data in a Na-illite. Both materials were well-characterised before starting sorption tests.

With the complexation constants obtained independently for the two minerals, it was possible to simulate selenite sorption data in two different mixed clays with smectite and illite in different proportions (70 - 30 and 43 - 57), assuming an additive model, as shown in Figure 28(c). This type of approach is promising and can be extended to even more complex materials.

In any case, it has to be recognised that this approach might not be realistically applied to very complex rocks or to consolidated solids, also because the behaviour of some mixed system is not necessarily additive, in relation to its mineralogical composition.

In some cases, the minerals may interact with each other, and some properties as the particle size or the surface area, very relevant adsorption processes, may be affected. For example, clay particles and oxides together, under certain chemical conditions, may suffer hetero-aggregation processes (Mayordomo *et al.*, 2017).

11.3 DISPERSED AND CONSOLIDATED MATERIALS

An especially interesting question for the description of real systems is related to the transferability of laboratory data obtained in powdered material (batch experiments) to compacted / consolidated systems (and to real systems). This topic is quite complex and involves questions related both to the experimental methodologies and to data interpretation. Most of the information on sorption is gathered through batch experiments, because this relatively simple, methodology allows investigating retention processes under a wide range of experimental conditions, which is basic for the development of mechanistic models.

However, the “real” structure of the (consolidated/compacted) materials may influence the overall retention; for example, apart from adsorption, absorption and diffusion processes are

expected; additionally, the sorption sites *accessibility* or the electrical double layer structure in the porous surfaces might not be the same as in powdered materials, etc..

When working with consolidated materials, firstly it has to be considered that the kinetics may play a very important role and that the time needed to reach the equilibrium may be extremely large for direct experimental evaluations, being necessary an evaluation of the experimental techniques.

As an example, Figure 29 shows the comparison of the distribution coefficients obtained for cesium ($[Cs]=1 \cdot 10^{-9}$ M) in a granitic rock in the powdered material and in a small block of the same materials. In both cases, the water in contact with the solids was the same and the solid to liquid ratio very similar. In the powdered rock, the equilibrium was reached in a few days, whereas the distribution coefficient measured in the small block was still increasing after more than 300 days. Additionally, the K_d obtained in the crushed rock (~ 140 g·mL⁻¹) was almost one order of magnitude higher than the maximum obtained in the small piece of rock (~ 33 g·mL⁻¹).

Indeed, this comparison might not be significative if the two values are not taken at the equilibrium. Nevertheless, this is a clear example of the potential problems that can be encountered when the data obtained in conventional sorption tests have to be extrapolated to compacted/consolidated materials.

Apart from problems related to the attainment of the sorption equilibrium, several additional aspects have to be considered, especially those related to geochemical and physicochemical characteristics of the systems, that must be evaluated in detail. In this sense, geochemical and thermodynamic modelling are essential tools for a better comprehension of the underlying mechanisms.

Typical tests to determine the transport/retention properties of compacted/consolidated materials are diffusion tests (García-Gutiérrez *et al.*, 2006 a and b). Many diffusion data are available for the compacted bentonite, which is a very important material in the frame of high-level radioactive waste disposals. Effective and apparent diffusion coefficients, D_e , and, D_a , are very important parameters in the safety assessment calculations. In fact, in compacted clays the radionuclide mobility is mainly controlled by diffusion retarded by sorption.

The apparent diffusion coefficient D_a , is given by the expression:

$$D_a = \frac{D_e}{\theta + \rho K_d} = \frac{D_e}{\alpha} \quad \text{Equation 45}$$

The term α (capacity factor) is dimensionless. The capacity factor includes parameters defining the porous medium (porosity and density) and the distribution coefficient, K_d , which represent the (eventual) adsorption of the contaminant in solid. According to this relation, if the effective and apparent diffusion coefficients are known, the K_d of the contaminant can be calculated.

Nevertheless, when comparing the value of the K_d obtained with Equation 46, applied to the compacted system, and the measurement of the K_d obtained with the same material in batch experiments, it is possible to find a difference even of about one of two orders of magnitude, similarly to what occurred in the case explained in Figure 29.

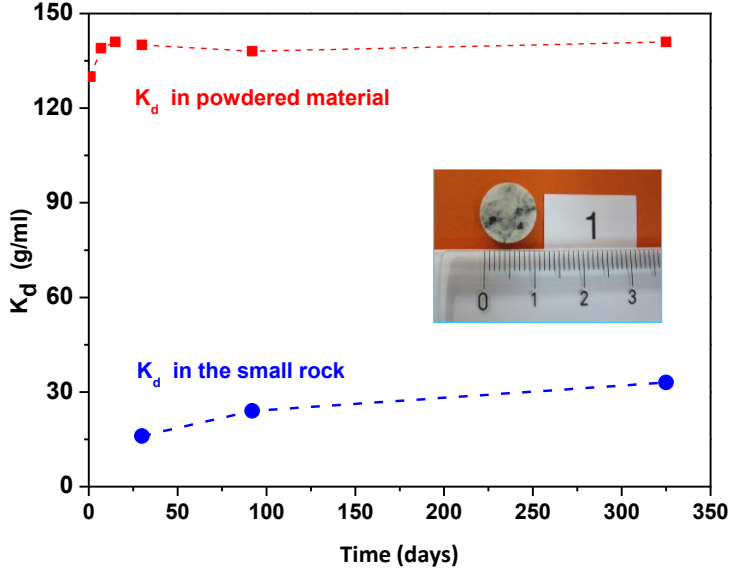


Figure 29. Comparison between the distribution coefficients of Cs ($[Cs]=1\cdot 10^{-9} M$) in granite obtained with powdered solid (red line) and in a small block of rock (blue points).

Trying to solve these (sometimes apparent) incongruences, it is fundamental to develop experimental methodologies that include different types of tests and experimental techniques. The models should integrate both macroscopic and microscopic concepts, to favour understanding of both sorption and diffusion results (Ochs *et al.*, 2001; Tachi *et al.*, 2014).

12 FINAL CONSIDERATIONS

In this document the most important methods to carry out sorption studies have been described considering both practical and theoretical aspects.

To analyse the sorption equilibrium in various systems, different types of models exist: some of them are semi-empirical (distribution coefficients or sorption isotherms); thermodynamic models are based in the concept of the electrical double layer, describing the solid-solution interface, and of surface complexation.

Due to the complexity of natural systems, semi-empirical models have been (and still they are) widely used for the analysis of experimental sorption data in complex materials. The use of thermodynamic models for the analysis of the experimental data represents a very powerful tool to figure out sorption mechanism and, above all, they have the capacity of predicting them when the chemical conditions vary; thus, it is important to carry out efforts to make possible their application in various contexts.

Surface complexation models must be based in a bottom-up approximation and in a solid experimental base, including the best as possible knowledge of the sorbing materials (type and quantity of surface sites, surface area, acidity constants., etc.). The knowledge of the real chemistry of the scenario in which contaminant are present and its possible evolution are essential for long-term predictions.

To carry out a feasible analysis of sorption processes, it is necessary to design detailed experiments covering a wide range of experimental conditions and accounting for all the issues that can have a role on contaminant migration. The impact of the most important geochemical parameters, amongst which pH, ionic strength, contaminant concentration, presence of organic or inorganic ligands, of competitive ions, colloidal particles must be studied in a systematic way.

Once the scenario is defined in detail, the most important factors will be selected to perform the necessary simplifications. *Indeed, the mechanistic comprehension of the systems helps carrying out simplifications without a relevant loss of information.*

It is also important to implement possible strategies to decrease the number of adjustable parameters, when the surface complexation models are applied. Additional experimental information gives higher solidity to the modelling step. In particular, spectroscopic techniques represent a very important instrument for the identification of aqueous and surface complexes and an undisputable support to the development of sorption models. The validity of a sorption model does not depend exclusively on its capability of simulation a single set of data, but on its capability of explain different magnitudes obtained with different type of experimental methods; for this reason, it is extremely important to obtain data from independent sources.

Finally, it must be pointed out that the main objective of the modelling is not the attainment of a set of parameters providing a nice fit of the experimental data, else it must be applied as a support for a better knowledge of the sorption mechanisms. It has to be considered that the set

of parameters obtained for the “data fit” is not necessarily unique, being this one of the main problems related to the application of surface complexation models.

The application of thermodynamic models to real systems is still a challenge, even if the existence of modern geochemical codes and the development of detailed and reliable thermodynamic database improves continuously and significantly the modelling tasks, and the consequent inclusion of surface complexation models in transport codes.

13 SIMBOLS AND CONSTANTS

Símbol	Constant	Value	Unit	Observations
e	<i>Electron charge</i>	$1.6 \cdot 10^{-19}$	[C]	
T	<i>Absolute Temperature</i>		[K]	
N_A	<i>Avogadro's number</i>	$6.02 \cdot 10^{23}$	[at]·[mol ⁻¹]	
k_B	<i>Boltzmann constant</i>	$1.38 \cdot 10^{-23}$	[J]·[K ⁻¹]·[mol ⁻¹]	
F	<i>Faraday constant</i>	96,485	[C]·[mol ⁻¹]	$F = N_A \cdot e$
R	<i>Gas constant</i>	8.31	[J]·[K ⁻¹]·[mol ⁻¹]	$R = N_A \cdot k_B$
ϵ_0	<i>Vacuum dielectric constant</i>	$8.85 \cdot 10^{-12}$	[F·m ⁻¹]	$[F] = [C^2] \cdot [J^{-1}]$
ϵ_r	<i>Relative dielectric constant</i>	78.54	adim.	Water
ϵ	<i>Dielectric constant</i>		[F·m ⁻¹]	$\epsilon = \epsilon_r \cdot \epsilon_0$
ρ	<i>Bulk density</i>		[Kg]·[m ⁻³]	
η	<i>Viscosity</i>	0.1	[Pa]·[s]	Water
θ	<i>Porosity</i>			
v	<i>Velocity</i>		[m]·[s ⁻¹]	
A	<i>Section. Área</i>		[m ²]	
I	<i>Ionic strength</i>		[mol]·[L ⁻¹]	$0.5 \cdot \sum c \cdot z^2$

Símbol	Constant	Value	Unit	Observations
z	<i>Ion charge</i>		Entire number	
S_A	<i>Surface area</i>		$[m^2] \cdot [Kg^{-1}]$	
S	<i>Solid to liquid ratio</i>		$[Kg] \cdot [L^{-1}]$	
CEC	<i>Cation Exchange capacity</i>		$[eq] \cdot [Kg^{-1}]$	
σ_0	<i>Surface charge density</i>		$[C] \cdot [m^{-2}]$	
Γ	<i>Volumetric Surface charge</i>		$[C] \cdot [m^{-3}]$	
ζ	<i>Zetapotential</i>		[V]	
Ψ_0	<i>Surface potential</i>		[V]	
C, C₁, C₂	<i>Capacitances</i>		$[F][m^{-2}]$	$[F] = [C][V^{-1}]$

14 BIBLIOGRAPHY

1. AEN-NEA. Engineered Barrier Systems (EBS) in the Context of the Entire Safety Case, Workshop Proceedings, Oxford 27 September 2002 (2002).
2. Al-Ghouti M.A., Khraisheh M.A., Allen S.J., Ahmad M.N. The removal of dyes from textile wastewater: a study of the physical characteristics and adsorption mechanisms of diatomaceous earth. *Journal of Environmental Management* (2003), 69(3), 229-38.
3. Alonso U., Missana T., Fernandez A.M., García-Gutierrez M. Erosion behaviour of raw bentonites under compacted and confined conditions: relevance of smectite content and clay/water interactions. *Applied Geochemistry* (2018), 94, 11-20.
4. Amman L., Bergaya P., Lagaly G. Determination of the CEC of clays with copper complexes revisited. *Clay Minerals* (2005), 40, 441-453.
5. Anirudhan T.S., Ramachandran M. Adsorptive removal of basic dyes from aqueous solutions by surfactant modified bentonite clay (organoclay): kinetic and competitive adsorption isotherm. *Safety and Environmental Protection* (2015), 95, 215–225.
6. Antelo J., Fiol S., Perez C., Marino S., Arce F., Gondar D., Lopez R. Analysis of phosphate adsorption onto ferrihydrite using the CD-MUSIC model. *Journal of Colloid and Interface Science* (2010), 347, 1, 112-119.
7. Azizian S. Kinetic models of sorption: a theoretical analysis, *Journal of Colloid and Interface Science* (2004), 276 47-52.
8. Baeyens B. & Bradbury M.H. A Quantitative Mechanistic Description of Ni, Zn and Ca Sorption on Na-Montmorillonite. Part I: Physico-Chemical Characterisation and Titration Measurements, PSI Bericht N° 95-10 (1995).
9. Barakat M.A. New trends in removing heavy metals from industrial wastewater. *Arabian Journal of Chemistry* (2011), 4, 361-377.
10. Berubé Y.G., Onoda G.Y, de Bruyn P.L. Proton adsorption at the ferric oxide/aqueous solution interface. *Surface Science* (1967), 7, 448-464.
11. Bethke C.M. & Yeakel S. *The Geochemist's Workbench, Release 10, Essential Guide, Aqueous Solutions*, LLC Champaign Illinois USA (2014).
12. Bhattacharyya K.G. & Gupta S.S. Adsorption of a few heavy metals on natural and modified kaolinite and montmorillonite: a review. *Advances in Colloids and Interface Science* (2008) 140(2), 114-131.
13. Blesa M.A. & Kallay N. The metal oxide-electrolyte solution interface revisited, *Advances in Colloid and Interface Science* (1988), 28,111-134.

14. Bonilla-Petriciolet A., Mendoza-Castillo D., Reynel-Ávila (Eds). Adsorption Processes for Water Treatment and Purification, Springer (2017).
15. Bradbury M.H. & Baeyens B. A mechanistic description of Ni and Zn sorption on Namontmorillonite Part I: titration and sorption measurements, *Journal of Contaminant Hydrology* (1997), 27, 199-222.
16. Bradbury M.H & Baeyens B. A mechanistic description of Ni and Zn sorption on Namontmorillonite. Part II: Modelling. *Journal of Contaminant Hydrology* (1997), 27, 223-248.
17. Bradl H.B. Adsorption of heavy metals on soils and soils constituent. *Journal of Colloids and Interface Science* (2004) 277, 1-18.
18. Cai Z, Sun Y, Liu W, Pan F, Sun P, Fu J. An overview of nanomaterials applied for removing dyes from wastewater. *Environ. Sci. Pollut. Res Int.* (2017), 24(19),15882-15904.
19. Chapman D.L. A contribution to the theory of electrocapillarity. *Phil. Mag.* (2013) 25(6), 475-481.
20. Davies J.A. & Leckie J.O. Effects of adsorbed complexing ligands on trace metal uptake by hydrous oxides. *Environ. Sci. Technol.* (1978) 12, 1309-1315.
21. Davis J.A. & Kent D.B. *in* Mineral-Water Interface Geochemistry (ed. Hochella & White), Surface complexation modelling in aqueous geochemistry. *Rev. Mineral* (1990), 177-259
22. Davis J.A. & Leckie J.O. Surface ionisation and complexation at the oxide/water interface II: Computation of the electrical double layer properties in simple electrolytes, *Journal of Colloids and Interface Science* (1978a) 67(1) 90-107.
23. Davis J.A., James R.O., Leckie J.O. Surface ionisation and complexation at the oxide/water interface I: Surface properties of amorphous hydrous oxyhydroxide and adsorption of metal ions, *Journal of Colloids and Interface Science* (1978b) 63(3), 480-499.
24. Davis J.A., Conston, J.A., Kent D.B., Fuller C.C. Application of the surface complexation concept to complex mineral assemblage. *Environ. Sci. Technol.* (1998), 32, 2820-2828.
25. Delgado A.V., Gonzalez-Caballero F., Hunter R.J., Koopal L.K., Lyklema J. Measurement and interpretation of electrokinetic phenomena, *Journal of Colloids and Interface Science* (2007), 309, 194-224.

26. Ding C., Cheng W., Wang X., Wu Z., Sun Y., Chen C., Wang X., Yu S. Competitive sorption of Pb(II), Cu(II) and Ni(II) on carbonaceous nanofibers: a spectroscopic and modelling approach. *Journal of hazardous materials* (2016), 313, 253-261.
27. Dohrmann R. An efficient model for the detection of incorrect CEC and exchangeable cations results. *Applied Clay Science* (2006), 34 (1-4), 31-37.
28. Dzombak D.A & Morel F. "Surface Complexation Modelling" Ed. John Wiley & Sons (1980).
29. Felipe-Sotelo M., Edgar M., Beattie T., Warwick P., Evans N.D.M., Read D. Effect of anthropogenic organic complexants on the solubility of Ni, Th, U(IV) and U(VI). *Journal of Hazardous Materials* (2015) 300, 553-560.
30. Fetter C.W. *Contaminant Hydrogeology*, 2nd Ed. Prentice Hall, New Jersey (1999).
31. Foo K.Y. & Hameed B.H. Insights into the modelling of adsorption isotherm systems, *Chemical Engineering Journal* (2010), 156, 2-10.
32. Ford R.G., Scheinost A.C., Sparks D.L. Frontiers in metal sorption/precipitation mechanisms on soil mineral surfaces. *Advances in Agronomy* (2001), 74, 41-61.
33. Gaines G. L. & Thomas H. C. Adsorption studies on clay minerals. II. A formulation of the thermodynamics of exchange adsorption. *J. Chem. Phys.* (1953) 21(4), 714-718.
34. García-Gutiérrez M. & Missana T. Análisis del transporte de contaminantes en medios porosos. *Soluciones analíticas. Colección documentos CIEMAT* (2018).
35. García-Gutiérrez M., Cormenzana J.L., Missana T., Mingarro M., Martín P.L. Large-scale laboratory diffusion experiments in clay rocks. *Physics and Chemistry of the Earth* (2006a), 31, 10-14.
36. García-Gutiérrez M., Cormenzana J.L., Missana T., Mingarro M., Molinero J. Overview of laboratory methods employed for obtaining diffusion coefficients in FEBEX compacted bentonite. *Journal of Iberian Geology* (2006b) 32 (1), 37-53.
37. Geissen V., Mol H., Klumpp E., Umlauf G., Nadal M., van der Ploeg M., van der Zee S.E., Ritsema C.J. Emerging pollutant in the environment: a challenge for water resource management. *International Soil and Water Conservation Research* (2015) 3, 57-65.
38. Giffaut E., Grivé M., Blanc P., Viellard, Colás E., Gailhanou H., Gaboreau S., Marty N., Madé B., Duro L. Andra thermodynamic database for performance assessment: *Thermochimie. Applied Geochemistry* (2014), 49, 225-236.

39. Gogoi A., Mazumder P., Kumar V., Tyagic, G.G., Chamindad T. Kyoungjin A., Manish Occurrence and fate of emerging contaminants in water environment: a review. *Groundwater for Sustainable Development* (2018) 6, 169–180.
40. Goldberg S. Equation and Models describing adsorption processes in soils. *Chemical Processes in soils*, Soil Science Society of America (2005) 667, 489-517.
41. Goldberg S., Johnston C.T., Suarez D.L., Lesh S.M. Mechanism of Molybdenum adsorption on soils and soil minerals evaluated using vibrational spectroscopy and surface complexation modelling. *Adsorption of metals by geomedia II: variables, mechanisms and model applications* Barnett & Kent Eds. Vol7 (2008), 235-266.
42. Goldberg S., Lesch S.M, Suarez D.L Predicting Boron Adsorption by Soils Using Soil Chemical Parameters in the Constant Capacitance. *Soil Sci. Soc. Am. J.* (2000) 64,1356-1363.
43. Goldberg S., Modelling selenite adsorption envelopes on oxides, clay minerals and soils using the triple layer model. *Soil Sci. Am. J* (2013) 77, 64-71.
44. Goldberg S. & Sposito F. A chemical model of phosphate adsorption in soils: I. Reference oxide minerals. *Soil Sci. Soc. Am. J.* (1984) 48, 772
45. Goli E., Rahnemaie R., Hiemstra T., Malakouti M.J. The interaction of boron with goethite: experiments and CD-MUSIC modelling. *Chemosphere* (2011), 82, 1475-1481.
46. Gouy G. Sur la contribution de la charge electrique a la surface d'un electrolite. *Ann. Phys IV* (1910) 9, 457-468.
47. Grivé M., Duro L., Colás E., Giffaut E., Thermodynamic data selection applied to radionuclides and chemotoxic elements: an overview of the ThermoChimie-TDB, *Applied Geochemistry* (2014), 55, 85-94.
48. Gupta V.K. & Suhas. Application of low-cost adsorbents for dye removal--a review. *Journal of Environmental Management* (2009), 90(8), 2313-2342.
49. Hassaan M.A. & El Nemr A. Health and Environmental Impacts of Dyes: Mini Review, *American Journal of Environmental Science and Engineering* (2017), 1(3): 64-67.
50. Haworth A. A review of the modelling of sorption from aqueous solutions, *Advances in Colloid and Interface Science* (1990), 32, 43-78.
51. Hayes K.F. & Leckie J.O. Modelling ionic strength effects on cation adsorption at hydrous oxide/solution interfaces, *Journal of Colloids and Interface Science* (1987) 115(2) 564-572.

52. Hayes K.F., Redden G., Ela W., Leckie J.O. Surface complexation models: an evaluation of model parameter estimation using FITEQL and oxide mineral titration data, *Journal of Colloids and Interface science* (1991), 142(2), 448-469.
53. Hernández-Montoya V., Pérez-Cruz M.A., Mendoza-Castillo D.I., Moreno-Virgen M.R., Bonilla-Petriciolet A. Competitive adsorption of dyes and heavy metals on zeolitic structures *Journal of Environmental Management* (2013), 116, 213-221.
54. Hiemstra T. & Van Riemsdijk G.H. A surface structural approach to ion adsorption: the charge distribution (CD) model. *Journal of Colloids and Interface Science* (1996), 179, 488-508.
55. Hiemstra T., Van Riemsdijk G.H., Bolt J. Multisite Proton adsorption modelling at the solid-solution interface of (hydr)oxides. A new approach. 1. Model description and evaluation of intrinsic reaction constant. *Journal of Colloids and Interface Science*, (1989a), 133, 91-104
56. Hiemstra T., De Wit J.C.M., Van Riemsdijk W.H. Multisite proton adsorption modelling at the solid-solution interface of (hydr)oxides. A new approach. 2. Application to various important (hydr)oxides. *Journal of Colloids and Interface Science*, (1989b), 133 105-117.
57. Hohl H. & Stumm W. Interactions of Pb^{2+} with hydrous gamma-alumina. *Journal Colloid and Interface Science* (1976), 55, 281-288.
58. Hsi C. & Langmuir D. Adsorption of uranyl onto ferric oxyhydroxides – application of the surface complexation binding model. *Geochimica et Cosmochimica Acta* (1985), 49(9), 1931-1941.
59. Hunter J.R., *Zeta Potential in Colloid Science*. Academic Press (1981).
60. Iglesias A., Lopez R., Gondar D., Antelo J., Fiol S., Arce F. Adsorption of MCPA on goethite and humic acid-coated goethite. *Chemosphere* (2010) 78, 1403-1408.
61. James R.O. & Healy T.W. Adsorption of hydrolysable metal-ions at oxide-water interface 3. Thermodynamic model of adsorption. *Journal of Colloid and Interface Science* (1972), 40(1), 65-67.
62. Kah M. & Brown C.D. Adsorption of ionizable pesticides in soils. *Rev Environ. Contam. Toxicol.* (2006), 188, 149-217.
63. Kaufhold S., Dohrmann R., Klinkenberg M., Siegesmund S., Ufer K. N(2)-BET specific surface area of bentonites. *Journal of Colloid and Interface Science* (2010), 349(1), 275-282.

64. Keith-Roach M.J. The speciation, stability, solubility and biodegradation of organic co-contaminant radionuclide complexes: a review. *Science of the Total Environment* (2008), 396, 1-11.
65. Kersting A.B., Efurud D.W., Finnegan D.L., Rokop D.J., Smith D.K., Thompson J.L. Migration of plutonium in groundwater at the Nevada Test Site. *Nature* (1999), 397, 56-59.
66. Komulski M. pH-dependent surface charging and points of zero charge. VII. Update. *Advances in Colloid and Interface Science* (2018), 251, 115-138.
67. Koopal L.K., van der Riemsdijk W.H., Roffey M.G. Surface Ionization and complexation models: a comparison of methods for determining model parameters, *Journal of Colloid and Interface Science* (1987), 118, 117-135.
68. Kulik D.A. Sorption modelling by Gibbs energy minimisation: towards a uniform thermodynamic database for surface complexes of radionuclides. *Radiochimica Acta*, (2002), 90, 815-832.
69. Langmuir D.L. *Aqueous Environmental Geochemistry*. Prentice Hall (1997)
70. Largette L. Y & Pasquier R. A review of the kinetics adsorption models and their application to the adsorption of lead by an activated carbon. *Chemical Engineering Research and Design* (2016), 109, 495-504.
71. Leroy P. & Revil A. A triple-layer model of the surface electrochemical properties of clay minerals. *Journal of Colloid and Interface Science* (2004), 270(2), 371-380.
72. Leroy P., Tournassat C., Bernard O., Devau N., Azaroual M. The electrophoretic mobility of montmorillonite. Zetapotential and surface conductivity effects. *Journal of Colloid and Interface Science* (2015), 451, 21-39.
73. Liklema J. Points of zero charge in the presence of specific adsorption, *J. Colloid Interface Sci.* (1984), 99, 109-117
74. Limousin G., Gaudet J.P., Charlet, Szenknet S., Bartés V., Krimissa M. Sorption isotherms: a review on physical bases modelling and measurements. *Applied Geochemistry* (2007) 22, 249-275.
75. Lützenkirchen J. Parameter estimation for the constant capacitance surface complexation model: analysis of parameters interdependency. *Journal of Colloid and Interface Science* (1999), 210, 384-390.
76. Lützenkirchen J. Parameter estimation for the triple layer model. Analysis of conventional methods and suggestion of alternative possibilities. *Journal of Colloid and Interface Science* (1998), 204, 119-127.

77. Manning B.A., Fendorf S.E., Goldberg S. Surface structures and stability of arsenic (III) on goethite: spectroscopic evidence for inner-sphere complexes. *Environmental Science and Technology* (1998), 32(16), 2383-2388.
78. Mayordomo N. Experimental and theoretical studies of mixed smectite and alumina nanoparticles to improve pollutant retention in geochemical barrier. Doctoral Thesis, Universidad de Alcalà (2017).
79. Mayordomo N., Foerstendorf H., Heim K., Weiss S., Alonso U., Missana T., Schmeide K., Jordan N. Selenium (IV) sorption onto gamma-alumina: a consistent description of the surface speciation by spectroscopy and thermodynamic modelling. *Environmental Science and Technology* (2018), 52, 581-588.
80. Meier L.P. & Kahr G. Determination of CEC of clay materials using the complexes of copper (II) with triethylenetetramine and tetraethylenepentamine. *Clay and Clay Minerals* (1999), 47(3), 386-388.
81. Missana T., Alonso U., Albarran N., García-Gutierrez M., Cormenzana J.L. Analysis of colloid erosion from the bentonite barrier of a high-level radioactive waste repository and implications in safety assessment. *Physic and Chemistry of the Earth* (2011), 36, 1607-1615.
82. Missana T., Alonso U., Fernandez A.M., García-Gutierrez M. Colloidal properties of different smectite clays: significance for the bentonite barrier erosion and radionuclide transport in radioactive waste repository. *Applied Geochemistry* (2018), 97, 157-166.
83. Missana T., Alonso U., García Gutiérrez M., Mingarro M. Role of bentonite colloids on the migration of Eu and Pu in a granite fracture. *Applied Geochemistry* (2008), 23, 1484-1497.
84. Missana T., Alonso U., García-Gutierrez M. Experimental study and modelling of selenite sorption onto illite and smectite clays. *Journal of Colloids and Interface Science* (2009), 334, 132-138.
85. Missana T., Benedicto A., García-Gutierrez M., Alonso U. Modeling cesium retention onto Na-K-, and Ca- smectite: effects of ionic strength, exchange and competing ions on the determination of selectivity coefficients. *Geochimica et Cosmochimica Acta* (2014a), 128, 266-277.
86. Missana T., García-Gutierrez M., Benedicto A., Ayora C., de Pourcq C. Modelling of Cs sorption in natural mixed-clays and the effects of ion competition. *Applied Geochemistry* (2014b), 49, 95-102.
87. Mulligan C.N., Yong R.N., Gibbs B.F. Remediation technologies for metal contaminated soils and groundwater: an evaluation. *Engineering Geology* (2001) 60, 193-207.

88. Nie Z., Finck N., Herbeling F., Pruessmann T., Liu C.L., Lützenkirchen J. Adsorption of selenium and strontium on goethite: EXAFS study and surface complexation modelling of the ternary systems. *Environmental Science and Technology* (2017), 51, 3751-3758.
89. Nishimura S., Kodama M., Yao K., Imai Y., Tateyama H. Direct Surface Force Measurement for Synthetic Smectites using the Atomic Force Microscope. *Langmuir* (2002) 12, 4681-4688.
90. Noguera-Oviedo K., Aga D.S. Lesson learned from more than two decades of research on emerging contaminants in the environment. *Journal of Hazardous Materials* (2016) 316, 242-251.
91. Norris S. Clays in Natural and Engineered Barriers for Radioactive Waste Confinement: an introduction. *Geological Society London Special Publications* (2014), 400(1):1-5.
92. Ochs M., Lothenbach B., Wanner H., Sato H., Yui M. An integrated sorption-diffusion model for the calculation of consistent distribution and diffusion coefficients in compacted bentonite. *Journal of Contaminant Hydrology* (2001), 283-296.
93. Onoda G.Y. & De Bruyn P.L. Proton adsorption at ferric oxide/aqueous solution interface I. A kinetic study of adsorption. *Surface Science*. (1966), 4(1), 48-63.
94. Parkhurst D.L. & Appelo C.A.J. Description of input and examples for PHREEQC version 3: a computer program for speciation, batch-reaction, one-dimensional transport, and inverse geochemical calculations *Techniques and Methods 6-A43 Book 6 Modeling Techniques* (2013).
95. Parks G.A. The isoelectric points of solid oxides, solid hydroxides and aqueous hydroxo complex systems. *Chemical Reviews* (1965), 177-180.
96. Payne T.E., Brendler V., Ochs M., Baeyens B., Brown P.L., Davis J.A., Ekberg C., Kulik D.A., Lutzenkirchen J., Missana T., Tach Y., Van Loon L.R., Altmann S. Guidelines for thermodynamic sorption modelling in the context of radioactive waste disposal. *Environmental Modelling and Software* (2013), 42, 143-156.
97. Peri J.B. Infrared and gravimetric study of surface hydration of gamma-alumina. *J. Phys. Chem.* (1965), 69, 211-219.
98. Pieper J.H.A., Vooy's D.A. Direct measurement of the double layer capacity at the silver iodide aqueous electrolyte interface. *Journal Electroanal. Chem.* (1974), 53, 243-252.
99. Richter A., Brendler V., Nebelung C. Blind prediction of Cu(II) sorption onto goethite: current capabilities of the diffuse double layer model. *Geochimica et Cosmochimica Acta* (2005), 69, 2725-2734.

100. Righetto L., Azimonti G., Missana T., Bidoglio G. The triple layer model revised. *Colloid and Surfaces A* (1995), 95, 141-157.
101. Roberts H.E., Morris K., Law G.T.W., Frederick J., Mosselmans W., Bots P., Kvasnina, Shaw S. Uranium (V) Incorporation mechanisms and stability in Fe(II)/Fe(III) (oxyhydr)Oxides. *Environmental Science and Technology Letters* (2017), 4(10), 421-426.
102. Rötting, T. S., Caraballo, M. A., Serrano, J. A., Ayora, C., Carrera, J. Field application of calcite dispersed alkaline substrate (calcite-DAS) for passive treatment of acid mine drainage with high al and metal concentrations. *Applied Geochemistry* (2008) 23(6), 1660-1674.
103. Sahai N. & Sverjensky D.A. Evaluation of internally consistent parameter for the triple layer model by the systematic analysis of oxide surface titration data. *Geochimica et Cosmochimica Acta* (1997a), 61, 2801-2826.
104. Sahai N. & Sverjensky D.A. Solvation and electrostatic model for specific electrolyte adsorption, *Geochimica et Cosmochimica Acta* (1997b), 61 (14), 2827-2848.
105. Sahai N. & Sverjensky D.A. Theoretical prediction of single-site surface protonation equilibrium constants for oxides and silicates in water. *Geochimica et Cosmochimica Acta* (1996), 60 (20), 3773-3797.
106. Schulthess C.P. & Sparks D.L. Back-titration technique for proton isotherm modelling of oxide surfaces. *Soil Sci. Soc. Am. J.* (1986), 50, 1406-1411
107. Sellin P. & Leupin X.O. The use of clay as an engineered barrier in radioactive waste management. A review. *Clay and Clay Minerals* (2014), 1(6), 477-498.
108. Smith A. M., Maroni P., Borkovec M, Trefalt G., Measuring Inner Layer Capacitance with the Colloidal Probe Technique. *Colloids Interfaces* (2018), 2, 65-82.
109. Sparks D.L. (2003) *Environmental Soil Chemistry*, Academic Press.
110. Sparks D.L. Toxic metals in the environment: the role of surfaces. *Elements* (2005), 1, 193-197.
111. Sposito G. On the surface complexation model of the oxide-aqueous solution interface, *Journal of Colloid and Interface Science* (1983), 91(2), 329-340.
112. Sprycha R. & Szczyba S. Estimation of surface ionization constants from electrokinetic data. *Journal of Colloid and Interface Science* (1984), 102, 288-291.
113. Sprycha R. Electrical double layer at alumina-electrolyte interface 1. Surface-charge and zeta potential. *Journal of Colloid and Interface Science* (1989), 127, 1-11.

114. Steefel C.I., Software for modelling multicomponent reactive flow and transport, Rapport Technique Lawrence Berkley National Laboratory (2009).
115. Stumm W. Chemistry of the solid-water interface. Wiley (1992)
116. Stumm W., Hohl H., Dalang F. Interaction of metal ions with hydrous oxide surfaces. *Croatica Chemica Acta* (1976), 48, 491-504.
117. Stumm W., Huang C.P, Jenkins S.R. Specific chemical interaction affecting the stability of dispersed systems. *Croat. Chem. Acta* (1970), 42, 223-245
118. Sun Y., Li J., Wang X. The retention of uranium and europium onto sepiolite investigated by macroscopic, spectroscopic and modelling techniques. *Geochimica et Cosmochimica Acta* (2014), 140, 621-643.
119. Sverjensky D.A. Interpretation and prediction of triple-layer model capacitances and the structure of the oxide-electrolyte-water interface. *Geochimica et Cosmochimica Acta* (2001), 65(21), 3643-3655.
120. Sverjensky D.A. Zero-point charge prediction from crystal-chemistry and solvation theory. *Geochimica et Cosmochimica Acta* (1994) 58, 3123-3129.
121. Tachi Y., Yotsuji K., Suyama T., Ochs M. Integrated sorption and diffusion model for bentonite. Part 2: porewater chemistry, sorption and diffusion modeling in compacted systems, *Journal of Nuclear Science and Technology* (2014), 51, 1191-1204
122. Tadanier C.J. & Eick J.E. Formulating the charge distribution multisite surface complexation model using FITEQL. *Soil Sci. Soc. Am. J.* (2002), 66, 1505-1517.
123. Tian L., Shi Z.Q., Lu Y., Dohnalkova A.C., Lin Z., Dang Z., Kinetics of cation and oxyanion adsorption and desorption of ferrihydrite: roles of ferrihydrite binding sites and unified model. *Environmental Science and Technology*, 51, 10605-10614.
124. Tipping E. Cation binding by humic substances. Cambridge University Press (2002).
125. Toride N., Leij F.J., van Genuchten M.Th. The CXTFIT Code for Estimating Transport Parameters from Laboratory or Field Tracer Experiments" Version 2.1, U.S. Salinity Laboratory, Research report N° 137 (1999)
126. Tournassat C., Greneche J.M., Tisserand D., Charlet L. The titration of clay minerals I. Discontinuous backtitration technique combined with CEC measurements. *Journal of Colloid and Interface Science* (2004), 273(1), 224-233.
127. Uddin K. A review on the adsorption of heavy metals by clay minerals with special focus on the past decade. *Chemical Engineering Journal*. (2017) 308, 438-462.

128. Van der Lee J. & de Windt L. CHESS Tutorial and Cookbook. Update for Version 3. User Manual LHM/RD/02/13 Ecole de Mines Fontainebleu, France (2002).
129. Van Genuchten, M. Th., Šimůnek J., Leij F.L., Toride N., Šejna M. STANMOD: Model use, calibration and validation, special issue Standard/Engineering Procedures for Model Calibration and Validation, Transactions of the ASABE, 5(4), 1353-1366 (2012)
130. Villalobos M. & Leckie J.O. Surface complexation modelling and FTIR study of carbonate adsorption to goethite. Journal of Colloids and Interface Science (2001), 235(1), 15-32.
131. Westall J. & Hohl H. A comparison of electrostatic models for the oxide/solution interface Adv. Colloid Interface Sci. (1980), 12, 265-294.
132. WHO, developing drinking-water quality regulation standards (2018).
133. WHO, Pharmaceutical in drinking water (2012).
134. Yagub M.T., Sen T.K., Afroze S., Ang H.M. Dye and its removal from aqueous solution by adsorption: a review. Advances in Colloid and Interface Science (2014), 209, 172-184.
135. Yates D.E, Levine S., Healy T.W. Site-binding model of the electrical double layer at the oxide/water interface, J. Chem. Soc. Faraday Trans. (1974), 70, 1807-1818.
136. Yates D.E. & Healy T.W. The structure of the silica/electrolyte interface. Journal of Colloid and Interface Science (1976), 55, 9-19.
137. Yates D.E. & Healy T.W. Titanium-dioxide electrolyte interface 2. Surface-charge (titration) studies, Journal of the chemical society-Faraday transaction (1980), 76, 9-18.
138. Zachara J.M., Girvin D.C., Schmidt R.L., Resch C.T. Chromate adsorption on amorphous iron oxyhydroxide in the presence of major groundwater ions. Environmental Science and technology (1987), 21(6), 589-594.
139. Zhang P. & Sparks D.L. Kinetics of selenate and selenite adsorption/desorption at the goethite water interface. Environmental Science and Technology (1990), 24(12), 1848-1856.
140. Zhang Z., Fenter P., Cheng L., Sturchio N., et al. Ion adsorption at the rutile-water interface: linking molecular and macroscopic properties. Langmuir (2004), 20(12), 4954-4969.

